Invited Review

Long-Range $^1H-^{15}N$ Heteronuclear Shift Correlation at Natural Abundance

Gary E. Martin* and Chad E. Hadden

Rapid Structure Characterization Group, Pharmaceutical Development, Pharmacia & Upjohn, Kalamazoo, Michigan 49001-0199

Received July 2, 1999

Despite the inherently low sensitivity of ^{15}N NMR because of its low gyromagnetic ratio (γ_N) and its relatively low natural abundance (0.37%), this important nuclide still has useful potential as a structural probe even at natural abundance. Inverse-detected NMR methods coupled with major advances in NMR probe designs have made it possible to acquire long-range $^1H-^{15}N$ heteronuclear shift correlation data on samples as small as a micromole overnight. Chemical shift referencing schemes for ^{15}N and the range of ^{15}N shifts are discussed, followed by a discussion of the currently available pulse sequences, pulse calibration, parametrization and processing of long-range $^1H-^{15}N$ data, and the implications of probe selection. These topics are followed by a review of the applications contained in the literature that have utilized $^1H-^{15}N$ heteronuclear shift correlation experiments at natural abundance, with emphasis placed on the observed long-range coupling pathways.

Introduction

Early ^{15}N NMR studies employed direct observation uniformly. The low natural abundance of ^{15}N (0.37%) coupled with a low gyromagnetic ratio (γ_N), roughly only 10% that of the proton (60.68 MHz for ^{15}N vs 599.75 MHz for ^1H at 14.1 T), combine to make ^{15}N a difficult nuclide to employ as a structural probe. Despite the unfortuitous intrinsic properties of ^{15}N, there still exists a wealth of information on ^{15}N chemical shifts and scalar couplings to various other nuclides. Much of the available information is contained in reviews ranging from chapter to monograph length by Witanowski, Stefaniak, and Webb.[1−6] There are several additional monographs[7−10] and the 1986 review of von Philipsborn and Müller,[11] although all are now becoming dated. Inverse-detected methods for $^1H-^{15}N$ heteronuclear shift correlation have not been specifically reviewed before now; however, there is some coverage of this topic in the most recent contribution of Stefaniak, Witanowski, and Webb.[6]

Difficulties of direct ^{15}N observation were largely circumvented by the advent of inverse-detected methods. Work by Bax, Griffey, and Hawkins[12,13] directed at the proton detection of directly coupled $^1H-^{15}N$ resonant pairs was first reported in 1983. These studies utilized heteronuclear multiple quantum coherence, or HMQC, based on earlier work by Müller in 1979.[14] To position these developments chronologically, the corresponding multiple quantum methods for $^1H-^{13}C$ heteronuclear shift correlation, now a very widely utilized method in natural product structure elucidation, did not follow until 1986.[15] Heteronuclear single quantum methods based on the work of Bodenhausen and Ruben[16] have also been developed and predate the $^1H-^{15}N$ multiple quantum work by several years.

From these beginnings, there followed the development of the inverse-detected long-range heteronuclear shift correlation experiment pioneered by Bax and Summers.[17] Although developed for $^1H-^{13}C$ heteronuclear shift correlation, there is no reason the HMBC experiment could not also be applied to $^1H-^{15}N$ long-range coupled pairs. In practice, however, the very weak long-range correlation signals between $^1H-^{15}N$ long-range coupled pairs preclude the successful utilization of HMBC in most instances at natural abundance. The earliest nongradient application of HMBC to $^1H-^{15}N$ correlation of which we are aware was to a biosynthetically ^{15}N-labeled sample of the marine alkaloid tantazole-A by Moore and co-workers.[18] The first $^1H-^{15}N$ long-range applications at natural abundance were a poster presentation by one of the authors in 1993[19] and a presentation in Japan by Koshino and co-workers[20] that same year that employed gradient methods. Before going any further, however, it is useful to digress slightly.

Perhaps the single factor that "set the stage" for practical $^1H-^{15}N$ heteronuclear shift correlation, whether direct or long-range, was the report of the gradient-enhanced GHMQC and GHMBC pulse sequences by Hurd and John.[21] The role of gradients in these experiments will be treated briefly below, but the interested reader is referred to the excellent paper by Ruiz-Cabello and co-workers[22] or the recent review by Parella[23] for a more detailed treatment. While gradients can be used to select coherence pathways,[24] thereby minimizing phase cycling requirements, for $^1H-^{15}N$ heteronuclear shift correlation they more importantly suppress t_1 noise. By lowering the t_1 noise floor, the observation of the relatively weak $^1H-^{15}N$ correlations is correspondingly facilitated, thereby making long-range $^1H-^{15}N$ heteronuclear shift correlation experiments at natural abundance a viable technique.

From this brief introduction, we will first consider issues of ^{15}N chemical shift referencing scales. Unfortunately, at present, there is not a single, universally accepted chemical shift scale for ^{15}N NMR. Next, the overall range of ^{15}N shifts will be briefly considered, as will the chemical shifts for ^{15}N resonances typically encountered for nitrogen-containing moieties incorporated into natural product structures. Methods now available for various types of $^1H-$

* To whom correspondence should be addressed. Tel.: (616) 833-6283. Fax: (616) 833-2030. E-mail: gary.e.martin@am.pnu.com.

10.1021/np9903191 CCC: $19.00
Published on Web 03/18/2000

^{15}N heteronuclear shift correlation will be discussed, beginning with a very brief treatment of pulse calibration and the implications of ^{15}N pulse length on the F_1 spectral width that is effectively excited. Next, gradient vs nongradient experiments will be briefly contrasted, followed by a discussion of the optimization of gradient ratios for ^{15}N, which differ from those used for ^{13}C heteronuclear shift correlation experiments even though the pulse sequences may be identical. Following these introductory sections, the pulse sequences currently available that are amenable to direct and then long-range ^{1}H−^{15}N heteronuclear correlation experiments will be discussed. This segment of the review will conclude with sections that address the extraction of long-range ^{1}H−^{15}N data from suitable long-range experiments and the implications of probe selection on sample size. The following section of the review presents a brief treatment of setting experimental parameters for ^{1}H−^{15}N heteronuclear shift correlation experiments followed by a brief discussion of the optimization of data processing. Next, the applications of ^{1}H−^{15}N heteronuclear shift correlations that have appeared to date, with particular emphasis on the long-range coupling pathways observed in these studies, will be presented. The review concludes with a discussion of what may become possible in terms of long-range ^{1}H−^{15}N heteronuclear shift correlation experiments at natural abundance over the next few years.

^{15}N Chemical Shift Referencing

Before embarking on any discussion of the methods or applications of inverse-detected ^{1}H−^{15}N heteronuclear shift correlation, it is almost mandatory to visit the issue of chemical shift referencing. Unlike ^{1}H and ^{13}C, for which chemical shift referencing has been agreed on for years, there is not presently a single, universally accepted chemical shift referencing scheme for ^{15}N. Rather, ^{15}N chemical shifts have been primarily referenced to three different "standards" over the years. Chemical shift references include nitromethane, nitric acid at various molar concentrations, and various forms of ammonium, including "liquid" ammonia. The use of nitric acid as a ^{15}N shift reference, fortunately in the opinion of the authors since a broken tube could be devastating to probe hardware, appears to be falling into disfavor. The other reference schemes are still in common, competing usage.

When used as a chemical shift reference, the ^{15}N shift of nitromethane is taken to be zero. Resonances observed upfield of nitromethane are assigned a positive (+) chemical shift, much as with the now unused tau (τ) scale for referencing proton shifts. Resonances downfield of nitromethane are assigned a negative (−) chemical shift in the nitromethane convention. More recently, some reports have begun to reverse the sign convention of using nitromethane as a shift reference, with resonances upfield of nitromethane given a negative sign and those downfield a positive sign, analogous to the TMS shift reference convention. Relative to nitromethane, liquid ammonia resonates ca. +379.5 ppm upfield. The sign convention for nitromethane [positive (+) shifts upfield] is unfortunately contrary to ASTM and IUPAC recommendations that resonances deshielded relative to the shift reference should be given algebraically positive shifts.

Liquid ammonia, though obviously less convenient to handle than nitromethane, affords a chemical shift reference scale that more closely resembles the TMS scale used for ^{1}H and ^{13}C chemical shift referencing. In this convention, resonances downfield of liquid ammonia are assigned a positive (+) chemical shift, while those upfield are assigned a negative (−) chemical shift. It is also worth noting that when chemical shifts are reported downfield of liquid ammonia, the plus sign is normally omitted. Hence, relative to liquid ammonia, nitromethane resonates at 379.5 ppm downfield. Aqueous solutions of ammonia are more conveniently handled.

Table 1. Inter-relation of the ^{15}N Chemical Shifts of the Substances Employed as ^{15}N Chemical Shift Reference Standards for Long-Range ^{1}H−^{15}N Heteronuclear Shift Correlation Studies Discussed in this Review

	chemical shift reference standard				
	liquid NH_3	CH_3NO_2	$^{15}NH_4NO_3$	$NH_4{}^{15}NO_3$	$^{15}NH_4Cl$
liquid NH_3	0.0	+379.5	−19.9	+383.5	−26.6
CH_3NO_2	379.5	0.0	359.6	+4.0	352.9
$^{15}NH_4NO_3$	19.9	+359.6[a]	0.0	+363.6	−6.7
$NH_4{}^{15}NO_3$	383.5	−4.0[a]	363.6	0.0	356.9
$^{15}NH_4Cl$	26.6	+352.9[a]	6.7	+356.9	0.0

[a] Saturated aqueous solution.

Several ammonium-containing ionic compounds have also been used as ^{15}N chemical shift reference standards for the long-range natural abundance experiments reviewed below. Reference substances have included $^{15}NH_4NO_3$, $^{15}NH_4Cl$, and $NH_4{}^{15}NO_3$. The first two substances have both been used in a manner analogous to ammonia; chemical shifts downfield are assigned positive chemical shifts. When ammonium nitrate has been utilized, it has been employed in a manner analogous to nitromethane; resonances upfield are assigned positive shifts, while those downfield are negative.

Which chemical shift scale will ultimately predominate is still an open question. It is worth noting, however, that protein ^{15}N NMR data are referenced using the ammonia shift referencing convention. The sheer bulk of ^{15}N NMR data now being generated for multiply labeled proteins may be sufficient, over time, to nudge the ammonia scale into predominance. Obviously, and unfortunately, only time will resolve this issue. Until then, individuals working in the area of ^{1}H−^{15}N heteronuclear chemical shift correlation will first have to make a decision as to which chemical shift scale they prefer to use in reporting data. At this point, it should be noted explicitly that the ^{15}N chemical shift data contained in this review are reported relative to liquid ammonia. Table 1 contains a compilation of the interrelation of the nitrogen shifts of the various materials that have been used as chemical shift reference standards. We have converted all shifts to the ammonia scale, noting in each case the original chemical shift referencing system employed when the data were reported. Second, workers must take care when resorting to data reported in the literature to ascertain which chemical shift referencing convention was used in reporting the data and to re-reference chemical shifts, if necessary, to correspond to the chemical shift referencing system that they are employing. It is imperative that the referencing convention used is specified when ^{15}N shift data are reported in the literature. Finally, it is also worth noting here that several authors have used the ^{15}N resonances of various solvents as chemical shift references for their respective studies. These have included *N*,*N*-dimethylformamide-d_7 (103.2 ppm downfield of liquid ammonia) and formamide (112 ppm downfield of liquid ammonia).

^{15}N Chemical Shift Ranges

The full range of ^{15}N chemical shifts, relative even to that of ^{13}C, is quite large. The range across which ^{15}N

resonances have been observed is >800 ppm. Practically, insofar as natural products are concerned, the useful range of ^{15}N chemical shifts is somewhat more restricted, but is still well in excess of 300 ppm. Before setting up a long-range $^{1}H-^{15}N$ heteronuclear shift correlation experiment, it is useful to have at least a reasonable expectation of the range of the ^{15}N chemical shifts that may be encountered in a molecule. There is the implicit assumption that an investigator will have conducted potentially numerous $^{1}H-^{13}C$ heteronuclear shift correlation experiments prior to acquiring long-range $^{1}H-^{15}N$ heteronuclear shift correlation data and will thus have at least some idea of the type(s) of nitrogens contained in the structure being studied.

Over the past twenty plus years since the advent of pulsed Fourier transform methods, which have provided convenient experimental access to ^{13}C NMR data, spectroscopists and natural products chemists have developed an appreciation of the range of ^{13}C chemical shifts for a diverse assortment of carbon types. This fundamental knowledge correspondingly facilitates setting transmitter frequencies and chemical shift windows in the second (F_1) frequency domain of heteronuclear 2D NMR experiments, both direct and long-range. In contrast, a corresponding knowledge of ^{15}N chemical shifts does not exist for most investigators simply because they have not had the experience to develop such a knowledge base. For this reason, we have provided the following example and the supplemental tables which summarize the chemical shifts of a number of different types of ^{15}N resonances in an effort to provide investigators with an interest into delving into these experiments with at least a reasonable starting point for their efforts.

Because of the relatively wide range of ^{15}N chemical shifts, one would ideally like to locate the X-transmitter in about the center of the expected range of ^{15}N shifts when there are multiple types of nitrogen contained in the structure being investigated. This is desirable to be certain that all of the ^{15}N resonances will be excited as efficiently as possible. Unlike ^{13}C experiments, in which the full chemical shift range seldom exceeds 200 ppm, the bandwidth for ^{15}N excitation can approach or even exceed 300 ppm. The excitation of this broad potential range of ^{15}N chemical shifts is further complicated by the fact that ^{15}N 90° pulses are typically somewhat longer in duration than for ^{13}C, thereby leading to less efficient excitation at the limits of the excitation bandwidth. Indeed, using the Varian INOVA 600 MHz NMR in the authors' laboratory, the 90° pulses for ^{15}N and ^{13}C are 22.8 and 11.0 μs, respectively, for a Nalorac Z·SPEC 3 mm gradient inverse triple resonance probe (MIDTG-600-3). We will return to the issue of the falloff of excitation with increasing F_1 spectral widths below, but before doing so, it is useful to examine a real world, natural product example.

Before considering other nitrogen species incorporated into natural products, we will examine the assigned ^{15}N chemical shifts of the semisynthetic bisindole anticancer drug vinorelbine [Navelbine (**1**)] to give an example of the considerations inherent in setting up long-range $^{1}H-^{15}N$ experiments at natural abundance.[25]

Vinorelbine is a semisynthetic bisindole alkaloid containing four nitrogen resonances. As might be expected of the types of nitrogens encountered in natural products, aliphatic nitrogens generally resonate the farthest upfield. Typical aliphatic nitrogens generally resonate in the range ~30−70 ppm. Aralkyl nitrogens resonate somewhat farther downfield, in the general range ~60−80 ppm. Indole nitrogens resonate still farther downfield in the range

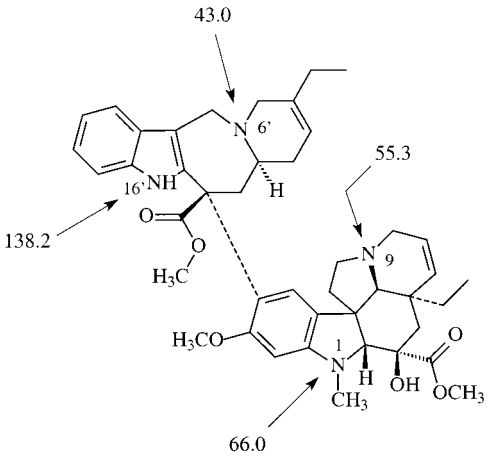

1

~120−150 ppm. 2,3-Dihydroindoles, which are commonly encountered in natural products, may essentially be considered as an aralkyl nitrogen and correspondingly resonate upfield of the indole nitrogen. Using these general guidelines, we would set the ^{15}N F_1 spectral window from ~20 to 160 ppm, placing the transmitter in the center at ~90 ppm downfield of the ammonia resonance.

The two aliphatic nitrogen resonances of vinorelbine, N-9 and N-6′, resonate at 55.3 and 43.0 ppm, respectively, well within the general range of chemical shifts for this type of nitrogen. The aralkyl N-1 resonance is observed downfield of the simple aliphatic nitrogens, resonating at 66.0 ppm, again inside the range suggested above. Finally, the indole N-16′ resonance was observed at 138.2 ppm.

When the long-range $^{1}H-^{15}N$ heteronuclear shift correlation data for vinorelbine were acquired, correlations to three of the four nitrogens contained in the molecule's structure were observed within a few hours of initiating interleaved data collection. The correlation to the N-6′ resonance, in contrast, required a data acquisition of >40 h before this correlation was observed with acceptable, albeit weak, intensity. The reason for the difference potentially can be accounted for, in part, by a mismatch between the actual long-range coupling and the experiment optimization. Alternately, another potentially major factor impacting on the observation of the response to N-6′ is the conformational flexibility of the azocine ring containing N-6′. Molecular modeling studies of the *Strychnos* alkaloids have shown the alkaloid holstiine to be conformationally much more flexible than either strychnine or brucine because of the lack of a bond between C-16 and N-19 in the former that both of the latter possess. Despite optimizing experiments for the same long-range coupling for all three *Strychnos* alkaloids, there were significantly fewer long-range correlations to the N-19 resonance of holstiine which were attributed to conformational flexibility.[26] Similar behavior of the azocine ring containing the N-6′ resonance of navelbine may account for the difficulty in observing long-range correlations to N-6′.

Supplemental Table S1 contains ^{15}N chemical shift data for some commonly encountered functional groups such as aliphatics, amides, nitriles, and oximes. No effort has been made to provide an exhaustive listing of the range of nitrogen functional group chemical shifts. The reader interested in the ^{15}N shift of less commonly encountered substituents is referred to the comprehensive reviews of Witanowski, Stefaniak, and Webb.[1−6]

Chemical shifts of the nitrogens of five-membered ring heterocycles frequently encountered with or incorporated

into natural products are summarized in Supplemental Table S2. Where enough examples exist, ranges are provided for chemical shifts, although by no means should these chemical shift ranges be assumed to be anything more than a guideline.

Nitrogen chemical shifts for an assortment of six-membered ring heteroaromatic molecules are presented in Supplemental Table S3. Here again, the listing given is by no means comprehensive. Included in Supplemental Table S3, in addition to the simple heteroaromatic systems, are various benzo-fused analogues including indoles, carbazole, etc.

Unfortunately, there are not yet a large number of examples contained in the literature for alkaloids despite the very diverse range of alkaloids known. The relative dearth of alkaloid ^{15}N chemical shift data, as would be expected, has been limited by the low sensitivity and relative abundance of ^{15}N. In contrast, as surveyed below, the database for alkaloid nitrogen shifts is growing relatively quickly since the first reports of long-range inverse-detected ^{1}H−^{15}N heteronuclear shift correlation experiments at natural abundance appeared in the literature in 1995.

Methods for Direct and Long-Range ^{1}H−^{15}N Heteronuclear Shift Correlation at Natural Abundance

Unlike conventional ^{1}H−^{13}C heteronuclear chemical shift correlation, for which there is a plethora of inverse-detected methods, the number of experiments used to date for both direct and long-range ^{1}H−^{15}N heteronuclear shift correlation at natural abundance is relatively few. Although direct correlation experiments can be done successfully without gradients at natural abundance, as noted below, this is not a generally recommended approach. Following a brief discussion of the desirability of using gradient experiments, the experiments available for direct and long-range ^{1}H−^{15}N correlation at natural abundance will be considered. There are a growing number of inverse-detected long-range heteronuclear shift correlation experiments that can potentially be applied to ^{1}H−^{15}N long-range heteronuclear shift correlation. These are surveyed in the following sections, with information pertaining to the application of these experiments to ^{1}H−^{15}N heteronuclear shift correlation where available. Following the discussion of available experiments, the parametrization of the experiments will be presented, followed by a brief treatment of the extraction of long-range ^{1}H−^{15}N coupling constant information. Finally, a survey of the published applications now in the literature is presented.

Pulse Calibrations. A wide assortment of molecules can be used for the calibration of ^{15}N pulses. One standard that has been in use for many years is 90% formamide. With the improvements in the separation of stable isotopes and the preparation of labeled materials for biosynthesis, other materials are available that are perhaps more attractive than formamide for pulse calibration. We have found it to be generally useful to employ doubly labeled *N*-acetyl glycine, enriched 99% at both the nitrogen and the glycine α-position, in DMSO-d_6. The molecule is useful in that both ^{15}N and ^{13}C pulses can be calibrated using the same sample. In addition, being doubly labeled, the molecule also provides a useful test sample for experiments involving one-bond transfers of magnetization from ^{15}N to ^{13}C or vice versa. Although these experiments are now generally limited to the study of labeled proteins and peptides, there may be occasions in the future when such experiments will be devised for natural products, particularly if it is possible to biosynthetically label the molecule of interest with ^{15}N.

Calibration of ^{15}N Pulses. Nitrogen pulses are readily calibrated using the simple sequence of pulses shown by Supplemental Figure S1A or by the spin−echo variant of the sequence shown in Supplemental Figure S1B. By arraying the length of the ^{15}N pulse across a range of values in rather coarse steps (initially), the ∼90 Hz ^{1}H−^{15}N doublet will start antiphase when the duration of the pulse is shorter than 90° if the sequence in Supplemental Figure S1A is employed. The sequence shown in Supplemental Figure S1B, which differs only by the inclusion of a 180° pulse, will have both limbs of the doublet with the same phase initially. Regardless of which sequence is used, as the duration of a 90° pulse is approached, the intensity of the "limbs" of the multiplets will decrease and will then null when a 90° pulse is actually applied. This behavior can be simply explained by considering what the pulse train in Supplemental Figure S1A does; the pair of pulses, separated by the delay τ, when $\tau = 1/2(^{1}J_{NH})$, creates unobservable heteronuclear multiple quantum coherence when a 90° pulse is applied to nitrogen. As the duration of the pulse goes beyond 90° toward 180°, the phase of the limbs of the multiplets are inverted. By using a series of coarse increments of the duration of the ^{15}N pulse, a quick approximation of the 90° ^{15}N pulse can be obtained. A more careful second experiment can then be performed with smaller increments spaced about the anticipated duration of the 360° ^{15}N pulse. We find it preferable to calibrate the 90° pulses as a function of the 360°/4 pulse length since t_1 relaxation times need not be considered when 360° pulses are applied. Data from the calibration of a 90° ^{15}N pulse using the authors' 600 MHz Nalorac 3-mm MIDTG gradient inverse-detection triple resonance NMR probe are shown in Supplemental Figure S2.

The Importance of Pulse Length. As noted earlier in the section of ^{15}N chemical shift ranges, the duration of 90° ^{15}N pulse is generally considerably longer than for ^{13}C because of the lower observation frequency of nitrogen. In the specific case of the authors' 1.7-mm SMIDG NMR probe, the 90° ^{13}C and ^{15}N pulses are 11.1 and 21.1 μs, respectively, at power settings of 58 and 59 dB, respectively, using channels 2 and 3 of a three-channel Varian INOVA 600 NMR spectrometer. To illustrate the desirability of calibrating ^{15}N pulses at the highest power without either arcing the probe or saturating the amplifier, the results of a pair of experiments are shown in Supplemental Figure S3. The data shown in Supplemental Figure S3A were acquired with the 90° ^{15}N pulse set to 21.1 μs at a power setting of 59 dB (63 dB max, at 60 or 61 dB the same effective 90° pulse was measured, indicting that the amplifier is in saturation). An ^{15}N satellite 1D GHSQC experiment was performed using the ^{15}N/^{13}C doubly labeled *N*-acetylglycine sample recommended above. The transmitter location for ^{15}N was arrayed across a range of 300 ppm in 1 ppm steps centered about the ^{15}N resonance position at ∼105.5 ppm. Only the ^{1}H−^{15}N satellite resonance is shown in the horizontal plot summary of the 300 spectra. All spectra were phased and scaled identically prior to plotting. As will be quickly noted from these data, the intensity of the ^{1}H−^{15}N satellite resonance begins to fall off as the transmitter is moved successively further off-resonance. We have arbitrarily selected 40% as a useful level of excitation (relative to the intensity obtained when the transmitter is on-resonance). In the case of a 21.1 μs ^{15}N pulse, it is possible to excite a 190 ppm (±95 ppm)

bandwidth with 40% intensity or better using a 90° pulse of this duration. There is still excitation of resonances >95 ppm upfield or downfield of the transmitter, the degree of excitation being a function of the separation from the transmitter. Practically, it is desirable to keep the maximum F_1 window to about 200 ppm total to ensure that resonances at the edge of the window are still being reasonably excited.

Data shown in Supplemental Figure S3B were recorded in an identical fashion to those in Supplemental Figure S3A, except that the power level was attenuated by 3 dB to 56 dB, giving a 29.5 μs 90° ^{15}N pulse. Using the same arbitrary 40% cutoff, note that the bandwidth excited decreases from 190 to 116 ppm with a 3 dB attenuation (a factor of 1.4) of the pulse power. At the edges of the 300 ppm window chosen for this example, using a ^{15}N 90° pulse of 29.5 μs potentially leaves resonances at the edge of the F_1 window that are not excited at all. Pulse lengths for ^{15}N in the range of 30 μs or slightly longer are typical of the performance encountered with most 5-mm gradient inverse-detection probes in the authors' experience. Using this type of hardware, it would be desirable to keep the F_1 window restricted to about 125 ppm total for long-range ^{1}H−^{15}N heteronuclear shift correlation experiments, assuming that the experiment being performed involves 180° ^{15}N pulses. The GHMBC experiment (see Figure 2), which applies only 90° pulses to ^{15}N, is somewhat more "forgiving" in terms of effective bandwidths of useful excitation.

Gradient vs Nongradient Inverse-Detected Experiments. Gradient NMR pulse sequences are hardly new. The first reported utilization of gradients in an NMR pulse sequence appeared nearly 20 years ago.[27] The question of the desirability of using gradients in ^{1}H−^{15}N heteronuclear shift correlation is much more recent. Gradients are used in three fundamental capacities in NMR experiments. First, gradients may be used to suppress t_1 noise. In this capacity, they are highly desirable for ^{1}H−^{15}N correlation experiments at natural abundance. Second, gradients can be used to select coherence pathways, thereby eliminating extensive and time-consuming phase cycling schemes.[24] Since significant numbers of transients will generally be accumulated per t_1 increment when performing ^{1}H−^{15}N correlation experiments at natural abundance, gradients do not offer a particular advantage in this regard. Third, gradients can be used for solvent suppression. In most cases, this will also not be a major concern with natural products unless one is seeking to establish ^{1}H−^{15}N direct ($^1J_{NH}$) or long-range correlations for water-soluble compounds, in which case it may be necessary to use H_2O/D_2O solvent mixtures. Hence, the primary benefit that derives from using gradient-based or -enhanced NMR pulse sequences for ^{1}H−^{15}N correlation comes from t_1 noise suppression.

Direct ^{1}H−^{15}N heteronuclear shift correlation data recorded without the use of gradients have been reported for several alkaloids. These include a submilligram sample of the simple indoloquinoline alkaloid quindolinone[28] (**2**) and a sample of cryptospirolepine (**3**) with a protonated indole nitrogen.[29] Chemical shifts for the two *N*-methyl nitrogen resonances of **3** were determined separately from a gradient long-range experiment.[30] More recently, the remaining amide nitrogen, N-3, was finally detected via a $^4J_{NH}$ long-range correlation observed in a 2.5-Hz optimized experiment.[31] The only long-range data reported at natural abundance at that time, of which we are aware, were those contained in a poster presented by one of the authors in 1993.[19] These efforts represented our initial attempts at

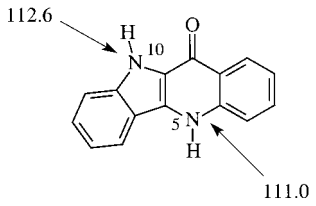

2

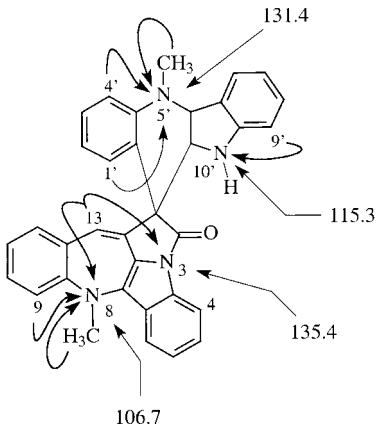

3

^{1}H−^{15}N long-range heteronuclear shift correlation at natural abundance and were only partially successful. Those data were recorded prior to the widespread availability of spectrometers with pulsed gradient capabilities. Long-range ^{1}H−^{15}N HMBC data have also been reported for the ^{15}N-labeled marine alkaloid tantazole-A (**4**).[18] At present,

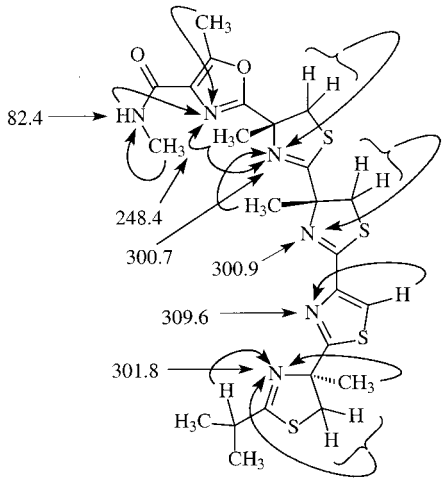

4

it is decidedly preferable to take full advantage of the use of gradient pulse sequences to minimize t_1 noise.

Gradient Pulse Sequences and Gradient Ratio Considerations. Gradient ratios used in NMR pulse sequences are derived from the ratio of the gyromagnetic ratios of the nuclides being correlated in the experiment. In the more familiar case of ^{1}H−^{13}C heteronuclear shift correlation experiments, the ratio of the gyromagnetic ratios are ~4:1 for ^{1}H and ^{13}C, respectively. For ^{1}H−^{15}N correlation, the gradient ratio is ~10:1 for ^{1}H and ^{15}N, respectively, or more precisely 9.9869:1. One might reasonably ask the question, does the difference between 10 and 9.9869 really make a difference? The answer, quite emphatically, is yes (for the long-range experiment). To illustrate the effect of optimization or misoptimization of

the gradient ratio, the results of a series of $^1H-^{15}N$ satellite spectra in which the power of the final gradient was varied are shown in Supplemental Figure S4.

The initial setup of a gradient NMR pulse sequence for $^1H-^{15}N$ shift correlation can be based on a 10:1 ratio of gradient strengths. Indeed, if only direct $^1H-^{15}N$ correlations are to be measured, the precise optimization of the gradient ratios is unnecessary when large samples are being studied. In contrast, when the extremely weak signals for long-range $^1H-^{15}N$ correlation pathways are to be examined, the difference of ~5−10% that can be obtained by careful optimization of the gradients can represent the savings of hours in data acquisition time to attain a specific signal-to-noise level. Ratios of the gradient pulses relative to one another in the various pulse sequences are discussed in more detail in the treatment of the individual experiments below.

Pulse Sequences. At present, there are a growing number of pulse sequences that are applicable to the acquisition of $^1H-^{15}N$ heteronuclear shift correlation data, either direct or long-range. In terms of the direct correlation experiments, the choice is fundamentally between single or multiple quantum-based experiments. Both can provide the investigator with phase-sensitive data. The former is probably the preferred experiment in that ^1H multiplet structure is segregated in the F_2 (proton) frequency domain, which affords better resolution in the F_1 frequency domain than is available using data from a multiple quantum-based experiment acquired with exactly the same digitization in the second frequency domain.[32] For the types of compounds of interest to readers of this review, the improvement in F_1 resolution would probably be most beneficial with peptides (see the subsection entitled Peptides and Cyclic Peptides).

Direct Correlation Experiments. Direct $^1H-^{15}N$ heteronuclear chemical shift correlations can be accomplished using either the GHSQC or GHMQC pulse sequences. As an alternative, workers with older instruments can reasonably perform the nongradient versions of the experiments to obtain usable data in reasonable periods of time. On instruments equipped with 3-mm inverse-detection probes, nongradient direct correlation data, as shown by one of the authors, can even be recorded at the submilligram level in a few hours without particular difficulty.[28]

GHSQC (Gradient Heteronuclear Single Quantum Coherence). Direct correlations can be established via either single (SQC) or multiple quantum coherence (MQC) pathways. Of the two available choices, the former is preferable in that proton−proton spin coupling information is segregated into the F_2 frequency domain, affording correspondingly better digital resolution in the second frequency domain, F_1. Response density in most $^1H-^{15}N$ heteronuclear shift correlation experiments performed on natural products is not sufficiently high, perhaps other than in the case of the peptide antibiotics, etc., for response overlap to be a major concern. The single quantum variant also affords correspondingly higher S/N since relaxation effects due to proton transverse magnetization during t_1 are absent.[33]

The earliest version of the HSQC experiment was that described by Bodenhausen and Ruben.[16] A gradient version of the experiment, GHSQC, was subsequently described by Bax and Pochapsky.[34] The version of the pulse sequence currently in use in the authors' laboratory is shown in Supplemental Figure S5. The experiment begins with a TANGO (testing for adjacent nuclei with a gyration operator) pulse[35] following the interpulse delay. The TANGO pulse is a pulse operator that serves to selectively reorient direct and long-range components of magnetization, the final orientation a function of the phases of the various pulses in the pulse operator. Vector diagrams of the operation of the various TANGO pulses are presented in the monograph by Martin and Zektzer.[36] In the pulse sequence shown in Supplemental Figure S5, the TANGO pulse serves to selectively orient the component of $^1J_{NH}$ component of magnetization in the *xy*-plane for randomization by the homogeneity spoiling gradient which follows.

The application of gradients in the GHSQC experiment differs somewhat from the GHMQC experiment discussed below. Since the proton 180° pulse midway through evolution has no effect on the evolving heteronucleus chemical shift (recall that the experiment is based on heteronuclear single quantum coherence), a single gradient pulse may be located during the evolution period, t_1. A second gradient is then located following the paired 180° pulses of the reverse INEPT step. If the phase of the second gradient, G3, is not alternated on successive scans, a magnitude mode spectrum is obtained. By alternating the phase of G3, N- and P-type data can be created on successive scans and stored separately, giving a phase-sensitive spectrum after appropriate processing, albeit with a sensitivity loss of $2^{1/2}$.

GHMQC (Gradient Heteronuclear Multiple Quantum Coherence). The second method for direct heteronuclear shift correlation is via the exploitation of multiple quantum coherence pathways. These experiments had their beginning with the 1979 report of Müller.[14] The most familiar form of the experiment for investigators working with small molecules is probably the sequence described by Bax and Subramanian in 1986.[15] The first gradient version of the experiment was reported in 1991 by Hurd and John.[21] The variant of the experiment presently in use in the authors' laboratories is shown in Supplemental Figure S6.

The TANGO pulse operator in this version of the experiment serves to "park" the $^1J_{NH}$ component of magnetization in the *xy*-plane. Following the null delay, heteronuclear multiple quantum coherence is generated by the pair of 90° pulses applied to ^1H and [$1/2(^1J_{NH})$ later] ^{15}N. Heteronuclear multiple quantum coherence begins to evolve as zero and double quantum coherences during evolution (t_1). The gradients applied flanking the 180° ^1H pulse serve to select coherence pathways. The 180° ^{15}N pulses that precede and follow the first (G1) and second (G2) gradient pulses, respectively, refocus the effects of evolution during the duration of the gradient pulse application (typically 1−2 ms). The desired component of magnetization following evolution is proton single quantum coherence, which is recreated by the second 90° ^{15}N pulse. For $^1H-^{13}C$ systems ($\gamma_H/\gamma_C \approx 4$), the gradient ratio 2:2:±1, G1:G2:G3, gives the desired result, as does the ratio 5:3:4. For the $^1H-^{15}N$ system ($\gamma_H/\gamma_N \approx 10$), the gradient ratio 5:5:±1, G1:G2:G3, or an equivalent must be employed.

PEP-GHSQC-TOCSY. A novel report has recently appeared that takes advantage of the dispersion of ^{15}N to sort the ^1H homonuclear spin systems of amino acids via a GHSQC-TOCSY experiment.[37] This is the first reported application of any form of hyphenated 2D experiment involving ^{15}N at natural abundance. The pulse sequence, which is shown in Figure 1, utilizes the preservation of equivalent pathways, or PEP, approach to improve sensitivity.[38] Quite simply, protons directly attached to nitrogens are first labeled with the ^{15}N chemical shift of the directly bound nitrogen in a manner identical to the normal

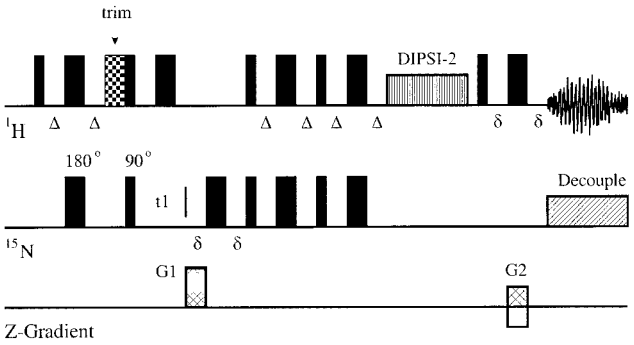

Figure 1. Pulse sequence for the heteronuclear single quantum coherence-based shift correlation with sensitivity improvement by preservation of equivalent pathways, coupled with the homonuclear isotropic mixing (PEP-HSQC-TOCSY).[37] Narrow bars correspond to 90° pulses; broader bars denote 180° pulses. The "TOCSY" transfer of magnetization is accomplished with the DIPSI-2 segment of the experiment.

GHSQC experiment. Recalling that gradient 2D NMR experiments "capture" only one component or half of the available signal, the sequence shown in Figure 1 first "stores" one component of magnetization on the *z*-axis. The other component of magnetization, which is squandered in conventional GHSQC experiments, is then refocused and added to the magnetization parked on the *z*-axis. A good description of the sensitivity-enhanced GHSQC experiment is to be found in the chapter by Griesinger and co-workers.[33] After both components of magnetization are collected as *z*-magnetization, magnetization is propagated from the directly bound proton to its vicinal neighbors in the TOCSY portion of the experiment using a DIPSI-2[39] spin lock. Ultimately, entire amino acid homonuclear spin systems can be "read out" and sorted by the ^{15}N chemical shift of the nitrogen directly bound to the individual α protons. Williamson and co-workers[37] demonstrated the application of the PEP-GHSQC-TOCSY experiment using the peptide bombesin as a model system (see the subsection entitled Peptides and Cyclic Peptides).

Long-Range Correlation Experiments. Until recently, in terms of long-range ^{1}H−^{15}N experiments, there was the single choice of the well-established GHMBC experiment developed by Hurd and John[21] derived from the nongradient HMBC experiment of Bax and Summers.[17] More recently, additional variants have begun to appear. Long-range experiments now available include the D-HMBC experiment proposed by Furihata and Seto,[40] which provides for X-nucleus decoupling during acquisition. Furihata and Seto[41] have also proposed a 3D-HMBC experiment in which the long-range optimization is varied in the third dimension. These data are intended for presentation as the projection through the third frequency domain, in which the long-range delay is systematically varied to take advantage of responses across a range of optima. Unfortunately, because of the very low sensitivity of ^{1}H−^{15}N long-range heteronuclear shift correlation experiments at natural abundance, it is unlikely that the 3D-HMBC experiment will ever have any practical utility for these applications. A useful alternative to the GHMBC sequence has been proposed by Marek, Králík, and Sklenář[42] that employs single quantum coherence (SQC). Their experiment, which has been given the acronym GSQMBC, offers improved F_1 resolution relative to the multiple quantum-based sequences in the same sense that GHSQC differs from GHMQC.[32] Sheng and van Halbeek[43] have also reported a phase-sensitive long-range experiment, which they have labeled PS-GHMBC. In mid-1998, Wagner and Berger[44] reported a different approach to a more uniform long-range coupling excitation in an experiment they called ACCORD-HMBC. Unlike the 3D-HMBC experiment of Furihata and Seto,[41] which for ^{1}H−^{15}N long-range experiments impractically varies the optimization of the long-range coupling in the third frequency domain, the ACCORD-HMBC experiment varies the long-range optimization in a systematic fashion from one increment of the t_1 evolution period to the next. This approach appears to have promise for long-range ^{1}H−^{15}N correlation experiments where there is a diverse range of possible long-range couplings. The first application of ACCORD-HMBC to long-range ^{1}H−^{15}N is presented below.

Late 1998 saw a further report by Furihata and Seto[45] of a pair of constant time (CT-HMBC-1 and CT-HMBC-2) long-range heteronuclear correlation experiments. To date, there has not been a reported application of either of these experiments to long-range ^{1}H−^{15}N heteronuclear shift correlation. It remains to be seen if these experiments will have any utility for such studies, although the nature of one of the experiments does lead to the sampling of a limited, albeit much less flexible, range of potential long-range couplings.

Finally, in early 1999, an experiment was developed in the authors' laboratories that was given the acronym IMPEACH-MBC (improved performance accordion long-range heteronuclear multiple bond correlation spectroscopy).[46] The IMPEACH-MBC pulse sequence is similar to ACCORD-HMBC in that it employs the accordion principle to excite a broad range of potential long-range couplings. It differs, however, in that the variable delay of the ACCORD-HMBC experiment, which serves as a pseudo third evolution period for homonuclear frequency modulation of long-range responses in F_1, is replaced by a new pulse sequence element, a constant time variable delay. The net result of replacing the simple variable delay by the constant time variable delay is complete suppression of homonuclear frequency modulation of the long-range responses in F_1 with correspondingly improved resolution when limited numbers of increments of the second frequency domain are collected.

Comparisons among the choices of long-range experiments now available are unfortunately only beginning to appear; it may be some time until definitive suggestions on which are the most appropriate experiments can be offered. Each of the experiments just briefly described above is, however, considered in somewhat greater detail below. Where long-range ^{1}H−^{15}N applications or any form of comparison between the various experiments exists, these results are noted explicitly.

GHMBC (Gradient Heteronuclear Multiple Bond Correlation). The gradient HMBC (GHMBC) experiment reported by Hurd and John[21] shown in Figure 2 is derived from the earlier nongradient version described in 1986 by Bax and Summers.[17] After a preparation period, which may involve homospoiling gradient pulses or other preparation, the pulse sequence begins with a 90° ^{1}H pulse followed after a short period by a 90° ^{15}N pulse. The first nitrogen pulse, applied after a delay of duration $1/2(^1J_{NH})$ (~5.6 ms for $^1J_{NH}$ = 90 Hz), serves to create heteronuclear multiple quantum coherence for nitrogens with a directly attached proton. By alternating the phase of this pulse in the fashion 0022 while the receiver phase is alternated 0202, the signal for the direct proton−nitrogen correlation is alternately added and subtracted on successive scans and is thereby effectively canceled. The pulse sequence element is known as a low-pass J-filter and was first described by Kogler et

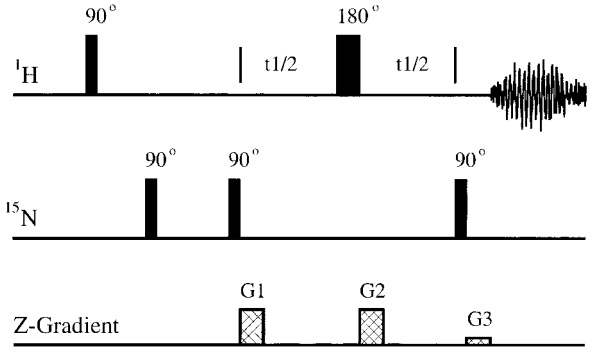

Figure 2. Gradient HMBC (GHMBC) pulse sequence developed by Hurd and John.[21] The low-pass J-filter is based on the one-bond proton−nitrogen coupling which can be assumed to be in the range of 90−95 Hz. Alternatively, the delay can be intentionally misoptimized for ~160 Hz if one wants to allow the one-bond correlation doublets to be seen in the experiment. The long-range delay is typically based on an assumed value for the two- or three-bond long-range proton−nitrogen coupling. This delay has been variously optimized for values ranging from about 1.7 to 16 Hz in two-dimensional ^{1}H−^{15}N long-range heteronuclear shift correlation experiments. Gradient ratios are typically optimized to 5:5:1, with the exact value of the last gradient ideally optimized experimentally. In our laboratory and for our particular instrument, we've found that the gradient ratio of 10:10:2.02 G cm^{-1} is optimal (see text).

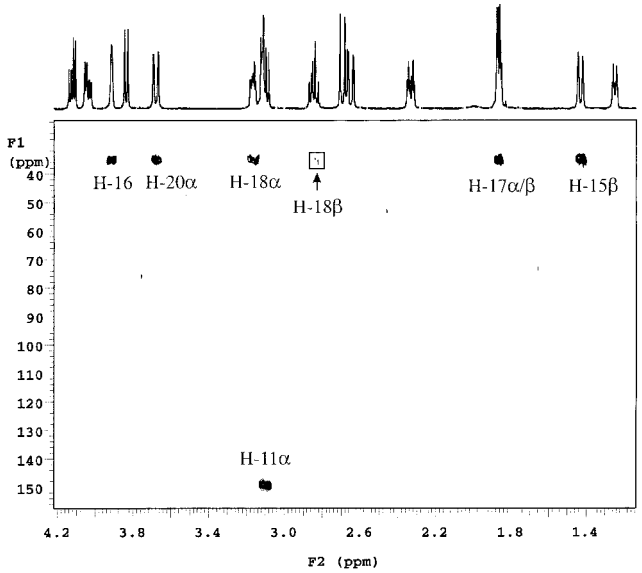

Figure 3. ^{1}H−^{15}N GHMBC spectrum of 1 mg (~3 μmol; 0.11 M) of strychnine (**5a**) at natural abundance in 30 μL of $CDCl_3$. The experiment was optimized for an assumed 10-Hz (50 ms) long-range coupling. The high-resolution proton spectrum is plotted atop the contour plot. Data acquisition parameters are specified in the text. Total acquisition time was 18 h. Correlations from H-8 and H-13 to N-9 were observed in the experiment but are below the threshold level of the contour plot.

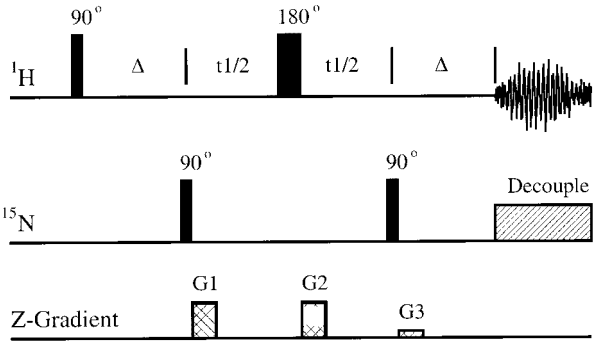

Figure 4. Decoupled gradient heteronuclear multiple bond (D-HMBC) experiment proposed by Furihata and Seto.[40] Gradient ratios are identical to those used in the conventional GHMBC experiment. The duration of the refocusing delay in which the final gradient (gt3) is located is optimized on the assumed size of the long-range coupling.

al.[47] The single low-pass J-filter can also be replaced by a gradient dual-stage low-pass J-filter to remove responses for a range of potential one-bond couplings. [The gradient dual-stage low-pass J-filter, originally developed by Sørensen and colleagues,[48] has been incorporated into the ACCORD-HMBC pulse sequence of Wagner and Berger[44] (see section entitled ACCORD-HMBC).] While it is highly effective for ^{1}H−^{13}C long-range experiments where the one-bond coupling may range from 125 to >210 Hz, it is likely that it will be less beneficial for ^{1}H−^{15}N long-range experiments where there is only a very narrow range of one-bond ^{1}H−^{15}N couplings. The desired long-range correlation information, in contrast, continues to evolve and is converted into the desired heteronuclear multiple quantum coherence (zero and double quantum coherence) only after the completion of the long-range delay, which is proportional to $1/2(^nJ_{NH})$.

The 10-Hz optimized ^{1}H−^{15}N GHMBC spectrum of a 1 mg (3 μmol) sample of strychnine (**5a**) in 30 μL of $CDCl_3$ is shown in Figure 3. Correlations are observed from the protons within two or three bonds of the amide N-9 and aliphatic N-19 resonances, which are observed at 148.0 and 35.0 ppm, respectively. The specific couplings observed and the size of the long-range couplings are discussed in the subsequent section of this review.

GHNMQC. The GHNMQC pulse sequence is a very simple derivative of the GHMBC experiment. It differs simply in that the low-pass J-filter, which is superfluous in most long-range ^{1}H−^{15}N experiments, has been omitted. The pulse sequence is identical to that shown for the GHMBC sequence in Figure 2 except that the very first ^{15}N 90°pulse is omitted from the sequence. The application of the GHNMQC sequence was first reported in a study of the long-range ^{1}H−^{15}N correlations for the HIV reverse transcriptase inhibitor Delavirdine.[49] An application of the GHNMQC sequence was also reported in a study of the effects of *N*-oxidation on the ^{15}N shifts of the oxazolidinone antibiotic Eperezolid and an investigational antipsychotic (PNU-101387).[50] Allowing the direct correlation responses to be observed in ^{1}H−^{15}N long-range correlation experiments obviates the need to acquire a ^{1}H−^{15}N GHSQC or GHMQC experiment to determine the chemical shift of protonated nitrogens in cases where a long-range correlation might not be observed to these nitrogens. As an alternative to reprogramming the GHMBC pulse sequence, authors wishing to allow the direct correlations to be observed can do so by intentionally mis-setting the low-pass J-filter to a value such as 160 Hz. This approach has been used in a number of the long-range ^{1}H−^{15}N studies described below.[30,31,51]

D-HMBC. The decoupled or D-HMBC experiment described by Furihata and Seto[40] seeks to improve sensitivity by decoupling during acquisition. The experiment does not use a low-pass J-filter and employs a refocusing period following the re-creation of proton single quantum coherence analogous to that in the GHMQC experiment. The intent is to bring the antiphase components of proton single quantum magnetization into phase after they are re-created by the final 90° ^{15}N pulse in the sequence. In this way broad-band heteronuclear decoupling can be applied during acquisition as shown in Figure 4.

In the authors' attempts to employ the D-HMBC experiment to improve the sensitivity of ^{1}H−^{15}N long-range experiments the results were rather disappointing. It is

likely that the problems encountered can be attributed to the variability of the long-range $^1H-^{15}N$ couplings. When attempting to utilize the D-HMBC experiment in the assignment of the nitrogen resonances of the peptide antibiotic sulfomycin-I (**65**), the results obtained were actually inferior to data obtained with the conventional GHMBC experiment.[51] In cases where there are one or, at most, a few nitrogens, with relatively uniform couplings, the D-HMBC experiment could doubtless be used with success for long-range $^1H-^{15}N$ experiments. Clearly, additional comparative work will be necessary before a final pronouncement on the benefit or detriment of using this experiment for long-range $^1H-^{15}N$ experiments can be made. It is worth noting, however, that experiments such as ACCORD-HMBC and IMPEACH-MBC (these are discussed later in this review) do successfully apply broadband heteronuclear decoupling during acquisition while simultaneously coping with the variability of long-range couplings.

3D-HMBC. Furihata and Seto[41] have also proposed a 3D-HMBC long-range experiment in an effort to improve performance when a molecule contains a range of long-range couplings. Rather than using a single long-range delay, Furihata and Seto have instead used an incremented delay converting this to a 3D NMR experiment as shown in Supplemental Figure S7. Successive planes in this 3D experiment vary from one another in the delay used to excite the long-range couplings. After processing, the data are presented as an F_2F_3 projection.

To date, no applications of this experiment have been reported for long-range $^1H-^{15}N$ at natural abundance. It is quite probable that this experiment will not be useful for proton−nitrogen experiments because of the substantially lower sensitivity of these experiments relative to their proton−carbon counterparts, which could lead to unacceptably long data acquisition times. This comment is based on the observation that while $^1H-^{13}C$ long-range correlation data can be recorded for a 1.5 μmol sample of cryptospirolepine using a submicro gradient inverse probe in roughly 5−15 min, the acquisition of the corresponding $^1H-^{15}N$ experiment required an overnight acquisition.[30] Having to acquire perhaps 16−32 such spectra to digitize the third frequency domain would obviously be time prohibitive.

GSQMBC. Recognizing the desirability of being able to extract heteronuclear coupling constants from long-range experiments, Marek, Králík, and Sklenář[42] have devised a phase-sensitive single quantum-based long-range experiment to which they have given the acronym GSQMBC. The pulse sequence is shown in Figure 5.

The experiment does not employ a low-pass J-filter, although the authors note that this pulse sequence element can be inserted if necessary. The initial phase of the experiment generates heteronuclear single quantum coherence as in a GHSQC experiment except that the delays in the INEPT step are optimized for the long-range coupling(s) of interest as a function of $1/2(^nJ_{NH})$. The heteronuclear single quantum coherence is allowed to evolve through t_1, after which a pair of phase-encoding gradients are applied flanking the composite 180° pulse. Proton antiphase magnetization, as usual, is created by the final pair of simultaneous 90° pulses applied. The receiver is gated open immediately afterward, and the final decoding gradient, G3, is applied during the acquisition period.

The phase of the decoding gradient, G3, is alternated on successive scans, and the results are stored separately. By combining these data during processing, pure absorption phase data are obtained in both frequency domains, and the heteronuclear coupling is antiphase in a manner analogous to the results obtained when GHMBC data are mixed-mode processed.[26]

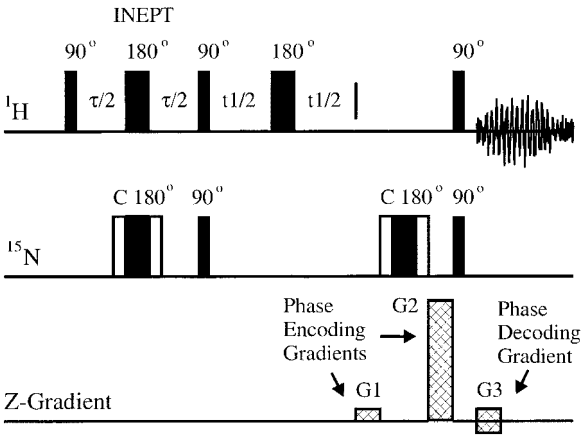

Figure 5. GSQMBC experiment devised by Marek, Králík, and Sklenář.[42] Heteronuclear single quantum coherence is generated by the INEPT step at the beginning of the experiment for which the delays are optimized for the desired long-range coupling constant. Magnetization is labeled with the heteronuclear chemical shift during evolution. Two phase encoding gradients (G1 and G2) are applied flanking the 180° pulse (which follows evolution) in a ratio of 4.8:52.8 G cm^{-1} (for proton−nitrogen experiments). The pair of 90° pulses transfers magnetization back to the protons. The receiver is enabled immediately as in the GHMBC experiment to record the antiphase proton magnetization. The final decoding gradient, G3 (±4.8 G cm^{-1}), is applied coincidentally with the initiation of the acquisition.

Unlike some of the experiments discussed above, the initial application of the GSQMBC experiment did demonstrate the acquisition of long-range $^1H-^{15}N$ data, as well as the measurement of coupling constants from these data. More recently, there have been an extensive number of applications of this experiment by Marek and colleagues that are discussed below.[112,114,124,125]

PS-GHMBC. Another approach to phase-sensitive long-range experiments is found in the PS-GHMBC pulse sequence described by Sheng and van Halbeek.[43] Their experiment is based on the conventional GHMBC experiment as shown in Supplemental Figure S8. The experiment does not utilize a low-pass J-filter during preparation. The authors explicitly note that the direct responses are necessary to establish the phase properties of the multiple bond correlations. Values of the long-range couplings in this experiment are extracted by applying the shift method introduced by Titman and colleagues.[53] Since the extraction of long-range coupling information from this experiment is less straightforward than from examining slices from the GSQMBC experiment of Marek, Králík, and Sklenář,[42] it is likely that PS-GHMBC will see less application to small molecules. It is worth noting, however, that Sheng and van Halbeek have reported being able to extract coupling constants from 30% uniformly enriched glucuronoxylomannan polysaccharides with molecular weights > 50 kDa.

The pulse sequence shown in Supplemental Figure S8 is essentially identical to the GHMBC sequence up to the application of the second 90° X-pulse. To obtain pure-absorption line shapes in the second frequency domain, it is necessary to retain both the $p = 1$ and $p = -1$ coherence pathways. There are several ways in which this task can be accomplished. One method is to perform two experiments, each selecting for one of the coherence transfer pathways followed by recombination of the data during processing.[54] A second approach is that of Hurd, John, and Plant,[55] in which the two coherence pathways are alter-

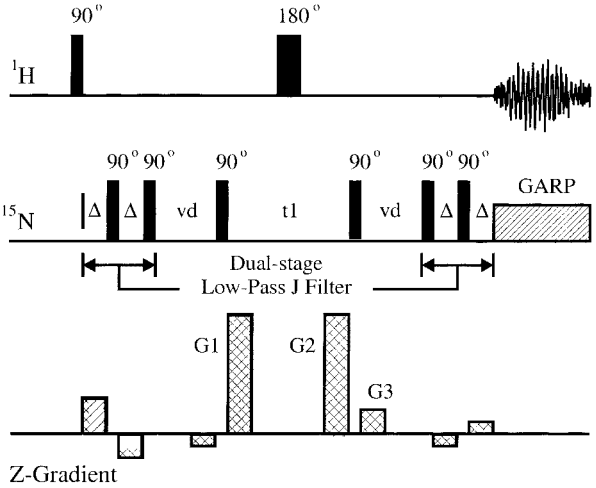

Figure 6. ACCORD-HMBC experiment proposed by Wagner and Berger,[44] providing uniform excitation across a wide range of long-range couplings. Gradient ratios can be optimized identical to those used in the conventional GHMBC experiment. Here, the first three gradients (unlabeled) must total to zero, e.g., 15:−10:−5, as shown. The gradients labeled G1−G3 select the coherence pathway and should be optimized for a 5:5:1 ratio for ^{1}H−^{15}N long-range experiments. The last two gradients must again cancel to zero, e.g., −5:5.

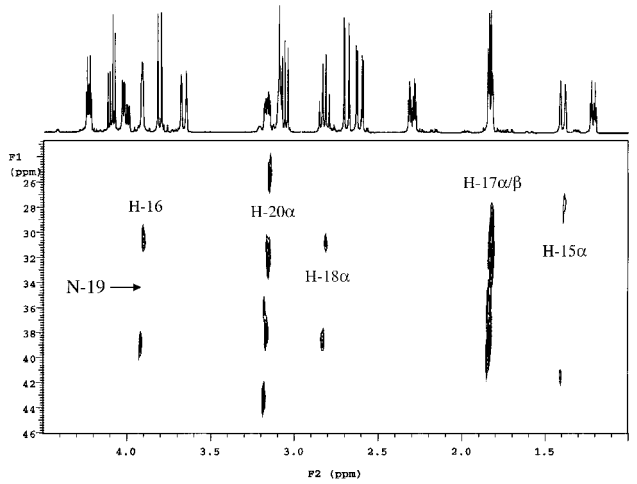

Figure 7. Plot of the correlations to N-19 observed in the ACCORD-HMBC spectrum of strychnine. The experiment was optimized for an accordion range of 2−16 Hz.

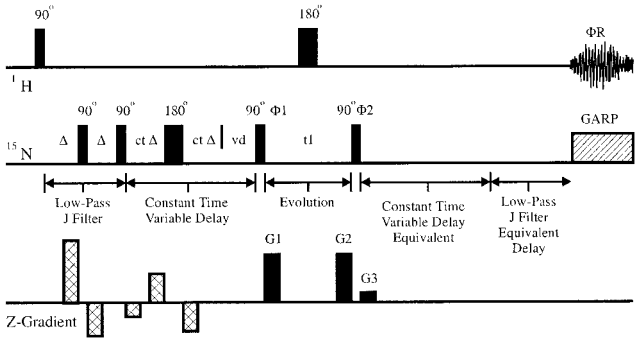

Figure 8. IMPEACH-MBC experiment developed by Hadden, Martin, and Krishnamurthy[46] eliminating the F_1 modulation inherent in the ACCORD-HMBC spectra.[44,60] Gradient ratios for G1−G3 are identical to those used in the conventional GHMBC experiment (5:5:1 for ^{1}H−^{15}N). Gradient ratios in the gradient dual-stage low-pass J-filter[48] must total to zero, e.g., 15:−10:−5 and 10:−10, as shown.

nately rephased and sampled during acquisition. A third approach, which avoids the application of gradients during evolution,[56−58] was employed by Sheng and van Halbeek.[43] The gradients are instead interspersed through the series of pulses applied to the X-nucleus after the reconversion of heteronuclear multiple quantum coherence to proton single quantum coherence prior to acquisition.

To date, there have been no applications of this experiment for long-range ^{1}H−^{15}N heteronuclear shift correlation at natural abundance. Given the complexity of extracting the long-range coupling constant information from the data, it is probable that this experiment will not see application for the purposes described in this review.

ACCORD-HMBC. A very novel and potentially useful approach to the problem of the variability of long-range coupling pathways in long-range ^{1}H−^{15}N heteronuclear correlation spectra has recently been proposed by Wagner and Berger.[44] The pulse sequence for this experiment is shown in Figure 6. Unlike the 3D-HMBC experiment of Furihata and Seto[41] (described above), in which a separate 2D experiment is performed for each increment of the long-range delay, Wagner and Berger instead use a systematically decremented variable delay (vd) flanking both the beginning and the end of the evolution period, using the accordion principle of Bodenhausen and Ernst.[59] The variable delays were decremented rather than incremented, and the pulse sequence was constructed in a symmetric fashion, keeping the proton 180° pulse exactly at the middle of the sequence to avoid phase distortions and frequency offsets in F_1 to a minimum. Gradients are applied for ^{1}H−^{15}N in the following ratio: 15:−10:−5:50:50:10:−5:5. A gradient two-stage low-pass J-filter[48] is applied at the beginning of preparation and following reconversion to proton single quantum coherence.

Because of the way in which the pulse sequence is constructed, i.e., using decremented variable delays, the smaller coupling constants are sampled near the beginning of the evolution, while the larger coupling pathways are sampled toward the end of the incrementation of the evolution period.

A drawback of the ACCORD-HMBC implementation of the accordion principle to sample a wide range of potential long-range heteronuclear couplings is the introduction of ^{1}H−^{1}H homonuclear frequency modulation during the variable delay. The variable delay serves as a pseudo-evolution time for homonuclear coupling processes, which are manifest in the ACCORD-HMBC spectra as an F_1 frequency modulation or "skew" of the long-range correlation responses.[44] Factors controlling F_1 modulation in ACCORD-HMBC spectra have been extensively studied in the recent work of Martin et al.[60]

The characteristic F_1 skew of long-range responses in ACCORD-HMBC spectra is shown in the ^{1}H−^{15}N spectrum of strychnine presented in Figure 7 (only correlations to the aliphatic N-19 resonances are shown). Response character is reminiscent of homonuclear 2D J-resolved spectra. The experiment was acquired with a 2−16 Hz optimization to examine the full range of ^{1}H−^{15}N couplings reported for strychnine.[26] [An expansion of the H-17α/β long-range correlations to N-19 is presented in Figure 10 (in a comparison of the same response in both the ACCORD-HMBC and IMPEACH-MBC experiments) to show the nature of the F_1 skew in more detail.] Because of the inherently low sensitivity of long-range ^{1}H−^{15}N experiments at natural abundance and the relatively broad range of ^{15}N shifts, most such experiments will be digitized rather coarsely in the second frequency domain. Indeed, we generally opt to digitize long-range ^{1}H−^{15}N experiments performed on molecules with spectral widths comparable to the 20−160 ppm F_1 window used in Figure 7 with 32 to

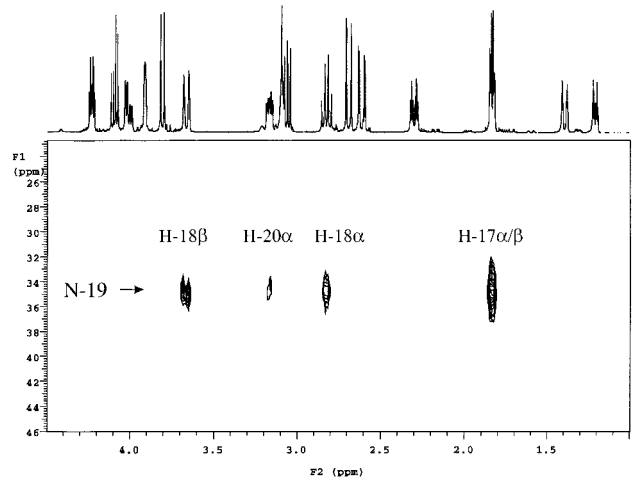

Figure 9. Plot of the correlations to N-19 observed in the IMPEACH-MBC spectrum of strychnine (**5a**).[138] The experiment was optimized for an accordion range of 2−16 Hz.

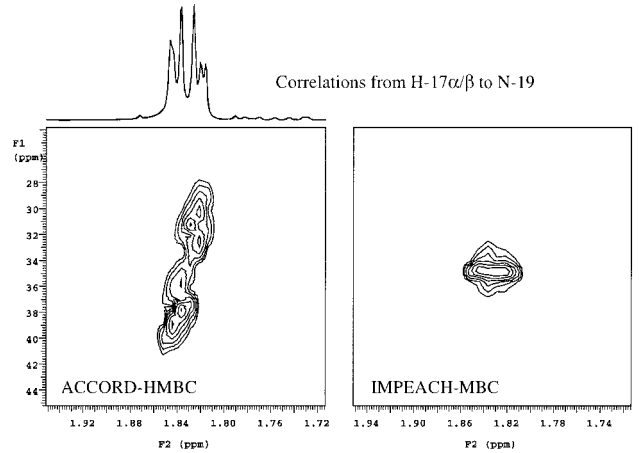

Figure 10. Comparison plot of the ACCORD-HMBC and IMPEACH-MBC correlations observed for H-17α/β to N-19, exhibiting the excessive F_1 skew inherent in the ACCORD-HMBC experiment and the resulting collapse of the proton−proton modulation in the IMPEACH-MBC experiment.

64 increments of the evolution time, followed by linear prediction to from 128 to 256 files in F_1 prior to Fourier transform. This level of F_1 digitization will lead to considerable F_1 modulation or "skew" (as is more evident by the data in Figures 7 and 10).[138]

Modulation in ACCORD-HMBC spectra is controlled by the scaling factor, N, which is defined by the expression

$$N = (2\tau/\Delta F_1) + 1$$

where the term ΔF_1 is the dwell time in the second frequency domain (1/sw1) and where the term τ is defined by

$$\tau = (\tau_{max} - \tau_{min})/\mathrm{ni}$$

where τ_{max} and τ_{min} are the optimization range of the experiment and ni is the number of increments used to digitize the second frequency domain. Simply, as broader excitation ranges are chosen, holding ni constant, the skew of long-range responses in F_1 correspondingly increases. Conversely, for a given excitation range, as the number of increments used to digitize the second frequency domain increases, the skew of long-range responses in F_1 diminishes.[60]

In ACCORD-HMBC long-range $^1H-^{13}C$ experiments, F_1 modulation can lead to severe overlap in congested regions of the spectrum, rendering the data uninterpretable. In contrast, for $^1H-^{15}N$ experiments, because of the much lower density of ^{15}N resonances, response overlap, despite relatively coarse digitization in F_1, is unlikely to be a significant problem for most compounds. Exceptions might include some of the peptide natural products such as quinomycin-A, crambin-A and -B, and sulfomycin-I (see section entitled Peptides and Cyclic Peptides).

One other attribute of F_1 modulation of long-range responses in ACCORD-HMBC spectra should also be noted explicitly. While overlap due to long-range response modulation in F_1 is obviously detrimental, F_1 modulation also provides a useful determinant of the authenticity of weak long-range responses in noisy spectra. While legitimate $^1H-^{15}N$ long-range responses will be skewed in F_1 (see Figures 7 and 10), spurious peaks cannot exhibit F_1 modulation. Hence, the authenticity of weak responses can be readily verified in ACCORD-HMBC spectra by the characteristic skew that they exhibit in F_1.[60] Given the inherent difficulty of acquiring long-range $^1H-^{15}N$ spectra of dilute samples, this attribute of the ACCORD-HMBC experiment may prove to be particularly useful in time.

Constant Time HMBC Experiments (CT-HMBC-1 and CT-HMBC-2). Furihata and Seto[45] in late 1998 reported a pair of constant time long-range heteronuclear shift correlation experiments, CT-HMBC-1 and CT-HMBC-2, which are shown in Supplemental Figures S9 and S10, respectively. The constant time elements flank the evolution period, t_1, by a pair of compensating decremented delays of the form

$$\Delta_3 - t_1/2$$

We have chosen to refer to these as compensating decremented delays in that they compensate for the normal incrementation of the evolution time, t_1, keeping the overall duration of evolution constant.

Proton−proton J-modulation normally present during evolution (t_1) is suppressed during the now constant evolution time of the experiment, thereby eliminating broadening of long-range correlation responses due to homonuclear scalar coupling in F_1. Long-range heteronuclear couplings are modulated both during the normal long-range delay, Δ_2, and during the variable delay, $\Delta_3 - t_1/2$, which precedes the creation and evolution of multiple quantum coherence with the second 90° X-pulse. The varied duration of the interval from the first 90° X-pulse to the second gives some measure of sampling for a broader range of potential long-range couplings. The range of long-range couplings that can be sampled in this fashion, however, is limited and is a function of $t_{1max}/2$, where t_{1max} is the maximum duration of the evolution time, which will typically only be in the range of about 5 to 20 ms.

The overall range of potential long-range couplings that can be sampled is from $[(\Delta_3 - t_1/2) + \Delta_2]$ to Δ_2. In contrast, the sampling possibilities opened through the use of the accordion principle are many times broader.

The second constant time long-range experiment proposed by Furihata and Seto,[45] CT-HMBC-2, is shown in Supplemental Figure 10. This experiment differs by the incorporation of the pulse sequence element

$$(\Delta_3 - t_1/2) - 180°_x\ ^1H - (\Delta_3 - t_1/2)$$

Again, the variable delay is decremented in concert with the incrementation of the delays in the evolution period,

keeping the overall duration of the experiment constant. The incorporation of a 180°$_x$ ^{1}H pulse in the center of Δ_3 suppresses ^{1}H−^{1}H *J*-modulation and ^{1}H−^{13}C couplings, thereby affording improved resolution in the experiment. Once again, the variable nature of Δ_3 allows the sampling of a modest range of potential long-range couplings.

Broad-band heteronuclear decoupling during acquisition is not an option in either of the constant time experiments proposed by Furihata and Seto,[45] although the authors do comment in a footnote to the paper that a modified sequence that allows broad-band heteronuclear decoupling during acquisition is under development. The application of the CT-HMBC experiments to long-range ^{1}H−^{15}N heteronuclear correlation experiments at natural abundance has not been demonstrated as of the time this review was written.

IMPEACH-MBC (Improved Performance Accordion Heteronuclear Multiple Bond Correlation Spectroscopy). The IMPEACH-MBC experiment is one of the newest long-range heteronuclear shift correlation pulse sequences to be reported.[46] The pulse sequence is shown in Figure 8 and is related to the ACCORD-HMBC experiment (see section ACCORD-HMBC and Figure 6). The variable delay of the ACCORD-HMBC sequence is replaced in the IMPEACH-MBC experiment by a new pulse sequence element known as a constant time variable delay, which is represented by

$$(D/2 - 180°\ ^{15}\mathrm{N} - D/2) - \mathrm{vd}$$

The portion of the constant time variable delay represented by vd is a decremented interval that functions in a manner analogous to the corresponding interval in the ACCORD-HMBC experiment. However, rather than the duration of the overall delay becoming progressively shorter with successive increments of the evolution time, t_1, the delay *D* (in two equal segments, *D*/2) is instead incremented by the time interval by which vd was decremented. In this fashion, the overall duration of the interval remains constant. This has the beneficial effect of suppressing ^{1}H−^{1}H homonuclear frequency modulation, which leads to the F_1 modulation or "skew" characteristic of the ACCORD-HMBC experiment.[44,60] The long-range heteronuclear couplings of interest are refocused at time *D* by the 180° ^{15}N pulse. In this fashion, long-range heteronuclear components of magnetization are refocused for a portion of the constant time variable delay (*D*) and evolve during the "variable" portion of the constant time variable delay, vd, which is successively decremented in concert with the incrementation of the evolution time, t_1. In this fashion, the range of potential long-range couplings selected is sampled with the benefit of the unwanted ^{1}H−^{1}H frequency modulation in F_1 being suppressed.

The N-19 correlations in the 2−16 Hz ^{1}H−^{15}N IMPEACH-MBC spectrum of strychnine are shown in Figure 9. Expansions of H-17a/b−N-19 long-range correlation multiplets from the ACCORD-HMBC and IMPEACH-MBC spectra are compared in Figure 10.

2D/Selective 1D Approaches to Low-Level ^{1}H−^{15}N Heteronuclear Shift Correlation at Natural Abundance. Sample limitations impose some rather significant restrictions on the acquisition of long-range ^{1}H−^{15}N heteronuclear shift correlation data. Submicro NMR probe technology reduces sample requirements to the range of perhaps 3−5 μmol for an overnight acquisition.[62] At still lower levels, e.g., 1 μmol or less, selective 1D experiments become a necessary undertaking if data are to be accumulated in reasonable periods of time.[61]

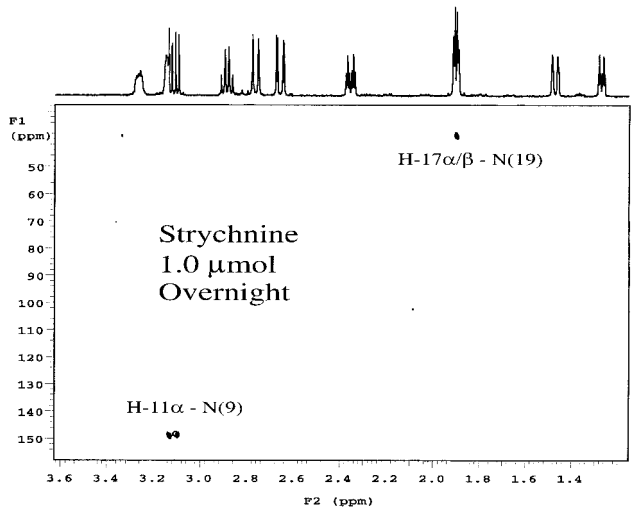

Figure 11. Overnight spectrum of 1 μmol of strychnine dissolved in 30 μL of deuteriochloroform.[61] The spectrum exhibited two responses that correlated H-17α/β to N-19 and also H-11α to N-9. From these 2D data affording the chemical shifts of the nitrogens, selective 1D ^{1}H−^{15}N long-range GHMBC experiments were acquired in excessively less acquisition time than would be possible for the acquisition of the traditional 2D experiment. (Copyright John Wiley & Sons, Limited. Reproduced with permission.)

An essential element of performing selective 1D long-range ^{1}H−^{15}N experiments is the ability to define the ^{15}N chemical shift of the resonance of interest. In some cases, it is possible to define the ^{15}N chemical shift from a coarsely digitized overnight 2D experiment. Once the shift of the resonance of interest is defined, albeit with minimal accuracy, it is possible to set up a selective long-range experiment in which the selectivity of the ^{15}N pulses is a function of the accuracy, or lack thereof, of the coarsely digitized 2D experiment used to define the shift.

To illustrate this approach, we recently demonstrated the acquisition of a 1 μmol 2D ^{1}H−^{15}N GHMBC spectrum of strychnine (**5a**) overnight.[61] As shown in Figure 11, only two resonances are observed in the spectrum (compare to the results shown in Figure 3 for a 1 mg, 3 μmol sample of strychnine) corresponding to correlations from the H-11α proton to N-9 and from the H-17α/β protons to N-19. The 2D data were acquired using only 24 files to digitize the second frequency domain, which were linear predicted to 96 files during processing. Chemical shifts were ∼35 and ∼148 ppm for the N-19 and N-9 resonances, respectively, which is in reasonable agreement with more accurately measured spectra.[26] A selective experiment was then set up calibrating the ^{15}N pulse to give an effective excitation of ca. ±5 ppm. The selective 1D result of an overnight acquisition on N-19 of a 1 μmol sample of strychnine is shown in Figure 12 (trace B). Data are plotted in combination with a proton reference spectrum (Figure 12, trace A) and the corresponding slice from a weekend 2D acquisition on the same 1 μmol sample of strychnine (Figure 12, trace C). The improvement in the quality of the responses in the selective 1D experiment acquired overnight is obvious. The lowest level to which this technology has thus far been pushed is the 0.5 μmol spectrum of N-19 shown in Figure 13 acquired using a selective 1D long-range experiment over a weekend.

Measuring ^{1}H−^{15}N Long-Range Couplings. To date, the majority of studies that have appeared have not reported the measurement of the long-range ^{1}H−^{15}N couplings. This is not an oversight on the part of any of the authors, but rather a function of the nature of the

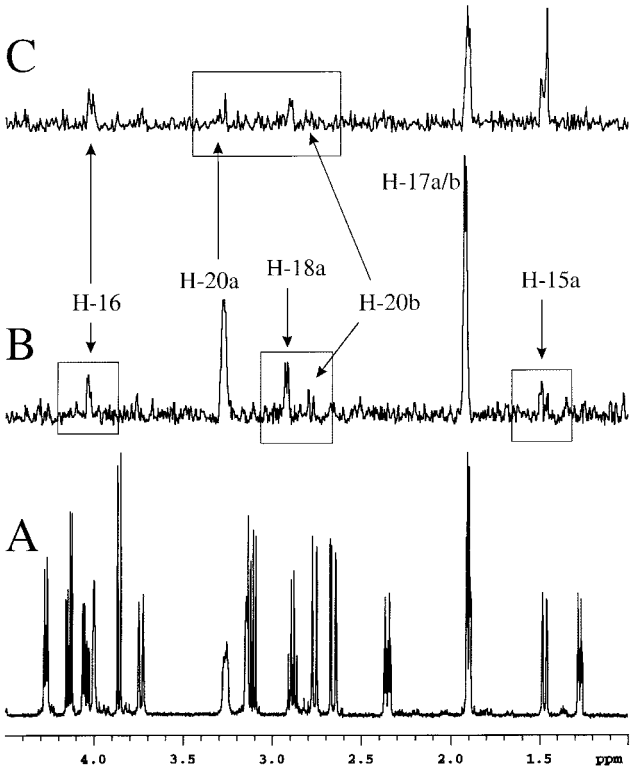

Figure 12. Slices showing a comparison of 2D and selective 1D long-range $^1H-^{15}N$ chemical shift correlation data acquired for a 1.0 μmol sample of strychnine dissolved in 30 μL of $CDCl_3$.[61] The slice taken at the ^{15}N chemical shift of the N-19 aliphatic nitrogen resonance is shown in trace C; data were acquired in 84 h over a weekend.[62] Selective 1D $^1H-^{15}N$ GHMBC spectrum of the N-19 resonance of strychnine (trace B); data were acquired overnight. The proton reference spectrum of the aliphatic region of strychnine (**5a**) is shown in trace A. All data were acquired at 600 MHz using a Varian INOVA three-channel instrument equipped with a Nalorac SMIDG-600-1.7 submicro inverse-detection gradient NMR probe. (Copyright John Wiley & Sons, Limited. Reproduced with permission.)

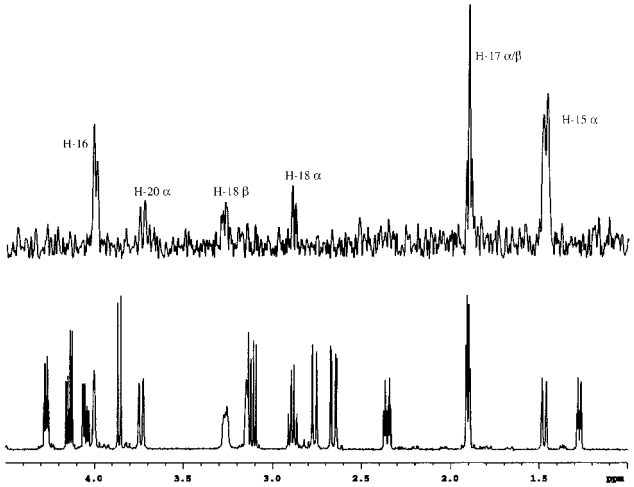

Figure 13. Selective 1D $^1H-^{15}N$ GHMBC spectrum of the N-19 resonance of strychnine (top trace) plotted above a ^1H reference spectrum.[61] Both experiments were performed at natural abundance using a 0.5 μmol sample dissolved in 30 μL of $CDCl_3$. All data were acquired using a Varian INOVA 600 spectrometer operating at a proton frequency of 599.75 MHz and equipped with a Nalorac Z·SPEC SMIDG-600-1.7 submicro probe. The selective GHMBC was optimized for an assumed 8 Hz (63 ms) long-range coupling. (Used with permission, John Wiley & Sons, Ltd.)

GHMBC data that have been most frequently acquired in long-range $^1H-^{15}N$ heteronuclear shift correlation experiments. There are, however, several approaches that allow long-range $^1H-^{15}N$ coupling constants to be determined. These will be treated briefly in the following paragraphs.

In most instances, GHMBC data are not acquired as phase-sensitive data in the second frequency domain. The data are instead intended to be presented in a magnitude-calculated format. GHMBC data can be recorded, however, with modified data storage that allows for mixed-mode processing. Although there is a phase shift across the second frequency domain that precludes the entire data matrix being presented in a phased manner, individual slices at the chemical shifts of a given nitrogen can be extracted from the data matrix and correctly phased to allow the measurement of the $^1H-^{15}N$ heteronuclear coupling. Since HMBC/GHMBC data acquisition begins immediately after the final proton pulse of the sequence (see below), the magnetization component for the long-range $^1H-^{15}N$ coupling is antiphase, while the proton−proton homonuclear coupling is in-phase. By plotting the data so that the proton−proton coupling is correctly phased, the antiphase components of the multiplet correspond to the long-range proton−nitrogen coupling and can be easily extracted. We have utilized this approach on several occasions.[25,26] If proton−nitrogen couplings are to be measured, however, it is advisable to acquire the data using 4K points in the proton frequency domain ($t_2 \rightarrow F_2$) and to zero-fill the data set to 8 or 16K points in F_2 to be certain that there is sufficient digital resolution available to permit the accurate determination of the proton−nitrogen long-range coupling.

A second approach that allows the extraction of long-range proton−nitrogen couplings is to optimize the delays in the GHSQC pulse sequence for the long-range coupling. Since GHSQC data are phase-sensitive, the data can be processed and the couplings measured in a fashion analogous to that described for mixed-mode processed GHMBC data above. The GHSQC pulse sequence is, however, longer and uses considerably more pulses than the GHMBC experiment in the manipulation of magnetization prior to detection. For this reason, it is possible that there will be some reduction in the intensity of the long-range responses, and, consequently, it might be prudent to reserve this approach for relatively strong samples. Despite potential shortcomings to this method of determining proton−nitrogen long-range couplings, it has been used successfully on several occasions.

The GSQMBC experiment of Marek, Králík, and Sklenář[42] explicitly offers phase-sensitive single quantum-based data from an experiment designed for the observation of long-range correlations. The experiment has been used with success for a variety of heteronuclides, which includes ^{15}N, although the long-range couplings have not always been reported in studies that have used this pulse sequence.

Finally, there is also the PS-GHMBC experiment proposed by Sheng and van Hallbeek.[43] The extraction of heteronuclear long-range coupling information from this experiment is considerably more cumbersome than the examination of a slice from the data matrix and the measurement of the antiphase limbs of a multiplet. Instead, it is necessary to use the shift method of Titman et al.[53] Because of the complexity of this method of extracting the coupling constants, coupled with what we feel to be a low likelihood that this experiment will be used for natural abundance long-range $^1H-^{15}N$ measurements of small molecules, we will not delve into the actual measurement of coupling constants from these data here. The interested reader is instead referred to the references cited above.

Probe Selection. The selection of probes available to an investigator will obviously vary from one NMR facility to the next. At present, there are two different commercially available probe formats capable of acquiring long-range $^1H-^{15}N$ data at natural abundance. The majority would be considered as "conventional" probes of varying diameter. Practically, for long-range $^1H-^{15}N$ experiments at natural abundance these would include 5-, 3-, or 2.5-, and 1.7-mm formats. Although 8- and 10-mm probes capable of performing these experiments are available, they are more amenable to studies involving labeled proteins. The second type of probe is the magic-angle gradient inverse gXH Nano-probe that has recently been developed by Varian NMR Instruments. Applications utilizing this type of probe hardware have not been reported for long-range $^1H-^{15}N$ at natural abundance to date. Finally, although not amenable to long-range $^1H-^{15}N$ experiments at natural abundance at this time, there are also a group of μ-coil NMR probes being developed that may offer the possibility of performing experiments with still smaller sample volumes than is currently possible with the 1.7-mm submicro NMR probe. The μ-coil probes, however, do not presently provide pulsed field gradient capabilities, and until this feature is added, they will not be amenable to the acquisition of long-range $^1H-^{15}N$ heteronuclear shift correlation data at natural abundance. These varied probe formats are described briefly in subsequent sections of this review. In addition, investigators using 5-, 3-, and 1.7-mm probes also have available to them specialized Shigemi NMR tubes (see section entitled Specialized NMR Sample Cells) intended for investigations with restricted sample volumes that offer an alternative to those unable to resort to a smaller probe format.

Conventional NMR Probes. Everyone will almost invariably have access to conventional 5-mm inverse-detection gradient NMR probes. Ideally, one would like to use this type of probe in the highest field spectrometer reasonably available and with the minimum possible sample volume to keep concentrations of the material being studied as high as possible in the coils of the probe. For conventional 5-mm NMR probes, sample volumes typically range from about 500 to 650 μL. Nominally, 5-mm probes have rf coils for which the average contained sample volume is about 220 μL. Thus, approximately a third of the 500−650 μL total sample volume is within the confines of the coil and available for experimental sampling.

For bulk samples of readily available alkaloids such as strychnine, **5a**, the sample volumes associated with 5-mm probes are not a limiting factor by any means. Indeed, in the first published long-range studies from 1995, both reported data recorded using instruments equipped with 5-mm probes.[26,63] Sample sizes for these studies were 40 and 20 mg, respectively, which would be prohibitive for compounds available in limited quantity.

The need to acquire data on smaller samples was a driving factor in the development of a variety of 3-mm NMR probes first reported in 1992.[64,65] The 3-mm, or micro, NMR probes utilize a total sample volume of 120 to 150 μL, roughly one-fourth that of the conventional 5-mm sample. Using 1 μmol of the small alkaloid norharmane dissolved in 130 and 500 μL for the 3- and 5-mm tubes, respectively, it was possible to acquire data with identical signal-to-noise (S/N) ratio in one-fourth the time with the 3-mm micro probe vs the conventional 5-mm probe.[65]

Further reductions in probe size have recently been reported by the authors for the characterization of extremely small samples. Results obtained for a 1.7-mm submicro inverse-detection gradient, or SMIDG, NMR probe have recently been described.[30,61,62] The probe utilizes a total sample volume of 25−30 μL, of which 19.2 μL is in the coil for the most recent design. For relatively concentrated samples (>1 μmol), the authors have shown that it is possible to acquire $^1H-^{13}C$ direct heteronuclear shift correlation data in as little as 34 s for a 1.5 μmol sample of cryptospirolepine (**3**).[30] Using the same sample, direct $^1H-^{15}N$ correlation spectra with excellent S/N were recorded in less than 1 h (S/N > 15:1). Long-range data for three of the four nitrogen resonances of **3** were obtained overnight using this sample in a 4-Hz optimized GHMBC experiment. The remaining amide nitrogen was observable only via a $^4J_{NH}$ correlation in a 2.5-Hz optimized GHMBC spectrum acquired in 120 h.[31] With ~0.5 μmol, $^1H-^{13}C$ direct and long-range correlation data were acquired in 12 min and 1.1 h, respectively.[66] At what represents the current limit of detection for $^1H-^{13}C$ heteronuclear shift correlation experiments, it was possible to record direct and long-range correlation spectra in 25.5 and 56.5 h, respectively, on 0.04 μmol of a cryptolepinone impurity (8%) contained in a 0.55 μmol sample of cryptolepine.[67] Exploiting the high sensitivity of the SMIDG probe for $^1H-^{15}N$ correlation experiments, the authors have also demonstrated that it is possible to acquire long-range data at natural abundance for a 1 μmol sample of strychnine (**5a**) over a weekend (see section entitled Strychnine).[62] Using a selective 1D approach, it is possible to acquire higher quality long-range $^1H-^{15}N$ correlation data on a 1 μmol sample overnight rather than over a weekend, assuming that the ^{15}N chemical shifts of the nitrogen(s) of interest can be determined or are known.[61] Pushing this approach to the extreme limit of detection, data have also been recorded for a 0.5 μmol sample in 84 h. It is likely that this size of sample represents the current limit of detection with the available probe technology. The development of cold metal or superconducting coil NMR probes may, however, reduce the limits of detection farther in the future.

Comparison of 5-mm and 3-mm NMR Probes. The performance of 5-mm conventional and 3-mm micro inverse NMR probes was compared in early 1992. As would be expected given the working sample volumes, the 3-mm probe was a factor of 4 more efficient in time for the acquisition of data to a given signal-to-noise (S/N) ratio.[65] In addition, it was also found that the 3-mm micro inverse probe was capable of acquiring data with smaller samples than was reasonable using a 5-mm probe. While the former gave a linear response to ~0.1 μmol, the 5-mm probe began to exhibit nonlinear performance below ~0.5 μmol of sample. For purposes of this review, linear performance is defined as requiring 4 times the number of transients to afford an identical S/N ratio when the amount of analyte is halved.

Comparison of 3-mm and 1.7-mm NMR Probes. The performance characteristics of 3-mm micro and 1.7-mm SMIDG NMR probes have also recently been compared.[68] Comparisons of $^1H-^{13}C$ GHSQC performance were reported for 1.0 μmol samples of strychnine (**5a**) and 0.5 μmol samples of ibuprofen. Crossover data were also reported for the 1.7-mm sample run in the 3-mm probe. For the former study, S/N ratios were 112:1 and 49:1 for the 1.7- and 3-mm probes, respectively. The S/N ratio for the 1.7-mm tube run in the 3-mm probe was 75:1. However, when sample columns are taken into account, the performance of the 3-mm probe with either 1.7- or 3-mm samples was

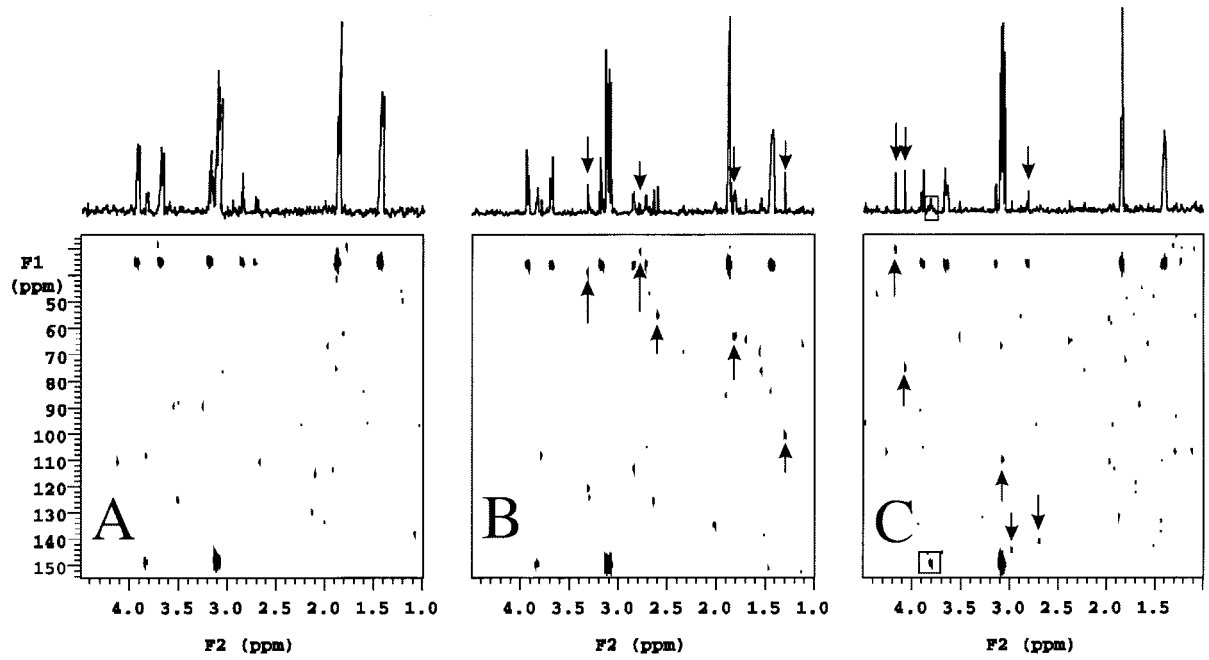

Figure 14. Comparative long-range $^1H-^{15}N$ GHMBC spectra of a 3.0 μmol sample of strychnine (**5a**) dissolved in 30 or 150 μL of $CDCl_3$.[68] Data were acquired using a Varian INOVA 600 NMR spectrometer equipped (panel A) with a Nalorac SMIDG-600-1.7 submicro inverse-detection gradient or (panels B and C) with a Nalorac MIDTG-600-3 micro gradient inverse triple resonance probe. All spectra were acquired in 18 h by accumulating 1024 transients at each of 40 increments of the evolution time. Data were linear predicted in the second frequency domain to 160 points followed by zero-filling to afford the final 2048 × 512 point files plotted in the individual panels. Data shown in panel A were acquired using a 3.0 μmol sample of strychnine (**5a**) dissolved in 30 μL of $CDCl_3$ using the Nalorac SMIDG-600-1.7 probe. The S/N ratio for the projection (taking the region from 4.5 to 5.5 ppm as representative noise) in panel A is 60:1. Panel B shows the contour plot from an identical experiment performed with the 1.7-mm sample inserted into the Nalorac MIDTG-600-3 NMR probe. The S/N ratio in this experiment was 41:1. There are, however, spurious peaks in the spectrum denoted by arrows that have intensities comparable to the weaker long-range correlations to the two nitrogen resonances. Panel C shows the data obtained using the 3.0 μmol sample of strychnine (**5a**) dissolved in 150 μL of $CDCl_3$; data were acquired using the Nalorac MIDTG-600-3 NMR probe. The S/N in this experiment was 26:1. Spurious peaks contained in the spectrum are now more intense than legitimate responses. Differences in the S/N ratios of the 1.7/3 and 3/3 mm tube/probe combinations are due to differences in the column height ratios in the tubes. In practical terms, the 3.0 μmol sample represents about the practical limit for the acquisition of 2D $^1H-^{15}N$ long-range correlation data overnight using submicro NMR probe technology. When dealing with an unknown at this level, it might be preferable to acquire data over a weekend. In the case of 3 mm micro NMR probe technology, it would clearly be necessary to acquire data on a μmole sample over a weekend.

essentially identical. These data do suggest, however, that slightly better performance can be obtained with the 3-mm probe by using shorter columns than those employed in this comparison study. (Sample volumes were 30 and 150 μL for the 1.7- and 3-mm probes, respectively.) For the 0.5 μmol ibuprofen samples, the S/N ratios are skewed somewhat higher because of the intensity of the *sec*-butyl methyl doublet in the spectrum. S/N ratios were 148:1 for the 1.7-mm sample, 75:1 for the 1.7-mm sample run in the 3-mm micro probe, and 62:1 for the 3-mm sample.

Perhaps more germane to the topic of this review, performances of the 3- and 1.7-mm probe formats for the acquisition of $^1H-^{15}N$ GHMBC spectra were also compared. Data were acquired using a 3 μmol sample of strychnine dissolved in either 30 or 150 μL of $CDCl_3$ and then sealed. The results of the three experiments performed are presented in Figure 14. The 1.7-mm sample gave a S/N ratio of 60:1 for an 18 h experiment (Figure 14A). All of the expected long-range responses were observed in the spectrum. In contrast, the 1.7-mm sample run in the 3-mm probe gave a spectrum with a 41:1 S/N ratio in which there were some spurious noise spikes that approached the intensity of some of the legitimate long-range correlations (Figure 14B). Again, all of the expected long-range correlations were observed in the spectrum. In contrast, for the 3-mm sample, the S/N ratio was down to 26:1, and not all of the expected responses were observed in the spectrum (Figure 14C). Furthermore, some of the spurious noise spikes were more intense than legitimate long-range correlations, which could be problematic in the case of unfortuitously located noise spikes. Projections of the three spectra shown in Figure 14 are presented in Figure 15. In the opinion of the authors, the 3 μmol sample run in a 3-mm probe gave unacceptable 18 h results, and it would be prudent to acquire data longer, perhaps over a weekend with a sample of this size in a 3-mm NMR probe.

Gradient Inverse or gXH Nano-probes. Nano-probes represent a departure from what would be considered a "normal" NMR probe. Nano-probes use a 40-μL NMR cell that is closed with a Teflon plug. The cell is fitted with a collar that rides in an air bearing in the probe of the type used for magic angle solid NMR probes. Indeed, the nano-probes are magic angle probes, and the sample is spun at a rate from 1 to 2 kHz when data are being acquired.

The gradient inverse nano-probe represents a new design announced in conjunction with the 39th Experimental NMR Conference held at Asilomar, CA, in the spring of 1998. Experiments such as GHSQC and GHMBC can be performed by syncing the application of the gradient pulse with the spin rate of the rotor.[69] The acquisition of direct and long-range $^1H-^{13}C$ heteronuclear shift correlation data has been demonstrated with this probe, although there are, as yet, no published data. For samples in the micromole range, acquisition times for $^1H-^{13}C$ data are generally comparable to those reported for the SMIDG NMR probe described in the section immediately preceding. A version of the probe that offers a tunable X-coil has also been announced, which would make the probe amenable to the acquisition of long-range $^1H-^{15}N$ heteronuclear shift cor-

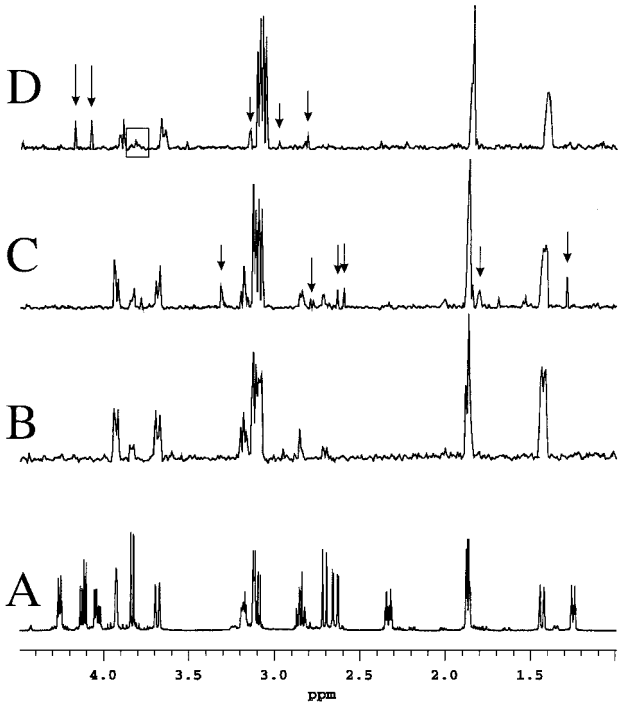

Figure 15. Comparative long-range $^1H-^{15}N$ GHMBC spectra of a 3.0 μmol sample of strychnine (**5a**) dissolved in 30 or 150 μL of $CDCl_3$.[68] The ^1H reference spectrum is shown in trace A. Trace B: Projection from the 1.7/1.7 mm tube/probe pairing shown in panel A in Figure 24. The S/N ratio in the projection (the region from 4.5 to 5.5 ppm was uniformly taken as representative noise) was 60:1. There are no spurious peaks observed in the trace. Trace C: Projection of the 1.7/3 mm tube/probe pairing. The S/N ratio was 41:1. Spurious peaks in the projection are denoted by arrows. Trace D: Projection of the 3/3 mm tube/probe pairing. The S/N ratio for the projection was 26:1. There are a number of spurious peaks designated by arrows. The boxed region of the projected spectrum contains a legitimate long-range correlation which is much weaker than the spurious responses. Two of the long-range correlations, those at ~2.85 and 2.71 ppm, are absent from the projected spectrum shown in trace D as well as from the contour plot shown in Figure 14C. (Copyright John Wiley & Sons, Limited. Reproduced with permission.)

relation data, although, again, these data have yet to be reported at the time that this review was written.

***μ*-Coil NMR Probes.** A series of papers have been published describing modifications and results obtained using a type of flow NMR probe that has been labeled as a μ-coil NMR probe following the initial 1995 publication of Olson et al.[70] Unlike conventional NMR probes, the coil is wound directly on a fused silica capillary, giving a coil volume in the range from 1 nL to 1 μL, depending on the diameter of the capillary.[71−74] Subramanian and Webb[73] have extended this probe design from ^1H only to ^{13}C observe and $^1H-^{13}C$ inverse designs. Unfortunately, only calculated limits of detection based on ^{13}C-labeled alanine and neat ethanol were specified for the direct observe and inverse probe designs, respectively, in the initial report. In the case of the latter, suppression of unwanted $^1H-^{12}C$ resonances was incomplete even when a 128-step phase cycle was employed with the initial probe design. A further drawback to the μ-coil NMR probe design is the fact that it is necessary to immerse the probe in a fluorocarbon bath in an effort to approximate the magnetic susceptibility of the coil. Although this may improve line shape somewhat, it is not without disadvantage in that it is necessary to acquire difference spectra to eliminate unwanted signals arising from incomplete fluorination of the fluorocarbon bath.[71] Finally, the percentage of the sample actually within the confines of the coil for analysis is also relatively low, ranging from about 2.5 to 15%, as opposed to 48 to 72% in the case of the 1.7-mm submicro NMR probe.

Overall, the μ-coil NMR probe design is interesting and may find application for CE-NMR. The practical applicability of the μ-coil design for natural products structural problems would seem to be quite low at the present time. In the specific case of long-range $^1H-^{15}N$ studies at natural abundance, the quantity of material within the confines of the coil of a μ-coil probe may well be so low as to preclude these experiments being successfully performed. In results presented at the 40th Experimental NMR Conference in Orlando, FL, in March, 1999, inverse-detected $^1H-^{13}C$ direct correlation HMQC and HSQC spectra were shown for samples of <0.1 μmol.[75] It will be interesting to see if some of the inherent technological problems can be surmounted to make this design more amenable to natural products structural problems in the future.

Specialized NMR Sample Cells. Sample volume requirements for NMR experiments are, in part, dictated by the need to have a column of solvent containing the sample that extends above and below the coil of the probe to make shimming manageable and line shape acceptable. This requirement mandates, for example, the 500−600 μL sample volume normally used in a 5-mm NMR tube despite the fact that the coil of the probe may contain only ~220 μL of the sample volume. To allow the reduction of sample volumes to near the coil volume, the Shigemi Company has developed a specialized NMR tube or sample cell. The composition of the glass used to make the tube is matched to the magnetic susceptibility of the solvent being used for the NMR experiment. Currently, tubes are available that are matched to D_2O, DMSO-d_6, $CDCl_3$, and MeOH-d_4. The tubes employ a solid glass bottom roughly 1 cm in length and a precision bore plunger with another 1-cm length of solid glass that is inserted inside the tube to the surface of the solvent. In this fashion, the solvent volume can be restricted to slightly larger than the coil volume. When in service, the coil in the NMR probe effectively "sees" the solvent containing the sample and a column of glass 1 cm above and below the sample that is, ideally, indistinguishable from the solvent.

Using a Shigemi NMR cell, in a 5-mm format, it is possible to reduce the total solvent volume to the range 250−300 μL. For 3-mm tubes, we have been able to reduce the solvent volume to the range 70−80 μL. Very recently, the availability of 1.7-mm Shigemi NMR cells matched to $CDCl_3$ and DMSO-d_6 has been announced. By restricting sample volumes, it is possible to maintain higher working concentrations, thereby either reducing acquisition times or making it possible to get data that might otherwise be inaccessible. Recalling that halving the sample volume and holding the amount of material in the sample constant quarters the acquisition time to a given S/N level in a given probe format,[65] the benefit of restricting sample volume is obvious. It remains to be determined how much of an additional advantage will be conferred on the 1.7-mm SMIDG NMR probe by using Shigemi NMR cells.

Using 3-mm Shigemi NMR sample cells, we have been able to acquire high-quality direct $^1H-^{13}C$ heteronuclear shift correlation data for ~0.1 μmol of Caribbean ciguatoxin.[76] Reynolds and co-workers[77] have also discussed the benefits inherent to using restricted volume Shigemi NMR cells for the acquisition of $^1H-^{13}C$ heteronuclear shift correlation data using ^{13}C detection when high levels of digital resolution are required in the carbon frequency domain.

Setting Up, Acquiring, and Processing Natural Abundance Long-Range $^1H-^{15}N$ Heteronuclear Shift Correlation Experiments

For purposes of experiment setup, it is useful to return to the example of vinorelbine (**1**) presented above.[25] Given the anticipated range of chemical shifts for the four nitrogens of vinorelbine (~30−150 ppm), we would generally set up the experiment to cover a chemical shift range in the F_1 frequency dimension (^{15}N) from ~25 to 155 ppm, locating the X-transmitter at 90 ppm. This experiment configuration would require an excitation bandwidth of only ±65 ppm from the transmitter, which is easily achieved.

A more aggressive example is provided by the HIV RT inhibitor Delavirdine (**16**).[49] Nitrogen shifts for Delavirdine range from an aralkylpiperazine nitrogen that resonates at 61.3 ppm to a pyridine nitrogen resonating at 290.2 ppm. Initially anticipating that the pyridine nitrogen would resonate in the vicinity of ~300 ppm, the first experiments were parametrized to cover the range from ~30 to 310 ppm in F_1, requiring excitation across an F_1 chemical shift range of ~280 ppm, for which the transmitter was set at 170 ppm in F_1. This required a necessary excitation bandwidth that was ±140 ppm from the transmitter. As noted in a previous section, the excitation efficiency at the limits of this range are expected to be relatively low (i.e., <40%) compared to "on-resonance" excitation. The ^{15}N 90° pulses in the range of 30−34 μs were employed with the 5-mm gradient inverse-detection probe used for this study. Despite this potential drawback, acceptable data were acquired for both the pyridine nitrogen resonating near 290 ppm and for the piperazine nitrogen, which resonated near 60 ppm. That acceptable data were acquired can probably be attributed, in part, to the generous size of the sample (25 mg of free base, mol wt 441 in 600 μL of DMSO). Using a 1-mg sample in a 3-mm probe, however, it was not possible to record data for the pyridine nitrogen over a weekend.

Generally, we find it useful to parametrize GHMBC experiments to acquire 4K points in t_2 (the proton frequency domain, F_2, after transformation. When performing experiments such as D-HMBC, ACCORD-HMBC, and IMPEACH-MBC, no more than 2K points should be accumulated in the first time domain, t_2, because of decoupler duty cycle considerations. In the second frequency domain, because there are relatively few nitrogen resonances, with the exception perhaps of cyclic peptides, it is generally possible to digitize coarsely. As a rule of thumb, we have found it acceptable to digitize using sufficient t_1 increments to provide a data point every 2 to 3 ppm in the second frequency domain. As an example, for a 120 ppm window in F_1, we would generally opt to acquire 40 or 48 files in the second time domain, t_1, followed by linear prediction to 128 or 160 files (if the S/N ratio in the experiment is sufficiently high to allow linear prediction to function properly).

During processing, zero-filling once without linear prediction prior to transformation with respect to t_2 is usually sufficient unless long-range $^1H-^{15}N$ coupling constants are to be extracted from the data set. In such cases, linear prediction and/or zero-filling prior to the first Fourier transform may also be necessary. We also find it useful and most often efficient to use linear prediction in the second frequency domain. By coarsely digitizing in the second frequency domain, the number of transients per t_1 increment can be correspondingly higher, generally providing better quality data than if more files and less transients/file were accumulated. This is particularly important when some of the long-range couplings may be rather weak. Generally, data in the second dimension can be linear predicted by about 3× without encountering any problems.

In terms of mathematical weighting factors, we have generally obtained the best results by utilizing Gaussian or shifted sine-bell multiplication prior to the first Fourier transformation and cosine multiplication prior to the second Fourier transform. It is beneficial to match the shape of the shifted sine-bell weighting function to the shape of the FID if it is visible, although this is an infrequent occurrence with long-range $^1H-^{15}N$ heteronuclear shift correlation data. It is also important to adjust the time constant for cosine multiplication prior to the second Fourier transformation to take into account any linear prediction that was done. Without the adjustment of the cosine time constant, the benefits of the linear prediction are squandered.

Presentation of long-range $^1H-^{15}N$ data as a contour plot is desirable when the S/N ratio in the data set is high. Investigators should, however, be certain to examine slices extracted from the data matrix at the chemical shift of the individual nitrogens to be certain that weak long-range correlations, which may be below the threshold used to prepare the contour plot, are not missed.

Long-range responses that are of questionable intensity may warrant the acquisition of a selective one-dimensional long-range $^1H-^{15}N$ experiment.[61] In this fashion, it is possible to achieve considerably higher S/N ratios than would ever be possible in a two-dimensional NMR experiment to confirm the authenticity of a questionable response. Alternatively, weak responses are confirmed as legitimate correlations by the F_1 frequency modulation characteristic of long-range correlations in ACCORD-HMBC spectra.[60]

Applications of Long-Range $^1H-^{15}N$ Heteronuclear Chemical Shift Correlation at Natural Abundance

The earliest results of the first attempted applications of long-range $^1H-^{15}N$ experiments at natural abundance were presented in 1993. Uzawa and co-workers,[20] in the first application of gradient long-range $^1H-^{15}N$ heteronuclear chemical shift correlation experiments, presented the results obtained with three model compounds, which included tubercidin cyclonucleoside, thiamine hydrochloride, and nicotine. These results are discussed separately below. That same year, one of the present authors[19] presented the results obtained using direct and long-range $^1H-^{15}N$ heteronuclear chemical shift correlation experiments with several indoloquinoline model compounds. There followed a gap of nearly two years before the next reports appeared in the published literature in 1995. In the several years since, the body of published work reporting applications of long-range $^1H-^{15}N$ heteronuclear chemical shift correlation at natural abundance has grown to exceed 50 citations in the literature.

We have tried to cite all of the papers published in the literature through late 1999; some of our own papers and those of colleagues who have provided preprints of work submitted more recently have also been included. As with any emerging field of investigation, there are undoubtedly examples in which applications are "tucked away" and cannot be uncovered by keyword searches, abstract and title searches, etc. It is possible that some worthy applications were missed, and the authors, therefore, apologize to any individuals whose work we may have inadvertently overlooked.

We have arbitrarily chosen to review the published reports by sorting them by chemical category, in the hope

that this will be the most meaningful organization for any reader wanting to apply the information contained in this review to a molecule of interest. Currently, there are insufficient numbers of reports to allow them to be logically grouped by any other means. Alkaloids were among the first compounds to be studied using long-range $^1H-^{15}N$ heteronuclear shift correlation techniques and have been, as a group, the most extensively studied using these methods. For this reason, we have chosen to begin first with the 1990 study of the tantazole alkaloids reported by Carmeli and co-workers.[18] These data, although acquired from a labeled compound using nongradient methods, were still the first reported application of long-range $^1H-^{15}N$ heteronuclear shift correlation in the study of a natural product. After discussing tantazole (**4**), we will next focus our attention on indole-containing species, of which there are more examples than for any other chemical category.

Oxazole/Thiazole-Derived Tantazole Alkaloids. The oxazole-/thiazole-derived alkaloids known as the tantazoles, biosynthesized by the blue-green alga *Scytonema mirabile*, were the first natural products we are aware of to be studied using long-range $^1H-^{15}N$ heteronuclear shift correlation. The 1990 report of Carmeli and co-workers[18] and a subsequent communication making minor structural corrections,[78] however, did not report natural abundance $^1H-^{15}N$ long-range heteronuclear shift correlation data. Rather, the samples of alkaloids studied were ^{15}N-labeled from a biosynthetic study, enabling these workers to employ the nongradient HMBC experiment.

The structure of one of the alkaloids reported in these studies, didehydrotantazole-A (**4**), is shown above. The chemical shifts of the six nitrogens in the molecule are shown as reported in the literature. Unfortunately, the ^{15}N chemical shift reference employed in these studies was not specified; the chemical shifts shown are reasonable based on our own work on the peptide antibiotic sulfomycin-I (**65**), which was referenced relative to liquid ammonia (see section entitled Peptides and Cyclic Peptides).

Numerous long-range correlations were reported for **4**, including a number of four-bond couplings, although most of the couplings are via three-bond correlation pathways. The four-bond couplings from the amide NH and from the oxazole methyl group to the oxazole nitrogen are noteworthy, particularly the latter coupling. Attempts to observe the corresponding four-bond couplings from an oxazole methyl to the oxazole nitrogen resonance in the GHMBC spectrum of sulfomycin-I were unsuccessful.[51] Couplings from the β-methyl substituents of two of the dihydrothiazoles were useful in that they located the specific methyl between the nitrogens of the adjacent dihydrothiazoles, thereby establishing the sequence of the oxazole and the dihydrothiazole rings. In the thiazole, the proton at the 3-position, unfortunately, couples only via three bonds to the nitrogen of that ring, not via four bonds to the nitrogen of the preceding ring. Our experiences with the cyclic peptide antibiotic sulfomycin-I were similar. Likewise, the α-methyl substituent of the terminal dihydrothiazole also couples only to the nitrogen of that ring. It is tempting to suggest that this is a function of the orientation of the methyl since β-methyl groups are long-range coupled. The coupling (or lack thereof) as a function of the methyl group stereochemistry may also have something to do with the orientation of the substituent relative to the nitrogen lone pair, which can have a considerable impact on the size of long-range $^1H-^{15}N$ coupling pathways.[26,79] The anisochronous prochiral methylene protons (indicated by brackets on the structure) both coupled to the nitrogen shown.

Overall, the ^{15}N chemical shifts reported for didehydrotantazole-A (**4**) are generally comparable to those we have observed for oxazole- and thiazole-based amino acids in sulfomycin-I.[51] As noted on the structure of **4** above, the oxazole nitrogen resonates at 248.4 ppm. For the one oxazole of the three contained in the structure of sulfomycin-I for which we were able to obtain long-range correlation data, the observed chemical shift was 255.8 ppm. The two thiazole nitrogens of sulfomycin-I resonated at 310.6 and 314.3 ppm, which compares favorably with the thiazole nitrogen of **4**, which resonates at 309.6 ppm. The chemical shifts of the three nitrogens contained in the dihydrothiazole residues of **4** resonate near 301 ppm, which is not unreasonable given the reduction of one of the double bonds.

Indole-Containing Compounds. Applications in this category include simple indole-containing molecules in addition to compounds into which indole moieties are incorporated in an integral fashion into more complex molecular structures. The latter include molecules such as the *Strychnos* alkaloids, carbolines, bisindole, and alkaloids. We will, however, begin with the *Strychnos* alkaloids since they were among the first compounds to be studied by long-range $^1H-^{15}N$ methods at natural abundance.

***Strychnos* Alkaloids.** To date, strychnine, **5a** (R = H),

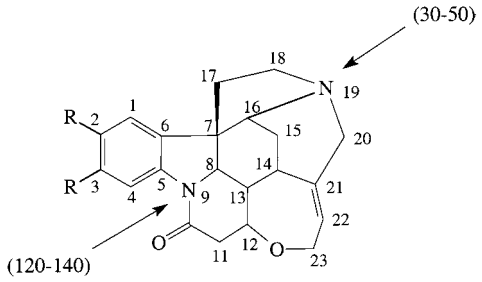

5a R = -H

5b R = -OCH_3

has been examined in four separate reports,[26,61−63] which is perhaps befitting given the original challenges of elucidating the structure of this interesting molecule. In addition, brucine, **5b** (R = OCH_3), which is closely related to strychnine, and holstiine, **6**, have also been studied using long-range $^1H-^{15}N$ heteronuclear shift correlation techniques at natural abundance.[26]

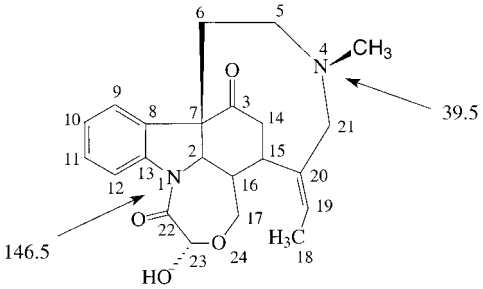

6

Strychnine. Strychnine, **5a**, is a complex indole-derived alkaloid isolated most commonly from the seeds of *Strychnos nux-vomica*. The molecule incorporates two nitrogens in its structure, the indole nitrogen, N-9, as a tertiary amide, and the tertiary bridgehead nitrogen, N-19. The

Table 2. Long-Range $^1H-^{15}N$ Couplings for the *Strychnos* Alkaloids Strychnine (**5a**), Brucine (**5b**), and Holstiine (**6**)

	strychnine (**5a**)		brucine (**5b**)		holstiine (**6**)	
coupling pathway[a]	N(9)	N(19)	N(9)	N(19)	N(1)	N(4)
H(3)−N(9) [H(12)−N(1)]	not observed[b]		2 Hz		not observed	
H(8)−N(9) [H(2)−N(1)]	4 Hz		4 Hz		not observed	
H(11α)−N(9)	4 Hz		4 Hz		n/a[c]	
H(13)−N(9) [H(16α)−N(1)]	not observed		weak[d]		6 Hz	
H(15α)−N(19)		7 Hz		7 Hz		n/a
H(15β)−N(19)		very weak[e]		not observed		n/a
H(16)−N(19)		16 Hz		15 Hz		n/a
H(18α)−N(19) [H(5α)−N(4)]		weak		8.5 Hz		not observed
H(18β)−N(19) [H(5β)−N(4)]		weak		∼2 Hz		6 Hz
H(20α)−N(19) [H(21α)−N(4)]		8 Hz		5 Hz		not observed
H(20β)−N(19) [H(21β)−N(4)]		weak		weak		5.5 Hz
[4Me−N(4)]		n/a		n/a		9 Hz

[a] Coupling pathway. Coupling pathways enclosed in square brakets pertain to holstiine, which has a different numbering system than strychnine and brucine. [b] Although possible, no response was observed for the indicated coupling pathway. [c] This coupling pathway is not physically possible where noted. [d] Couplings labeled as weak or very weak were not sufficiently well resolved and/or the response intensity was too low such that a reliable measurement of the coupling could not be made. [e] Coupling observed using a 1-mg sample in conjunction with a SMIDG 1.7-mm NMR probe.[62]

chemical environment of the two nitrogens leads to the expectation that the N-9 tertiary amide nitrogen will resonate in the range of perhaps 120−140 ppm, while the aliphatic N-19 will resonate in the range 30−50 ppm. There are a number of protons located within two or three bonds of both nitrogens that allow their respective chemical shifts to be readily determined.

The long-range $^1H-^{15}N$ study of Koshino and Uzawa[63] employed a sample prepared by dissolving 40 mg of the alkaloid in 300 μL of $CDCl_3$. Data were acquired in just under 10.5 h, with the long-range delays of a GHMBC experiment optimized for either 70 or 90 ms (7.1 or 5.6 Hz, respectively). A study that same year by one of the present authors[26] employed a lower concentration sample (20 mg/650 μL) and an overnight data accumulation. Experiments were optimized for 100, 62.5, and 50 ms corresponding to 5-, 8-, and 10-Hz optimizations, respectively.

Correlations to N-9, examining the structure of the alkaloid, might be expected from H-4, H-8, H-11α/β, and H-13. In the work of Koshino and Uzawa[63] correlations were observed from H-8, H-11α, and H-13 to N-9. In addition, a $^4J_{NH}$ coupling was, albeit weak, observed from H-3 to N-9 rather than what might be presumed to be the more likely $^3J_{NH}$ coupling from H-4. The N-9 chemical shift was not specified in the data reported by Koshino and Uzawa. Identical couplings were observed by Martin, Crouch, and Andrews[26] with the exception of the four-bond correlation from H-3, which was not observed in their study, probably due to the 4-fold lower concentration at which the data were acquired. In the authors' original report, the N-9 chemical shift was measured at 148.0 ppm relative to liquid ammonia. The long-range correlation from H-3 was, however, observed weakly in a long-range $^1H-^{15}N$ spectrum acquired on a 1-mg sample using SMIDG (submicro inverse-detection gradient) NMR probe technology.[62]

Couplings to the N-19 aliphatic nitrogen are considerably more numerous. Correlations were observed in the initial study by Martin, Crouch, and Andrews[26] from H-16, H-20α/β, H-18α/β, presumably H-17α and -17β (although it is difficult to be certain that both resonances are coupled to N-19 since these resonances are still heavily overlapped even at 600 MHz), and H-15b. The more recent submicro NMR study of Hadden and Martin,[62] in addition to the couplings just enumerated, also reported the observation for the first time of a very weak long-range coupling to H-15α. The long-range $^1H-^{15}N$ spectrum of strychnine (**5a**) recorded using a 1-mg sample of the alkaloid (∼3 μmol) is shown in Figure 3 (see also Figure 14).

As noted earlier, it is possible to acquire GHMBC data with ± alternation of the phase of the final gradient pulse using separate storage locations for alternate scans and to then process the data in what is known as mixed-mode processing,[52] to provide a data set from which individual slices at the nitrogen chemical shifts can be phased to allow the measurement of $^1H-^{15}N$ long-range couplings. Martin, Crouch, and Webb[26] applied this technique for their study of the *Strychnos* alkaloids. Couplings for all of the alkaloids in that study are summarized in Table 2.

Most remarkable of the couplings was that to N-19 from the H-16 resonance, 15 Hz, which is larger by essentially a factor of 2 relative to any of the other long-range couplings of the *Strychnos* alkaloids. Examination of a molecular model of strychnine, **5a**, suggests a plausible reason for the size of the $^2J_{N(19)-H(16)}$ coupling. The C-16/H-16 bond vector is strongly synclinal to the N-19 lone pair. This orientation is known to strongly enhance heteronuclear couplings to ^{15}N.[79] In similar fashion, the H-18α and H-20α proton−carbon bond vectors are also oriented synclinally and exhibited long-range couplings of 7 and 8 Hz, respectively. The balance of the couplings were considerably smaller. Those that could be measured were in the range ∼2−4 Hz; there were some correlation responses whose long-range couplings were too small to be measured in the GHMBC experiment used. It is possible, however, that these couplings could be measured using the GSQMBC experiment of Marek and co-workers,[42] described earlier.

Brucine. Brucine, **5b**, is structurally nearly identical to strychnine, **5a**, differing only by the incorporation of a pair of methoxyl groups at the 2- and 3-positions of the aromatic ring of the indole nucleus. Not surprisingly, the nitrogen chemical shifts of brucine were observed at 151.0 and 37.0 ppm for N-9 for N-19, respectively, which are quite comparable to strychnine. Likewise, the individual long-

range couplings observed and the size of the couplings were also very similar (see Table 2).

The only data reported for brucine, **5b**, are those in the initial report by Martin, Crouch, and Andrews.[26] These data were acquired using a 22-mg sample of the alkaloid dissolved in 650 μL of DMSO-d_6. A series of four long-range experiments were performed. Experiments optimized for 3-, 5-, and 8-Hz were 4.5 h acquisitions; a 10-Hz optimized spectrum was acquired for 9 h. The couplings reported in Table 2 were taken from the latter experiment.

Holstiine. The third *Strychnos* alkaloid to be studied thus far was holstiine, **6**. Although there are a number of structural similarities shared between holstiine and its congeners, there are also a few major differences. The aliphatic nitrogen of holstiine, N-4, is *N*-methylated rather than being linked to the equivalent of the 16-position of strychnine and brucine by a C−N bond. In addition, the oxepin ring of strychnine and brucine is opened in the structure of holstiine, while the δ-lactam incorporating N-1 has undergone an expansion to a seven-membered oxazepinone ring (ϵ-lactam).

The structural changes in holstiine relative to strychnine and brucine are not so large that the nitrogen chemical shifts would be substantially affected. Indeed, the N-1 and N-4 resonances of holstiine (**6**) resonate at 146.5 and 39.5 ppm, respectively, which compares very favorably with both strychnine and brucine. In contrast, there are expected to be considerable differences in the coupling pathways possible for the nitrogens of this alkaloid. While H-2 and H-16α would be capable of coupling to N-1, the prominent long-range coupling from H-11α seen in the spectra of strychnine and brucine is expected to be absent since this position is occupied by a hydroxyl group. Since N-4 is not linked to the equivalent of the 16-position of strychnine and brucine by a C−N bond, the prominent couplings from the positions equivalent to the 16- and 15-protons of strychnine and brucine are not possible. Indeed, the former is occupied by the carbonyl function at the 3-position of **6**. Couplings are expected from the ethylene bridge protons (H-5 and H-6) as well as from the protons at the 21-position and the 4-*N*-methyl group of holstiine.

A long-range spectrum of **6** was recorded using a 12-mg sample of the alkaloid dissolved in 650 μL of DMSO-d_6. A set of three experiments, each corresponding to an overnight acquisition, were acquired with the long-range delay optimized for 5, 8, and 10 Hz. The sole coupling observed to N-1 in the long-range ^{1}H−^{15}N spectrum of **6** is the 6-Hz coupling from H-16α.

The smaller number of long-range couplings to N-4 of **6** can likely be attributed to the greater flexibility of the aliphatic segment of the molecule in which N-4 is contained. A Monte Carlo simulation for strychnine revealed only two low-energy structures in the 50 kJ energy window. In contrast, there were 33 such structures for holstiine within the same 50 kJ window, six of which were within 3 kcal of the global energy minimum. As expected, the aliphatic region containing N-4 was conformationally quite mobile; three of the six lowest energy structures located H-5β, which strongly couples to N-4 such that the C-5/H-5β bond vector is oriented synclinally to the N-4 lone pair. This is consistent with the observed, relatively large coupling for this proton to N-4. While this does not offer definitive proof that conformational mobility makes the observation of long-range couplings to ^{15}N more difficult, we have observed that long-range couplings to nitrogens in regions of molecules that are very flexible are more difficult to observe, particularly when sample concentrations are low. It will be interesting to see if this trend continues and more molecules are studied using long-range ^{1}H−^{15}N heteronuclear shift correlation techniques.

Table 3. Long-Range ^{1}H−^{15}N Couplings Observed for Ajmaline (**7**)[80]

coupling pathway	N(1)	N(4)
H(2)−N(1)	3.5 Hz	4 Hz
H(2)−N(4)		
H(3)−N(1)	3.5 Hz	3.5 Hz
H(3)−N(4)		
H(5)−N(4)		not measured
H(6a)−N(4)		not measured
H(6e)−N(4)		3.5 Hz
H(21)−N(4)		6.5 Hz

Indole Alkaloids. There have been long-range ^{1}H−^{15}N correlation data reported at natural abundance for what is becoming a growing and diverse assortment of alkaloids containing indole moieties somewhere in their chemical structures. The majority of these are isolated reports; most do not warrant further subgrouping, although we have subgrouped various alkaloids when it was logical to do so. In general, we have reviewed examples chronologically beginning from the earliest reports that appeared in the published literature in 1995.

Ajmaline. Another interesting indole-derived alkaloid studied by long-range ^{1}H−^{15}N techniques in 1995 was ajmaline (**7**).[80] Using a sample containing 19.1 mg of **7**

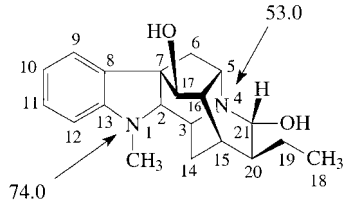

7

dissolved in 650 μL of DMSO-d_6, a series of four long-range ^{1}H−^{15}N spectra were acquired, the long-range delay optimized for 5, 8, 10, and 12 Hz. The 5-, 8-, and 12-Hz data were acquired in 4.5 h; the 10-Hz data were acquired in 9 h and were used for the measurement of the long-range coupling constants.

Both of the nitrogens of **7** are aliphatic. N-4 would be expected to resonate in the range 40−60 ppm as a tertiary aliphatic nitrogen; N-1, a 2,3-dihydroindole, would be expected to resonate somewhat downfield in the range of 60−80 ppm, analogous to the vinorelbine example (see section entitled ^{15}N Chemical Shift Ranges). As expected, the spectrum contained responses for two nitrogen resonances: the upfield resonance observed at 53.0 ppm was assigned as N-4; the downfield resonance at 74.0 ppm was assigned as N-1. Chemical shifts are reported downfield from liquid ammonia. Both resonance assignments were consistent with the observed long-range couplings. The observed long-range couplings are summarized in Table 3. All but one of the couplings was in the range 3.5−4 Hz. Based on molecular modeling, the H-21/C-21 bond vector is nearly synclinal to the N-4 lone pair, which can explain the observed, larger, 6.5-Hz coupling.

Vinorelbine. Vinorelbine (Navelbine) is a semisynthetic bisindole alkaloid used in the treatment of various forms of lung cancer.[25] The expectations for the chemical shifts of the four nitrogens were presented earlier and will not be repeated here. The data were acquired using a sample prepared by dissolving 21 mg of vinorelbine, **8**, in 650 μL of DMSO-d_6; chemical shifts are reported downfield from

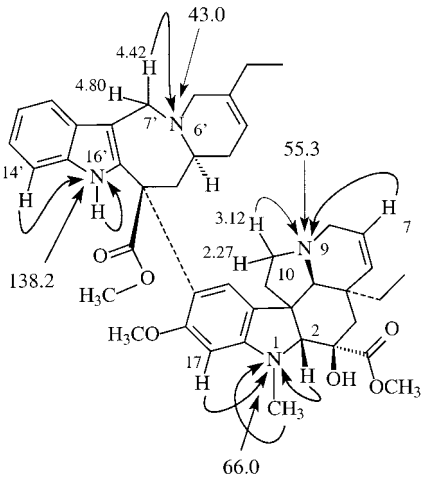

8

liquid ammonia. The experiment was optimized for 10 Hz. Within 4 h of the initiation of interleaved data acquisition, long-range correlations to N-1 and N-9 in the vindoline subunit and N-16′ in the velbanamine subunit were visible. It was necessary to continue data acquisition over the weekend before the single weak long-range correlation from the H-7′ proton resonating at 4.42 ppm was observed to the N-6′ resonance at 43.0 ppm. The weak H-7′/N-6′ correlation was attributed to the flexibility of the eight-membered azocine ring containing N-6′. On the basis of a study of the motional behavior of 3′,4′-anhydrovinblastine[81] and the conformational flexibility of the nine-membered azanonine ring contained in holstiine (**6**),[26] it is logical to suggest that the azocine ring of vinorelbine has similar conformational mobility, which could adversely affect the ability to observe correlations to N-6′ from protons located on the azocine ring.

Correlations observed to the nitrogens in the structure of navelbine are readily explained. Within the vincamine subunit, the dihydroindole nitrogen, N-1, which resonated at 66.0 ppm, exhibited correlations to the *N*-methyl group, the H-2 methine, and H-17 aromatic proton resonances. The N-9 resonance observed at 55.3 ppm was correlated to the H-7 vinyl methine proton and to the anisochronous methylene proton resonating at 3.12 ppm at the 10-position. In the velbanamine subunit, as noted above, only the H-7′ proton resonating at 4.42 ppm was very weakly correlated to N-6′, which resonated at 43.0 ppm. Finally, the N-16′ indole nitrogen resonating at 138.2 ppm was long-range coupled to the H-14′ aromatic proton and directly to the H-16′ N−H proton.

Vincamine. Vincamine (**9**), well-known in its own right, is also an important constituent of numerous bisindole alkaloids. The ^{15}N chemical shifts and long-range coupling

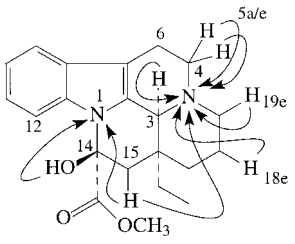

9

pathways of vincamine were reported in 1997 by Martin[82] at 500 MHz using a sample prepared by dissolving 15 mg of the alkaloid in 550 μL of DMSO-d_6. The data were acquired using the GHNMBC pulse sequence in which the long-range dependent delay was optimized for 5 Hz; shifts were referenced to liquid ammonia.

The ^{15}N resonances of vincamine were observed as expected; N-1 resonated at 143.0 ppm, while the aliphatic N-4 resonance was observed at 31.5 ppm. Correlations to the N-1 resonance were few in number. Only the 14-hydroxyl proton and the 15a (axial) proton were long-range coupled to N-1. Not surprisingly, there was no correlation from the H-12 resonance of the indole aromatic ring since these are generally very weak correlations and difficult to observe. In contrast, there were numerous correlations to the N-4 aliphatic resonance. The H-15a resonance was also long-range coupled to the N-4 resonance across four bonds. Four-bond, long-range couplings to ^{15}N are not particularly common, although they are sometimes observed to be strong correlations. The H-3a proton and both the H-5a/e (axial/equatorial) resonances were coupled to N-4 via two bonds. Finally, H-19e was coupled to N-4 via two bonds, while the H-18e proton coupled to N-4 via three bonds. Long-range coupling constants were not measured.

Indoloquinolines. The indoloquinoline alkaloids, as a group, have been the focus of considerable interest by several research groups. Recently, studies have begun to appear dealing with the ^{15}N chemical shifts and long-range couplings of these interesting alkaloids. Studies range from submilligram, nongradient data recorded for the two protonated nitrogen resonances of quindoline[28] to more recent studies of facile oxidation product mixtures.[89]

Quindoline. The earliest member of the indoloquinoline family of alkaloids to be studied by ^{15}N NMR spectroscopy was quindolinone (**2**).[28] The acquisition of ^{15}N chemical shift data for this alkaloid, despite a severely restricted samples of only 800 μg, were still a facile undertaking since both nitrogens are protonated.

Data were acquired in DMSO-d_6 using a nongradient HMQC experiment with the delay for the one-bond coupling constant optimized for 95 Hz in approximately 2 h at 400 MHz using a 3-mm micro inverse probe. The chemical shifts of the two nitrogens were consistent with expectations for the structure. The quinolone nitrogen, N-5, resonated at 111.0 ppm; the indole N-10 resonance was observed at 112.6 ppm, somewhat upfield of the normal indole nitrogen chemical shifts (133.5 ppm, see Supplemental Table S3). The chemical shift of N-10 of quindolinone is, however, consistent with its location in the structure β to the N-5 resonance, which would be expected to shift N-10 upfield. Since both nitrogens were protonated, no long-range data were acquired; nothing is known of the possible long-range coupling pathways for this alkaloid.

Cryptospirolepine. Three reports have appeared in the literature that have contained ^{15}N data on the complex alkaloid cryptospirolepine (**3**). The first report[29] described the elucidation of the structure of the alkaloid and reported the ^{15}N chemical shift of the one protonated nitrogen in its structure. These data were acquired on a 2.5 mg sample dissolved in 550 μL of DMSO-d_6 using a nongradient HMQC experiment. More recently,[30] the present authors have reported a study of this alkaloid using submicro NMR probe technology. Using a 750-μg sample of the alkaloid (~1.5 μmol) dissolved in 30 μL of DMSO-d_6, the present authors demonstrated the extremely rapid acquisition of direct and long-range ^{1}H−^{13}C heteronuclear shift correlation data (34 s and 15 min, respectively). Using the same sample it was also possible for the authors to acquire the direct ^{1}H−^{15}N GHSQC spectrum of the alkaloid in <50 min with >15:1 S/N. The long-range data were acquired over-

night (18 h) using a GHMBC experiment optimized for 6 Hz, which gave correlations to the two *N*-methyl-bearing nitrogen resonances in the structure of the molecule. The amide nitrogen did not give a response in the 6-Hz overnight experiment, nor was a response observed in a 3.3-Hz spectrum acquired over a weekend. Once again, the difficulty of three-bond ortho couplings to nitrogen likely hampered the assignment of the remaining amide nitrogen.

The most recent long-range $^{1}H-^{15}N$ experiment performed on cryptospirolepine was the acquisition of a 2.5-Hz optimized spectrum acquired in 120 h over a holiday break.[31] It was with these data that it was finally possible to establish the chemical shift of the remaining amide nitrogen, N-3. The N-3 resonance was observed at 135.4 ppm via a four-bond long-range coupling from the H-13 vinyl proton resonating at 6.27 ppm. No long-range correlation was observed from the ortho H-4 resonance. In addition to the $^{4}J_{NH}$ correlation from H-13 to N-3, a four-bond coupling was also observed from H-13 to the methyl-bearing N-8 resonance at 106.7 ppm. A third four-bond, long-range coupling was observed from the H-1′ proton resonating at 6.78 ppm to the methyl-bearing N-5′ resonance at 131.4 ppm. Finally, a three-bond ortho coupling was observed from the H-9′ proton resonance at 7.12 ppm to the protonated indole N-10′ nitrogen resonance at 115.3 ppm.

Cryptolepine. Cryptolepine (**10**) is the oldest of the

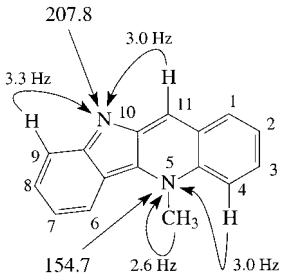

10

indoloquinoline alkaloids known from a natural source. The proton and carbon NMR spectra of the molecule have been well studied. It was with a sample of cryptolepine that our first attempts to observe long-range $^{1}H-^{15}N$ heteronuclear shift correlations at natural abundance were made in 1993.[19] Using a 10-Hz optimized, nongradient HMBC spectrum, we were only able to observe the two-bond, long-range correlation from the *N*-methyl singlet to N-5, which resonated at 154.7 ppm. It was not until 1996, using gradient methods, that we were successfully able to determine the ^{15}N chemical shifts and long-range coupling pathways of both nitrogen resonances in this molecule.[83] In the latter report, data were acquired using a sample prepared by dissolving 6.5 mg of the alkaloid in 650 μL of DMSO-d_6; a GHMBC experiment optimized for 4 Hz was acquired over 42 h. Chemical shifts are reported downfield of liquid ammonia.

The difficulty of observing long-range couplings to the two nitrogens of cryptolepine is exacerbated by the fact that three of the four observed couplings are three-bond ortho couplings. The two-bond coupling from the *N*-methyl to N-5, which resonates at 154.7 ppm, is the simplest to observe, aided by the fact that the resonance via which this correlation is detected is an *N*-methyl singlet. The three-bond coupling from the H-4 resonance was correspondingly weaker. The N-10 resonance is interesting in that it does not behave like an indole nitrogen. Rather, because of the conjugation, the C-9a═N-10 double bond is more imine-like in character and was thus expected to resonate substantially downfield of N-5. On the basis of a study by Kaczmarek and co-workers[84] of a series of azacarbolines such as **11**, it was expected that the N-10 resonance of

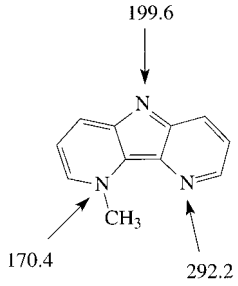

11

cryptolepine would be observed at ~200 ppm. Consistent with this expectation, the N-10 resonance of cryptolepine was observed at 207.8 ppm via long-range correlations to the ortho H-9 and H-11 proton resonances.

Long-range coupling constants were measured for cryptolepine (**10**) and are summarized on the structure. All of the observed long-range coupling constants were quite small, ranging from only 2.6 to 3.3 Hz, which in part accounts for the difficulty in observing these correlations.

Cryptolepinone. The alkaloid cryptolepinone (**13**) has

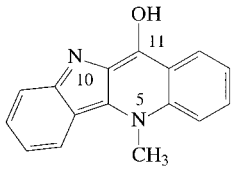

12

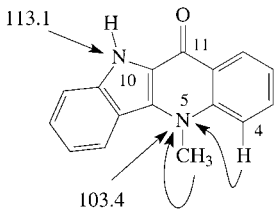

13

also been the subject of several reports in the literature. The earliest isolation and characterization of this alkaloid was in a doctoral thesis.[85] The proton and carbon spectra were assigned in DMSO-d_6 in this study. This report was followed by a report in the open literature by Paulo, Gomes, and Houghton[86] which described a molecule with the same physical properties and fundamentally the same proton and carbon chemical shifts (chloroform-*d*/methanol-d_4, 2:1) as 11-hydroxycryptolepine (**12**). This proposal for the structure invokes the extended conjugation of cryptolepine (**10**) and requires a C-9a═N-10 "imine" bond, which correspondingly requires N-10 to resonate in the vicinity of 200 ppm. A synthetic study of cryptolepinone was subsequently reported by Cooper, Lovell, and Joule[87] that suggested the molecule should be represented as the 11-one rather than the 11-ol. Finally, the question of substituent functionality and double-bond isomerization was resolved, in part, through an ^{15}N NMR study.[88] Quite simply, while 11-hydroxycryptolepine, **12**, requires a C-9a═N-10 imine double bond, with predictable consequences for the C-9a and N-10 chemical shifts, the 11-one, **13**, in contrast, has no imine character and N-10 is instead protonated.

The assignment of the ^{13}C NMR spectrum of cryptolepinone was unequivocal; C-9a was observed at 139.0 ppm, the assignment confirmed on the basis of long-range $^{1}H-^{13}C$ couplings. The assigned chemical shift of C-9a is inconsistent with the imine-like character required of this carbon if the molecule were indeed the 11-ol (**12**). In contrast, the C-9a resonance of cryptolepine is assigned at 160.0 ppm. More directly, the N-10 resonance was observed

in a $^{1}H-^{15}N$ GHSQC spectrum, optimized for a 95-Hz, one-bond coupling, at 113.1 ppm. The experiment was performed on a sample of 10 mg of **13** dissolved in 160 μL of DMSO-d_6 using a 3-mm micro probe. The long-range couplings to the N-5 resonance from H-4 and the *N*-methyl located this resonance at 103.4 ppm in an overnight 3-Hz optimized GHMBC experiment.

Cryptolepinone 5-Oxide. On standing for approximately 18 months, a sample of cryptolepinone, **13**, from the preceding study underwent a facile oxidation, presumably induced by DMSO, to afford approximately a 40% conversion to cryptolepinone 5-oxide (**14**).[89] Rather than

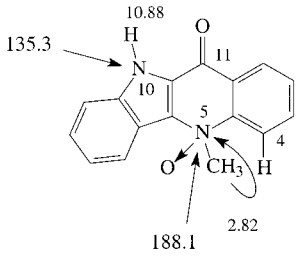

14

separating the *N*-oxide from its oxidative precursor, the mixture was studied directly. All experiments were performed on a sample containing ~5 mg of the mixture dissolved in 150 μL of DMSO-d_6. Chemical shifts are reported downfield from liquid ammonia. The two protonated nitrogens were assigned using a 95-Hz optimized GHSQC spectrum. In the mixture, the N-10 resonance of cryptolepinone was observed at 111.4 ppm, which is in reasonable agreement with the chemical shift of this resonance in a pure sample (113.1 ppm; see section entitled Cryptolepinone). The N-10 resonance of the 5-oxide, in contrast, was observed substantially downfield, resonating at 135.3 ppm.

Far more interesting were the results obtained from a 4-Hz optimized $^{1}H-^{15}N$ GHMBC experiment performed on the mixture. A single correlation was observed from the *N*-methyl group to the N-5 nitrogen, which resonated at 188.1 ppm following *N*-oxidation. The N-5 resonance of cryptolepinone present in the mixture resonated at 103.4 ppm, identical to its chemical shift in pure form.[88]

It is interesting to note here that the N-5 resonance was shifted downfield by +84.7 ppm following *N*-oxidation. The N-10 resonance of the N-5-oxidized alkaloid was also shifted downfield by +23.5 ppm. The downfield shift of N-5 is somewhat greater than the +68 ppm downfield shift noted for two alicyclic nitrogen containing systems (see section entitled Piperidine and Morpholine N-Oxides). The downfield shift of the N-10 resonance was consistent with the calculated partial charge on N-10 and is attributable to the transmission of the electronic effects of the *N*-oxide at the 5-position through the intervening double bond. *N*-Oxidation in a series of heteroaromatics gave a shift of the nonoxidized nitrogen of the same general magnitude as in the present case, albeit in the opposite direction. The calculated partial charge on the nitrogen of the heteroaromatic systems was opposite in sign of that of the present case, which is consistent with the upfield shift of the nonoxidized nitrogen.

11-Isopropylcryptolepine. The final member of the indoloquinoline family to be studied to date is 11-isopropylcryptolepine (**15**).[90] Originally isolated as <1 mg, the final characterization required the use of submicro NMR techniques. Despite a sample estimated at ~75 μg, it was possible to obtain a long-range $^{1}H-^{15}N$ GHMBC spectrum (3.3-Hz optimization) in 77 h over a weekend. In this

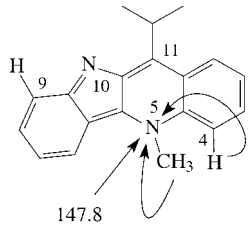

15

spectrum, the N-5 resonance was assigned at 147.8 ppm via long-range correlations to the *N*-methyl and weakly to H-4. The correlation from H-9 to N-10 observed for cryptolepine (**10**, see section entitled Cryptolepine) was not observed. The inability to observe the ortho, three-bond coupling for **15** is not surprising, however, since it is relatively weak and was difficult to observe even for a 6.5-mg sample of **10**. To date, this effort represents the smallest sample to be studied at natural abundance via $^{1}H-^{15}N$ long-range correlation techniques.

Delavirdine. The drug Delavirdine (Rescriptor, **16**) is

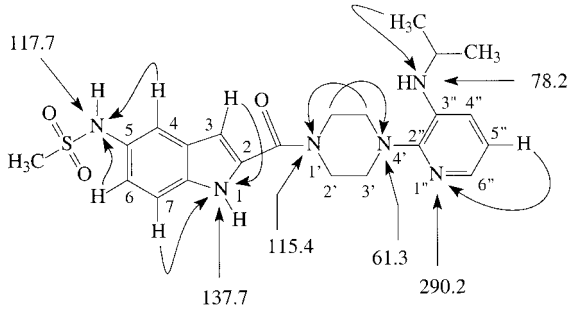

16

classified as a BHAP (bis-heteroarylpiperidine) and is used in the treatment of human acquired immunodeficiency syndrome (AIDS). This clinically active molecule is indole-derived and contains a total of six nitrogens in its structure. Two of the nitrogens, N-5 in the methylsulfonamido group and N4′ in the piperidine, were problematic in terms of observing responses to them.

Cursory inspection of the structure of Delavirdine shows three of the nitrogens to be protonated, leading to the expectation of three ~90-Hz doublets in the GHNMBC spectrum of the molecule.[49] A sample was prepared by dissolving 25 mg of Delavirdine free base in 650 μL of DMSO-d_6 followed by the acquisition of a 4-Hz optimized GHNMBC spectrum of the molecule. Two of the protonated nitrogens, N-1 in the indole nucleus and the N-3″ isopropyl amino nitrogen, gave the anticipated ~90-Hz doublets for the direct correlation response at 137.7 and 78.2 ppm, respectively. In contrast, the N-5 nitrogen of the methylsulfonamido group failed to give any direct response in GHNMBC spectra irrespective of the optimization. Hence, the lack of a response due to modulation effects can be ruled out. Other long-range correlations from the H-4 and H-6 indole aromatic protons pinpointed the ^{15}N chemical shift of N-5 at 117.7 ppm, which is reasonable for this type of functional group. Correlations were also observed from the H-3 and H-7 aromatic resonances to the N-1 indole resonance. Within the piperidine ring, a correlation from the H-3′/H-5′ methylene protons identified the N-1′ piperidine resonance at 115.4 ppm, which is again reasonable for an amide nitrogen. No response was observed for the piperidine N-4′ resonance in the GHNMBC data recorded regardless of the optimization of the experiment. Finally, the N-1″ pyridine nitrogen was located at 290.2 ppm via a

three-bond long-range correlation from the H-5″ resonance. Inexplicably, no correlation was observed via two bonds to the H-6″ proton resonance.

Addressing the problematic responses in turn, it was discovered that by preparing a sample of the drug in methylene chloride-d_2 and cooling the solution to −10 °C, it was possible to begin to see a direct response for N-5 H in a GHSQC spectrum. The intensity of the response increased at −20° and was at full intensity at −35°. The observation of the response at lower temperatures was attributed to slowing the exchange of the highly acidic N-5 H proton. Presumably, N-5 H autoprotonates the molecule, most likely at the N-3″ isopropylamino group. When a solution of the drug as the mesylate salt was examined in DMSO-d_6, the N-5 resonance was observed in a GHSQC spectrum at 117.3 ppm without any difficulty.

The remaining problem response, that of the N-4′ piperidine resonance, is attributable to the nature of the H-2′/H-6′ proton multiplet. Generally, as a proton resonance becomes progressively broader, the ability to observe long-range correlations from that response diminishes. Bax and co-workers[91] addressed this problem by applying selective 90° and 180° pulses to the broadened proton resonance of interest in $^1H-^{13}C$ GHMBC experiments. Using this approach, selective pulses were applied to the broad H-2′/H-6′ proton multiplet in the spectrum of **16**. This technique successfully long-range correlated the H-2′/H-6′ proton resonance to N-4′, which resonated at 61.3 ppm.

Brevicompanines A and B. Indole-derived plant growth regulators brevicompanines A and B (**17a** and **17b**) have

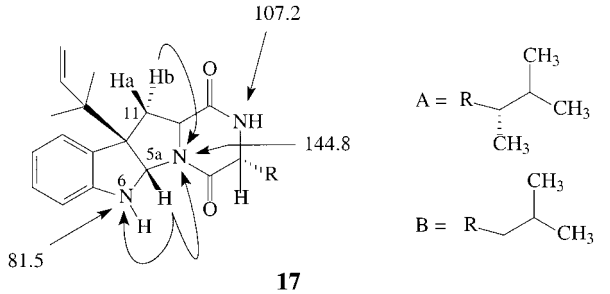

17

been isolated from the fungus *Penicillium brevicompactum*.[92] Direct and long-range $^1H-^{15}N$ heteronuclear shift correlation experiments were used in the elucidation of the structures of these interesting compounds. The protonated nitrogens were determined using a GHMQC experiment to correlate the dihydroindole proton resonating at 4.92 ppm with the nitrogen resonating at 81.5 ppm and the amide proton resonating at 6.69 ppm to its directly bound nitrogen resonating at 107.2 ppm. Chemical shifts were reported relative to $^{15}NH_4NO_3$, taken as 0 ppm. Chemical shifts shown here have been adjusted and are given relative to liquid ammonia.

Long-range $^1H-^{15}N$ correlations were observed using a GHMBC experiment. No details of the optimization were given in the report. Correlations were observed from the H-5a and H-11b protons to the remaining amide nitrogen, which resonated at 144.8 ppm. A correlation was also noted from the H-5a resonance to the dihydroindole nitrogen, N-6. No other long-range $^1H-^{15}N$ correlations were reported.

Carbolines. Carbolines are a logical progression from indole-containing molecules in that they are pyridoindoles. A useful survey of the ^{15}N chemical shifts of carbolines (direct observe ^{15}N NMR; see also Supplemental Table S2) has appeared.[93] To date, two long-range $^1H-^{15}N$ studies have appeared that involved carboline-containing molecules. We also report here the ^{15}N chemical shift assignments for the simple alkaloid norharmane (**18**) (β-carboline).

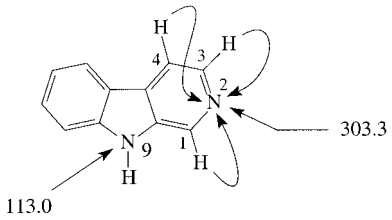

18

Norharmane (β-Carboline). The simplest of the carboline alkaloids is probably norharmane (**18**). Norharmane also provides a very useful model compound to learn to acquire and process $^1H-^{15}N$ long-range data at natural abundance since it is highly soluble in DMSO-d_6 and inexpensively available commercially.

The pyridine nitrogen resonance of norharmane (**18**) resonates downfield at 303.3 ppm and is long-range coupled via two bonds to the flanking H-1 and H-3 resonances and via three bonds to H-4. The protonated N-9 resonance is observed upfield, resonating at 113.0 ppm, typical of an indole.

Roemeridine. Roemeridine (**19**) is a complex β-carbo-

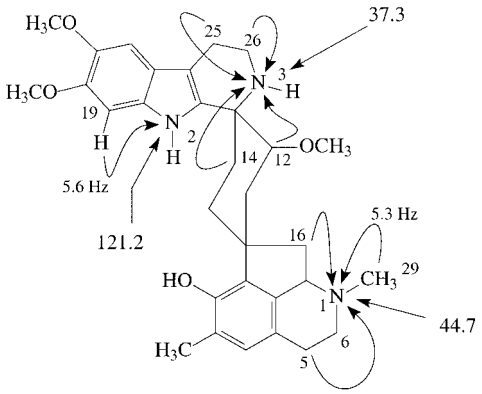

19

line-derived alkaloid that has been studied by Marek and co-workers.[94] The sample studied was prepared by dissolving 52 mg of the alkaloid in 500 μL of DMSO-d_6. A GHMBC experiment optimized for 7 Hz was performed and contained responses for the N-2 direct correlation doublet and a long-range response from H-19 to N-2 resonating at 121.2 ppm. Similarly, correlations from the H-5 and H-16 resonances to N-1, which resonated at 44.7 ppm, were observed in a 7-Hz optimized long-range experiment. A two-bond correlation from the 29-methyl resonance to N-1 was also observed. In contrast, it was necessary to reoptimize the GHMBC experiment for 4 Hz for correlations via two and three bonds to be observed to the N-3 resonance at 37.3 ppm.

Marek and co-workers reported the estimation of several long-range couplings from the acquisition of a $^1H-^{15}N$ HSQC experiment.[94] The measured couplings are shown on the structure. The authors also report the relative sign of the one-bond correlation from $^1J_{H-2/N-2}$ as negative on the basis of the $^1H-^{15}N$ HSQC data. In contrast, the long-range correlations were assigned positive coupling constants since the antiphase patterns of the long-range correlations were inverted relative to the antiphase sense of the direct response.

Mescengricin. One additional carboline, mescengricin (**20**), an α-carboline, has been studied using long-range $^1H-^{15}N$ techniques at natural abundance.[95] Mescengricin was isolated from *Streptomyces griseoflavus* during screening studies for compounds capable of protecting chick primary mescencephalic neuronal cells from l-gutamate toxicity.

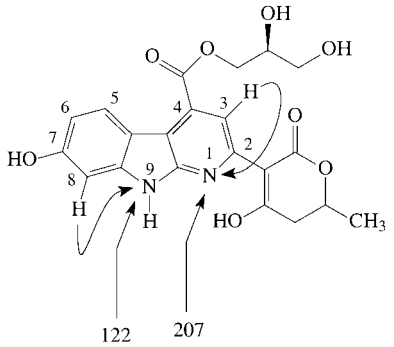

20

The two nitrogen atoms in the molecule were observed using a GHMBC experiment performed on a sample of **20** dissolved in DMSO-d_6. Details of the optimization were not given, nor was the chemical shift referencing scale reported in the communication. Chemical shifts are reproduced on the structure as reported by the original authors. Only two long-range correlations are described in the report. The indole nitrogen, N-9, which resonated at 122 ppm, was long-range coupled to the ortho H-8 aromatic proton via three bonds. The pyridine N-1 nitrogen resonance observed at 207 ppm was long-range coupled to the H-3 proton, again via three bonds. It is noteworthy that relative to the pyridine nitrogen chemical shift of α-carboline (266 ppm, see Supplemental Table S3),[93] the N-1 resonance of mescengricin (**20**) is shifted substantially upfield. The chemical shift of N-1 is also similar to the chemical shift reported for N-8 of tetradehydroisocalycanthine (**22**) at 202 ppm (see subsequent section).[97]

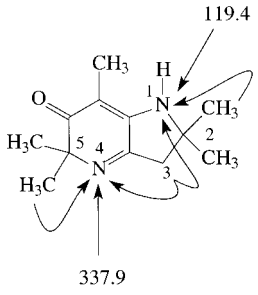

21

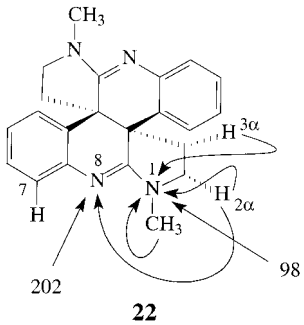

22

Pyrrole, Pyrazole, Imidazole, Thiazole, and Other Five-Membered Nitrogen-Containing Systems. Applications of long-range $^1H-^{15}N$ heteronuclear shift correlation experiments have also appeared for a significant number of molecules containing some form of five-membered nitrogen-containing ring. Examples include a diazaindane alkaloid from a Korean mushroom,[96] an isocalycanthine,[97] the pyrralomycin antibiotics,[98−100] pyrrolidine-containing structures,[101] imidazole-derived systems, substituted pyrazoles, and thiazole-derived systems.

Agrocybenine. An unusual diazaindane alkaloid, agrocybenine (**21**), has been isolated from the Korean mushroom *Agrocybe cylindrica*.[96] A broad proton resonating at 5.61 ppm in the proton spectrum, which failed to give a response in $^1H-^{13}C$ direct correlation experiment, was confirmed to be a N−H resonance on the basis of a 92-Hz doublet in a $^1H-^{15}N$ GHMQC experiment, with the nitrogen in question resonating at 119.4 ppm using a sample prepared in DMSO-d_6. Chemical shifts were originally reported downfield of $^{15}NH_4NO_3$ and are reported here relative to liquid ammonia.

A long-range $^1H-^{15}N$ GHMBC experiment was subsequently performed on the sample. Long-range correlations were observed from the 2,2-*gem*-dimethyl resonances and the 3-methylene resonances to N-1. The 3-methylene resonance was also long-range coupled to the N-4 resonance observed at 337.9 ppm, which was also long-range coupled to a 5,5-*gem*-dimethyl resonance. The ^{15}N data, in conjunction with the $^1H-^{13}C$ chemical shift correlation data, were interpreted to establish the diazaindane skeleton.

Tetradehydroisocalycanthine. In a study of the pyrrolidinoindoline alkaloids of *Psychotria colorata*, Verotta and co-workers[97] reported the elucidation of the structure of tetradehydroisocalycanthine (**22**). Long-range $^1H-^{15}N$ GHMBC was employed in the elucidation of the structure to define the two nitrogen types present in the symmetric structure.

The aliphatic nitrogen, N-1, resonating at 98 ppm in chloroform-*d*, was long-range coupled to the *N*-methyl, H-2α, and H-3α proton resonances. The "imine"-like N-8 nitrogen resonance at 202 ppm has a chemical shift similar to that of the N-10 resonance of cryptolepine (**10**),[83] the imino nitrogen of the diazacarboline (**11**),[84] and N-1 of mescengricin (**20**).[95] The N-8 resonance was coupled via three bonds to the ortho H-7 proton in what the authors referred to as a strong coupling. In addition, a weak four-bond correlation was also observed from the H-2α resonance to N-8. Nitrogen chemical shifts are reported downfield of liquid ammonia, the chemical shift of which was established indirectly from the chemical shift of neat nitromethane. Unfortunately, no details of the long-range optimization used in the experiments performed on **22** were reported.

Pyralomycins. The application of long-range $^1H-^{15}N$ heteronuclear shift correlation has been reported in three papers detailing the characterization of the pyrralomycin antibiotics. The first communication in which the use of $^1H-^{15}N$ GHMBC is mentioned describes the structures of these novel antibiotics from *Actinomadura spiralis*, although no actual proton−nitrogen data are presented or discussed.[98] Subsequently, the authors describe in detail the elucidation of the structures of the pyralomycins.[99] The long-range $^1H-^{15}N$ correlations of pyrralomycin 1a (**23**) were probed using a D-HMBC experiment[40] optimized for 2.8 Hz. A sample prepared by dissolving 66 mg of pyrralomycin 1a in 700 μL of *N*,*N*-dimethylformamide-d_7 was employed for the study. The ^{15}N chemical shift of N-1 of pyrralomycin 1a (**23**) was referenced using the ^{15}N chemical shift of the solvent, taken as 103.2 ppm downfield of liquid ammonia.

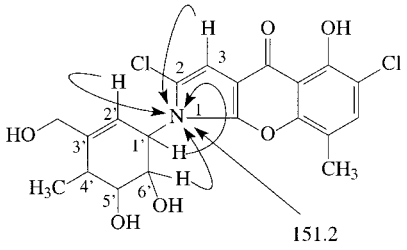

23

From the long-range $^{1}H-^{15}N$ spectrum published, all of the long-range correlations had reasonable intensity in the D-HMBC experiment.[40] The three-bond correlations from H-3 and H-6′ were more intense than the three- and two-bond correlations from H-2′ and H-1′, respectively, which may be a function of the proton multiplet structure. The H-3 and H-6′ resonances were a sharp singlet and a well-resolved apparent triplet, respectively. The H-2′ vinyl proton was less well resolved, and the H-1′ multiplet was relatively broad. Finally, the authors note that the reported chemical shift from the D-HMBC experiment (151.2 ppm) was in favorable agreement with the ^{15}N chemical shift of N-1 at 152.4 ppm from a ^{15}N direct observe experiment performed after the ^{15}N-labeling of **23** in a biosynthesis study.[100]

Kaitocephalin. Using a combination of $^{1}H-^{13}C$ GHMQC and GHMBC in conjunction with $^{1}H-^{15}N$ GHMBC, the pyrrolidine-containing substructure, **24**, of kaitocephalin (**25**) was successfully assembled.[101] Kaitocephalin was

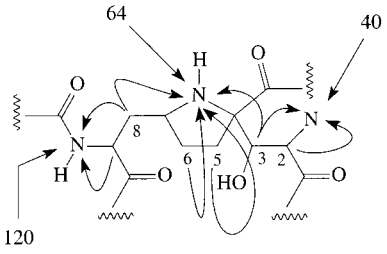

24

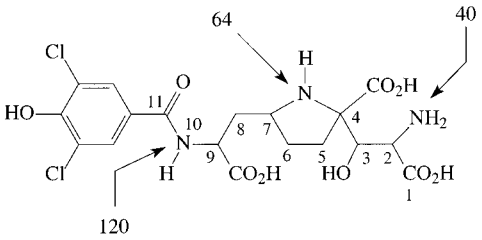

25

isolated from *Eupenicillium shearii* as a glutamate receptor antagonist which protected chick telencephalic neurons from kainate toxicity.

The direct response doublet observed at 120 ppm in the $^{1}H-^{15}N$ GHMBC spectrum of **25** established the presence of a secondary amide nitrogen when interpreted in conjunction with the long-range correlation from the N-10H resonance to a carbonyl in the $^{1}H-^{13}C$ GHMBC spectrum. The H-8 methylene protons were also coupled to N-10 as well as to an alicyclic nitrogen resonating at 64 ppm. The further correlations from the 6- and 5-methylene protons and the 3-methine proton supported the assembly of the pyrrolidine ring. Finally, the H-3 and H-2 methine protons were also coupled to a primary amino nitrogen resonating at 40 ppm. Correlations from the $^{1}H-^{13}C$ GHMQC and $^{1}H-^{13}C$ GHMBC spectra as well as from a double quantum filtered COSY experiment completed the assembly of the structural fragment represented by **24**. Unfortunately, no details on the concentration or optimization of the $^{1}H-^{15}N$ GHMBC were given in the report. It was noted, however, that the ^{15}N chemical shifts were referenced using formamide (δ ^{15}N = 112) as an external standard. This study provides an excellent example of the integral utilization of long-range $^{1}H-^{15}N$ heteronuclear shift correlation data in natural product elucidation.

Fungerin. Fungerin (**26**) is an imidazole alkaloid,

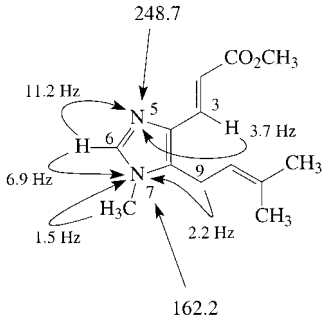

26

antifungal antibiotic isolated in a screening effort based on saprophytic fungi. The alkaloid was isolated from a *Fusarium* sp. fungus.[102] The long-range $^{1}H-^{15}N$ GHMBC spectrum, originally referenced to $^{15}NH_4NO_3$ and reported here relative to liquid ammonia, gave correlations to two nitrogens resonating at 248.7 and 162.2 ppm in DMSO-d_6, which were in agreement with data for a methylimidazole.[6] The locations of the double bond and the prenyl group were established at the 4- and 8-positions, respectively, based on the long-range correlation of the H-3 vinyl proton to N-5 and the correlation of the prenyl methylene, H-9, to N-7.

The measured long-range couplings from H-6 to the two nitrogens were reported as being determined from a $^{1}H-^{15}N$ GHMBC spectrum with high resolution. On the basis of the dependency of the GHMBC correlation peaks to the duration time for the long-range coupling (1/2J for the maximum and 1/J for the minimum), Koshino and co-workers determined the values of the other $^{n}J_{NH}$ couplings from 1D $^{1}H-^{15}N$ GHMBC and selective $^{1}H-^{15}N$ GHMBC experiments.[49,61,91]

Finally, it is interesting to note that the data reported by Koshino and co-workers[102] for fungerin were determined using a 30-mg sample of the alkaloid dissolved in 150 μL of chloroform-*d* using a Shigemi symmetrical NMR micro cell in a 5-mm probe. This is the only reported usage of a Shigemi NMR cell to facilitate the acquisition of natural abundance $^{1}H-^{15}N$ long-range heteronuclear shift correlation data of which we are aware. The long-range delay in the experiment was optimized for 8.3 Hz. Chemical shifts were referenced to external $^{15}NH_4NO_3$ and are shown re-referenced to liquid ammonia.

Amphistin. As a result of a screening program for melanogenesis inhibitors, a novel imidazole-derived alkaloid, amphistin (**27**), was isolated from an *Actinomyces*

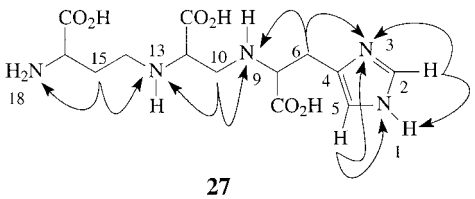

27

strain collected in China.[103] Amphistin, unfortunately, was

soluble only in water. COSY and $^1H-^{13}C$ GHMBC data were used to assemble the series of structural fragments shown by **28**. Ōmura and co-workers,[103] therefore, resorted

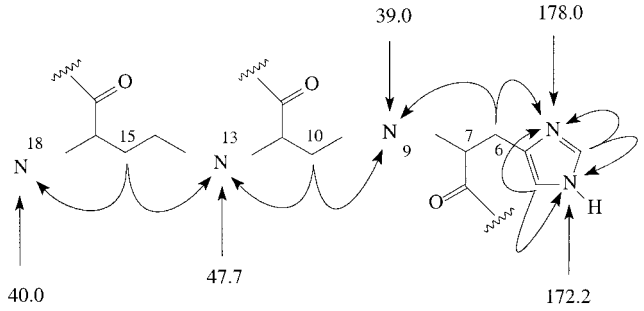

28

to a $^1H-^{15}N$ GHMBC experiment to link the various substructural fragments together via the ^{15}N resonances. Unfortunately, no details of the optimization of the $^1H-^{15}N$ GHMBC were contained in their report. The quantity of amphistin used for the long-range $^1H-^{15}N$ GHMBC experiment was not specified, nor was the ^{15}N chemical shift reference used given. Hence, ^{15}N chemical shifts are reported directly from the literature. Nevertheless, the study still makes interesting use of long-range correlations to nitrogen at natural abundance in the assembly of the overall structure of amphistin.

Differentiation of Pyrazole Regioisomers. The reaction of 6-(4-chlorophenyl)hexanoic acid (**29**) with 2-hydroazinopyridine (**30**) in a methanol/pyridine solvent mixture leads, as shown in the scheme below, to the formation of a pair of pyrazole regioisomers, **31** and **32**.[104] Long-range

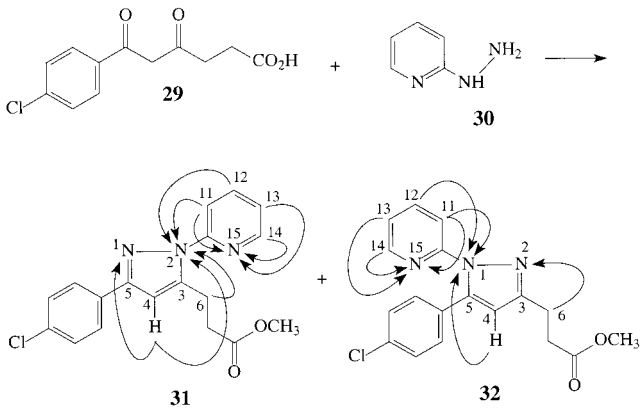

$^1H-^{15}N$ coupling data from a GHMBC experiment were used to differentiate the isomers from one another. Using samples containing 50 mg of each isomer in 600 μL of chloroform-*d*, GHMBC data were acquired using a 3.3-Hz optimization of the long-range delay.

The long-range $^1H-^{15}N$ coupling pathways are shown on the structures; ^{15}N chemical shifts for the three nitrogen resonances in the two isomers are given in Table 4. A long-range coupling from the 6-methylene proton resonance in **31** was observed to the nitrogen resonating at 217.7 ppm. Likewise, couplings were observed to this nitrogen resonance from the H-11 and H-12 protons of the pyridine ring in addition to a coupling from the H-4 pyrrole proton. These couplings to a nitrogen with this chemical shift are plausible only if the nitrogen carries the pyridine substituent as shown by **31**.

Table 4. ^{15}N Chemical Shifts Observed for Pyrazole Regioisomers **31** and **32** in Chloroform-*d* at 600 MHz[a]

position	**31**	**32**
N-1	296.4	214.2
N-2	217.7	304.2
N-15	285.5	294.9

[a] Chemical shifts are reported downfield of liquid ammonia.[104]

Table 5. ^{15}N Chemical Shifts of a Series of 5-*N*-Benzylideneaminopyrazoles (**33a**−**e**)[a]

R	N-1	N-2	N-5	other substituent
H	206.7	295.2	293.5	
H (TFA)	169.6	168.3	49.3	
4′-Me	206.1	292.4	291.6	
4′-NMe_2	201.1	288.8	276.5	53.9
4′-NO_2	208.2	297.1	306.5	366.2
2′-OH	205.8	295.1	266.8	

[a] Chemical shifts were measured as 0.5 M solutions in chloroform-*d* except as noted.[105]

In the case of the other regioisomer, the discriminatory long-range coupling from the 6-methylene resonance is observed to the nitrogen resonating at 304.2 ppm. The H-11 and H-12 pyridine resonances do not couple to this nitrogen. The pyridine aromatic protons are instead coupled to a nitrogen resonating at 214.2 ppm. Together, these couplings assign the structure of this regioisomer as **32**.

As illustrated by this example, long-range $^1H-^{15}N$ couplings have been advantageously used to differentiate a pair of pyrazole regioisomers that would otherwise be difficult to assign unequivocal structures to without resorting to X-ray methods. Undoubtedly further such examples will begin to appear as more laboratories begin using $^1H-^{15}N$ long-range heteronuclear shift correlation methods at natural abundance.

Protonation of *N*-Benzylidineamidopyrazoles. Kolehmainen and co-workers[105] in the course of a study of the protonation of a series of 5-*N*-benzylidineaminopyrazoles, **33a**−**e**, have utilized $^1H-^{15}N$ GHMBC experiments

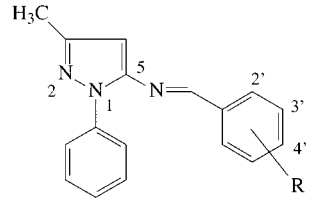

33a R = -H

33b R = 4' $-CH_3$

33c R = 4' $-N(CH_3)_2$

33d R = 4' $-NO_2$

33e R = 2' -OH

to assign the ^{15}N resonances of these molecules. Experiments were performed on 0.5 M solutions in chloroform-*d*; chemical shifts were referenced to external nitromethane. Details of the optimization of the long-range experiments were not reported.

Chemical shifts for the various nitrogens of the benzylideneaminopyrazoles are summarized in Table 5. For the unsubstituted analogue, **33a**, data were also obtained in trifluoroacetic acid. The large upfield shifts of all three nitrogen resonances is consistent with protonation at all three sites. An effort was made to determine the $^1J_{NH}$ couplings using a $^1H-^{15}N$ GHMBC experiment for which the one-bond dependent coupling was varied over the range from 70 to 120 Hz. Unfortunately, these efforts were uniformly unsuccessful, the failure attributed to proton exchange with the solvent.

Thiamine HCl. The application of long-range $^1H-^{15}N$ GHMBC to thiamine HCl (**34**) is one of the earliest

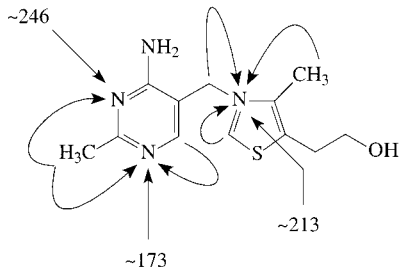

34

applications of this technique reported. This study was reported in 1993 in an abstract by Koshino and coworkers[20] using a sample prepared by dissolving 64 mg of thiamine HCl in 500 μL of solvent. The optimization of the GHMBC experiment used was not reported. Chemical shifts were referenced to external $^{15}NH_4NO_3$; actual shifts were not specified in the published work on thiamine, and consequently those shown are approximated from the published spectrum and are adjusted relative to liquid ammonia.

4-Methylaeruginoic Acid, a Cytotoxic Phenylthiazoline. A novel cytotoxic phenylthiazoline, 4-methylaeruginoic acid (**35**), has been isolated from a *Streptomyces*

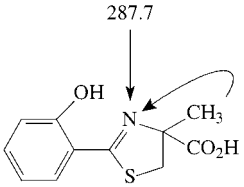

35

sp.[106] The thiazoline nitrogen exhibited a single long-range correlation to the methyl group attached to the thiazoline ring. Surprisingly, neither of the thiazoline methylene protons was coupled to the nitrogen. No details were given regarding the concentration or optimization of the $^1H-^{15}N$ GHMBC experiment performed on this compound, although it was noted that the ^{15}N chemical shift was referenced to $^{15}NH_4NO_3$; the chemical shift shown has been adjusted relative to liquid ammonia.

Piperidine and Morpholine *N*-Oxides. In an effort to develop an unequivocal method for the determination of the site of *N*-oxidation for the characterization of impurities and degradation products of pharmaceuticals, the oxazolidinone antibiotic Eperezolid (**36**) and its piperi-

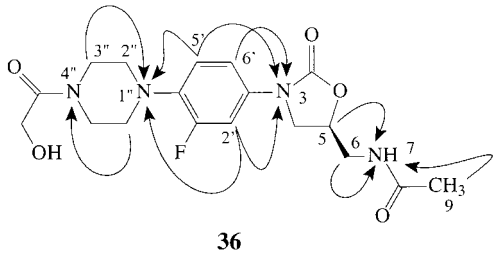

36

dine *N*-oxide (**37**) were studied to parametrize the perturbation of the ^{15}N chemical shift of the oxidized nitrogen atom. These data were subsequently used to unequivocally establish the site of *N*-oxidation of the anxiolytic PNU-101387 (**38**) as shown by **39**.[50]

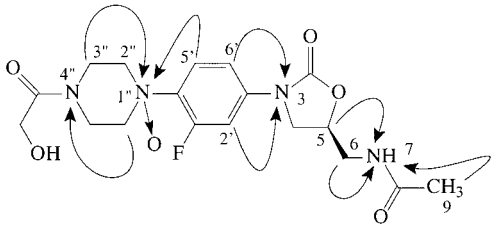

37

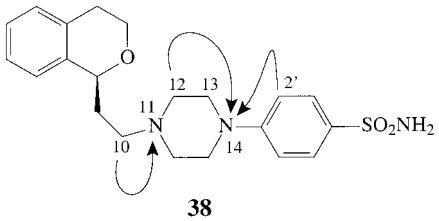

38

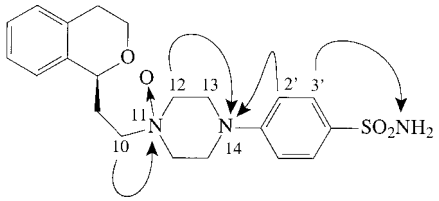

39

The long-range $^1H-^{15}N$ couplings observed for a 28 mg sample of Eperezolid (**36**) and a 37-mg sample of the corresponding *N*-oxide (**37**), both dissolved in 600 μL of DMSO-d_6, are shown with the structures. The GHMBC experiments performed on both compounds were optimized for 8 Hz. Chemical shifts are reported downfield of liquid ammonia in Table 6. The majority of the couplings observed were unremarkable with the exception of the two four-bond couplings observed from H-2′ to N-1″ and from H-5′ to N-3 for the parent drug, **36**. Neither of these long-range couplings was observed for the *N*-oxide, **37**, even though a more concentrated sample was used for the GHMBC experiment performed on the *N*-oxide.

The chemical shift differential, $\Delta\delta$ ^{15}N, following *N*-oxidation for Eperezolid (**36**) and its *N*-oxide (**37**) are also given in Table 6. As will be noted from even casual inspection of the table, there is a pronounced downfield shift of the oxidized nitrogen by +68.5 ppm, accompanied by smaller chemical shift perturbations at N-4″ (−5.2 ppm) and N-3 (+3.6 ppm). It was suggested by Martin et al.[50] that the upfield shift of N-4″ following *N*-oxidation might be mediated through space, while it was likely that the downfield shift of N-3 following oxidation was transmitted electronically through the phenyl ring. The latter effect is analogous to that observed for cryptolepine 5-oxide (**14**) although considerably smaller (see section entitled Cryptolepine 5-oxide).

Having a parametrized set of ^{15}N chemical shifts for piperidine *N*-oxidation, the ^{15}N chemical shifts and long-range $^1H-^{15}N$ couplings of the anxiolytic PNU-101387 (**38**) and its *N*-oxide degradant (**39**) were next examined. One fragment ion in the mass spectrum of **39** suggested that *N*-oxidation had occurred at N-11. The ^1H and ^{13}C NMR spectra had a pattern of chemical shift perturbations that were suggestive of *N*-oxidation at N-14, leaving the actual site of *N*-oxidation equivocal.

The acquisition of a pair of 8-Hz optimized $^1H-^{15}N$ GHMBC spectra of **38** and **39** using samples prepared by dissolving 15 and 9 mg, respectively, in 600 μL of DMSO-d_6, was undertaken in an effort to unequivocally establish

Table 6. ^{15}N Chemical Shifts Observed for Eperezolid (**36**) and Its *N*-Oxide (**37**) in DMSO-d_6[a]

position	**36**	**37**	$\Delta\delta$ ^{15}N
N-3	98.1	101.7	+3.6
N-7	109.3	109.2	−0.1
N-1″	52.3	120.8	+68.5
N-4″	111.0	105.8	−5.2

[a] Data were acquired from a 8-Hz optimized GHMBC experiment performed at 500 MHz. Chemical shifts are reported downfield of liquid ammonia.[50]

Table 7. ^{15}N Chemical Shifts Observed for PNU-101387 (**38**) and Its *N*-Oxide (**39**) in DMSO-d_6[a]

position	**38**	**39**	$\Delta\delta$ ^{15}N
N-11	44.9	113.0	+68.1
N-14	72.1	65.0	−7.1
$-SO_2NH_2$	96.5	96.2	−0.3

[a] Data were acquired from an 8-Hz optimized GHMBC experiment performed at 500 MHz. Chemical shifts are reported downfield of liquid ammonia.[50]

the site of *N*-oxidation of PNU-101387 (**38**). ^{15}N chemical shifts for both compounds are collected in Table 7 accompanied by the perturbations, $\Delta\delta$ ^{15}N, following *N*-oxidation.

The pronounced +68.1 ppm downfield shift of the N-11 resonance of **39** unequivocally established the site of *N*-oxidation in the *N*-oxidized degradant of PNU-101387. Overall, this appears to represent a reliable method for establishing the site of *N*-oxidation of pharmaceuticals, metabolites, alkaloids, and other nitrogen-containing compounds. When coupled with submicro NMR probe technology,[31,61,62] it should be possible to apply this method to milligram or even submilligram samples of drug impurities or degradants that can be realistically isolated and purified for structural characterization.

Six-Membered Ring Nitrogen Heterocycles. A number of reports have also appeared involving six-membered ring nitrogen heterocycles. Most examples presently contained in the literature incorporate the six-membered heterocycle into a larger molecular framework in some fashion.

Nicotine. Nicotine (**40**) was among the first compounds

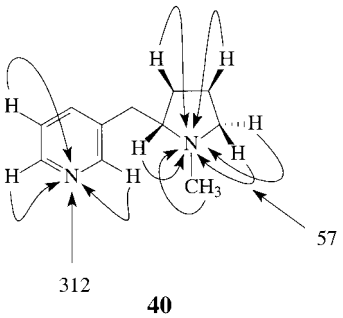

40

to be studied using long-range $^1H-^{15}N$ heteronuclear shift correlation techniques at natural abundance in the 1993 abstract of Koshino and co-workers.[20] Long-range correlations assigned the pyrrolidino nitrogen of nicotine at ~57 ppm in the published abstract. Although correlations were shown to the pyridine nitrogen on the structure in the abstract, no mention of the chemical shift was made in that report. Subsequently, Koshino and co-workers[63] again reported data for nicotine that were acquired using a 6-mg sample of the alkaloid dissolved in 300 μL of chloroform-*d* overnight (14.5 h). The experiment was optimized for 5.6 Hz; chemical shifts were referenced relative to $^{15}NH_4NO_3$ and are shown on the structure relative to liquid ammonia. Observed long-range $^1H-^{15}N$ couplings are also shown on the structure.

Ericamycin. The complex hexacyclic antibiotic ericamycin (**41**), a 2-azahexaphene isolated from *Streptomyces*

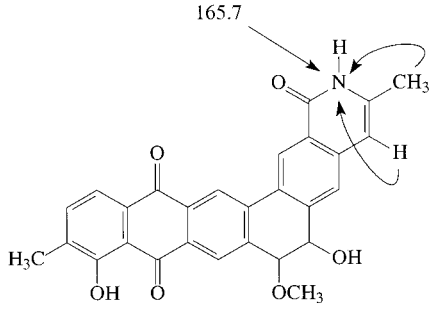

41

varius n. sp., was found to be active against various *Staphylococcal* sp. in an antibiotic screening program.[107] The 2-pyridone nitrogen was observed at 165.7 ppm using a GHMQC experiment. The reported chemical shift of the 2-pyridone nitrogen of ericamycin (**41**) is substantially downfield of the shift of the 4-quinolone nitrogen of cryptolepinone (103.4 ppm, see section entitled Cryptolepinone), but is consistent with expectation for this type of nitrogen functionality (see Supplemental Table S1). No details of the sample preparation or the optimization were given in the report. The ^{15}N chemical shift was referenced relative to $NH_4{}^{15}NO_3$, which is relatively uncommon. The chemical shift shown with the structure is reported relative to liquid ammonia. In a $^1H-^{15}N$ GHMBC experiment, three-bond couplings were observed from the 3-methyl group and the aromatic proton at the 4-position.

Clitidine. The pyridine nucleoside clitidine (**42**) has

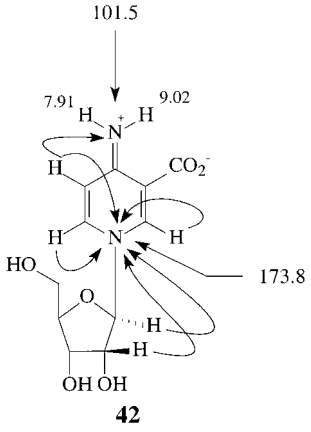

42

been isolated from the poisonous mushroom *Clitocybe acromelaga*.[108] Proton NMR and UV data suggested a 1,4-dihydropyridine rather than a pyridinium form, prompting the investigation of the tautomerism of the system using $^1H-^{15}N$ heteronuclear shift correlation methods. The study was conducted using a sample prepared by dissolving 10 mg of the nucleoside in 300 μL of D_2O or a mixture of 90:10 H_2O-D_2O. Chemical shifts were referenced downfield of $^{15}NH_4NO_3$ and are reported here relative to liquid ammonia.

A $^1H-^{15}N$ GHMQC spectrum of **42** at 4 °C showed the 4-amino nitrogen resonance, which resonated at 101.5 ppm, to be correlated to a pair of proton resonances at 7.91 and 9.02 ppm. The protons were specifically assigned as shown from NOE measurements. Two- and three-bond correla-

tions were observed from the 1′ and 2′ protons of the sugar ring to N-1, which resonated at 173.8 ppm. The upfield shift of this nitrogen resonance relative to pyridine is consistent with the 1,4-dihydropyridine structure shown.

Tubercidin Nucleoside. Another early study was that of the cyclic nucleoside tubercidin (**43**) reported in the 1993

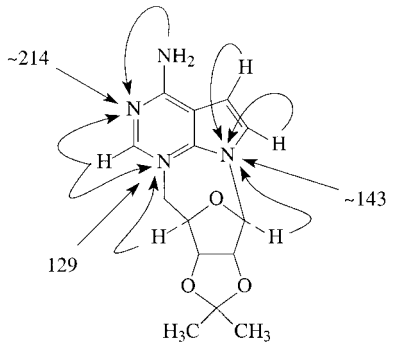

43

abstract of Koshino and co-workers.[20] Long-range correlations were observed to the three nitrogen resonances of the pyrrolopyrimidine nucleus using a sample prepared by dissolving 34 mg of the nucleoside in 400 μL of DMSO-d_6. The experiment was optimized for a 4.2-Hz, long-range coupling; the low-pass J-filter of the GHMBC sequence was used, eliminating the response from the 6-amino group. The chemical shift reference was not specified in the original report; ^{15}N chemical shifts are reported on the structure as they appeared in the original abstract and are only approximate, having been estimated from the published spectrum.

2-Azidoethylpyrimidin-2-ones. A study of the ^{15}N chemical shifts and long-range couplings of a series of 4-substituted 1-(2-azidoethyl)pyrimidin-2-ones (**44**) was

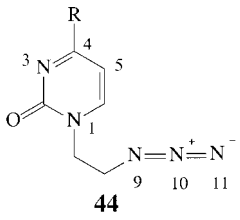

44

recently reported by Kolehmainen and co-workers.[109] Samples were prepared as saturated solutions in DMSO-d_6. The long-range delays were variously optimized for 5 or 2.5 Hz; chemical shifts were reported upfield of nitromethane and are reported here downfield of liquid ammonia.

For the unsubstituted analogue (R = H), a two-bond coupling from H-4 located the N-3 resonance at 283.5 ppm. In contrast, because of its amide nature, N-1 resonated in the range from 162 to 139 ppm, considerably upfield of N-3. The authors also report data for two of the three nitrogens of the azido group. The N-9 resonance was generally observed to resonate at ~69 ppm with relatively little variance. In contrast, the N-10 resonance was observed considerably downfield, resonating at ~248 ppm. Unfortunately, no correlations were observed to the N-11 resonance in the 2.5-Hz optimized ^{1}H−^{15}N GHMBC spectrum; the four-bond coupling from H-8 to N-11 is undoubtedly quite small. It is also interesting to note that the long-range correlation from H-5 to N-3 was not observed when the 4-position was substituted with electron-withdrawing groups. The authors suggest that by varying the electronic properties of the 4-substituent the biochemical activity of these compounds may also be affected.

Ritterazine A. The ritterazines, highly cytotoxic metabolites of the Japanese tunicate *Ritterella tokioka*, incorporate two hexacyclic polyoxygenated steroid units joined via a pyrazine ring.[110] A long-range ^{1}H−^{15}N GHMBC spectrum of ritterazine-A (**45**) was acquired at 600 MHz

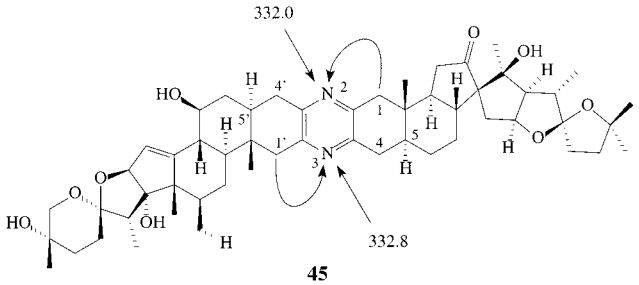

45

using a sample prepared by dissolving 20 mg of the cytotoxin in 200 μL of pyridine-d_5. The long-range delay was optimized for 8.3 Hz. The data were recorded overnight (16 h); chemical shifts are reported downfield of liquid ammonia.

The authors observed long-range correlations from the H-1 and H-1′ protons to two separate nitrogen resonances. The H-1β and H-1′β resonances were strongly coupled to their respective nitrogens, while the H-1α and H-1′α protons were more weakly coupled. No correlations were observed from the H-4 or H-4′ methylene protons or the H-5 or H-5′ methine protons, which the authors attributed to the more extensive homonuclear couplings and consequent broadening of these resonances. It is interesting to note here that a similar problem was successfully managed in the case of Delavirdine (see section entitled Delavirdine) through the use of selective 90° and 180° pulses.[49,91]

The structure of ritterazine-A, in terms of the orientation of the steroid nuclei relative to the pyrazine ring, was established by comparison to the ^{1}H−^{15}N GHMBC spectrum of the related compound ritterazine-B. The authors note that the long-range ^{1}H−^{15}N GHMBC experiment at natural abundance obviated the need for derivitization followed by the chromatographic separation and characterization of the resulting four isomers by NMR, to which ritterazine-B was subjected to establish its structure.

1,2,4-Triazolo[1,5-*a*]pyrimidine. In a very interesting experiment optimized for 1.7 Hz and performed on a 60-mg sample of 1,2,4-triazolo[1,5-*a*]pyrimidine dissolved in 350 μL of DMSO-d_6, Koshino and Uzawa[63] were able to observe all possible two-, three-, and four-bond proton−nitrogen couplings. These correlations are shown on structures **46** and **47**. The chemical shifts of the four nitrogens

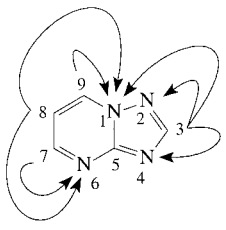

46

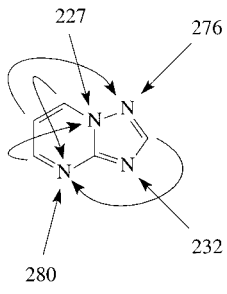

47

were originally reported relative to $^{15}NH_4NO_3$ and are adjusted relative to liquid ammonia.

To the best of our knowledge, these data represent the longest optimization (300 ms) of the long-range delay successfully employed in a $^{1}H-^{15}N$ GHMBC experiment at natural abundance. Although four-bond, long-range couplings from proton to nitrogen are not unknown, they are not common.

A Novel Endothelin-Converting Enzyme Inhibitor. A novel endothelin-converting enzyme inhibitor, B-90063, was isolated from a new marine bacterium, *Blastobacter* sp. SANK 71894.[111] The molecule is dimeric in nature, containing a pair of dihydropyridooxazole subunits linked together via a disulfide linkage as shown by **48**. The

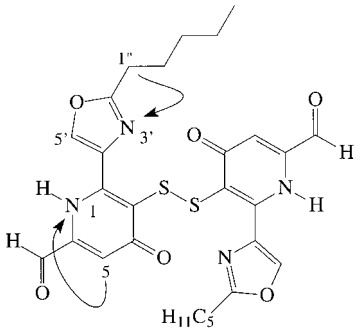

48

structure of the molecule was deduced from a series of 2D NMR experiments with heavy reliance on $^{1}H-^{13}C$ and $^{1}H-^{15}N$ GHMBC long-range correlation experiments. The *n*-pentyl moiety was attached to the 2′-position of the dihydropyridooxazole via long-range correlations from the H-1″ and H-2″ protons to C-2′. A long-range correlation was also observed from the H-1″ resonance to N-3′, which resonated at 225 ppm. Curiously, a correlation from the H-5′ resonance of the oxazole ring to N-3′ was not observed, in contrast to the work of Martin et al.,[51] on the assignment of the ^{15}N resonances of sulfomycin-I (see section entitled Sulfomycin-I), in which this correlation was observed.

Although the inability to observe the H-5′ to N-3′ long-range correlation may have been due to the optimization chosen, no details of the optimization were reported, nor did the authors specify the chemical shift referencing scheme employed. It is worth noting that the ^{15}N chemical shift of N-3′ reported in this study is somewhat upfield of the normal ^{15}N shift of oxazole, which is perhaps due to the location of N-1 β to N-3′.

The other ^{15}N resonance in **48** in the dihydropyridone portion of the molecule was located via a correlation from the H-5 resonance. N-1, which resonates at 130 ppm, confirms that the pyridyl-derived portion of the molecule is in the 1,4-dihydropyridone form on the basis of the N-1 chemical shift. In contrast, if the molecule existed as the fully aromatic pyridine, the chemical shift of N-1 would be expected to be in the range of ~320 ppm (see Supplemental Table S3).

Benzo[*c*]phenanthridine Alkaloids. In a growing series of reports, Marek and co-workers have investigated a series of benzo[*c*]phenanthridine alkaloids. The earliest of these reports dealt with chelerythrine chloride (**49a**) and sanguilutine chloride (**49b**) in a study dealing with several types of alkaloids.[94] The next report in this series dealt with C_2 symmetric benzo[*c*]phenanthridine alkaloids.[112] The structure and transformations of the alkaloid sanguilutine were also examined,[113] followed by a study of the structure of chelirubine and chelilutine free bases.[114] The most recent study in this series of papers has been a reexamination of the NMR assignments of sanguinarine pseudobase.[115]

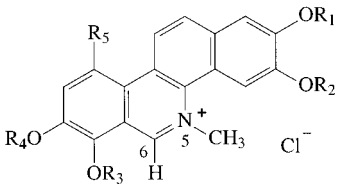

chelerythrine	**49a**	$R_1 + R_2 = -CH_2-$, $R_3 = R_4 = -CH_3$, $R_5 = -H$
sanguilutine	**49b**	$R_1 = R_2 = R_3 = R_4 = -CH_3$, $R_5 = -OCH_3$
chelirubine	**49c**	$R_1 + R_2 = R_3 + R_4 = -CH_2-$, $R_5 = -OCH_3$
sanguinarine	**49d**	$R_1 + R_2 = R_3 + R_4 = -CH_2-$, $R_5 = -H$
chelilutine	**49e**	$R_1 + R_2 = -CH_2-$, $R_3 = R_4 = -CH_3$, $R_5 = -OCH_3$

Chelerythrine Chloride and Sanguilutine Chloride. The alkaloids chelerythrine chloride (**49a**) and sanguilutine chloride (**49b**) were the first of a series of benzo[*c*]phenanthridine alkaloids to be examined using long-range $^{1}H-^{15}N$ GHMBC experiments at natural abundance beginning in 1996.[94] Samples of the alkaloids were prepared by dissolving 10−15 mg of the alkaloid in 500 μL of DMSO-d_6. The long-range experiments were optimized from 4.2 to 8.3 Hz. As noted below, the N-5-methyl and H-6 resonances had long-range couplings to N-5 of 4.4 and 5.6 Hz, respectively. The long-range couplings were estimated from $^{1}H-^{15}N$ GHSQC spectra. Given the similarity of the structures of chelerythrine (**49a**) and sanguilutine (**49b**), it is not surprising that the N-5 resonance of both alkaloids was observed at 186.2 ppm.

Chelirubine, Sanguinarine, and Chelilutine. Marek and colleagues[112] continued their study of the benzo[*c*]-phenanthridine alkaloids in 1997 with a conformational study of C_2 symmetrical analogues. Chelerythyrine (**49a**), chelirubine (**49c**), and sanguinarine (**49d**) were confirmed to form dimers using gradient inverse-detection methods. As a part of this study, Marek and co-workers determined the ^{15}N chemical shifts of a number of these compounds. The ^{15}N chemical shifts are collected in Table 8 for the compounds for which data were reported. Unfortunately, no details of the long-range $^{1}H-^{15}N$ experiments utilized or the acquisition parameters were given in the report. ^{15}N chemical shift data were also reported for the ether dimers, **50a**, **50c**, and **50d**, as well as for the amine dimers **51a** and **51d**.

Sanguilutine Chloride. Dostál and colleagues[113] have also studied the structure and transformations of **49b**. Treatment of **49b** with ammonium hydroxide afforded the corresponding dimeric ether (**50b**) and amine (**51b**). Long-range $^{1}H-^{15}N$ data were reported for only the dimeric ether and amine, **50b**, and **51b**, respectfully, in which N-5 resonated at 32.4 and 34.3 ppm, respectively, in this study. The ^{15}N chemical shifts were determined using a $^{1}H-^{15}N$ GHMBC experiment; no details of the optimization of the experiments were given.

Table 8. ^{15}N Chemical Shifts of Chelerythrine (**49a**), Chelirubine (**49c**), Sanguinarine (**49d**), and Their Corresponding Ether and Amine Dimers[112]

compound	δ ^{15}N-5
50a	39.0
51a	35.8
49c	49.7
50c	40.1
49d	50.3
50d	41.2
51d	38.4

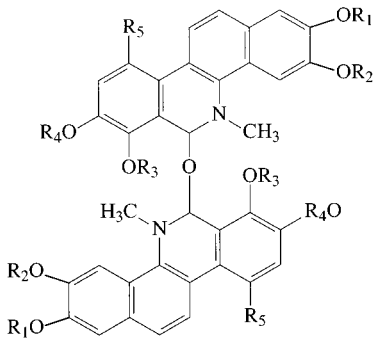

chelerythrine	**50a**	$R_1 + R_2 = -CH_2-$, $R_3 = R_4 = -CH_3$, $R_5 = -H$
sanguilutine	**50b**	$R_1 = R_2 = R_3 = R_4 = -CH_3$, $R_5 = -OCH_3$
chelirubine	**50c**	$R_1 + R_2 = R_3 + R_4 = -CH_2-$, $R_5 = -OCH_3$
sanguinarine	**50d**	$R_1 + R_2 = R_3 + R_4 = -CH_2-$, $R_5 = -H$
chelilutine	**50e**	$R_1 + R_2 = -CH_2-$, $R_3 = R_4 = -CH_3$, $R_5 = -OCH_3$

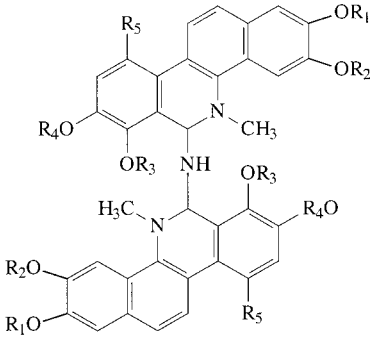

chelerythrine	**51a**	$R_1 + R_2 = -CH_2-$, $R_3 = R_4 = -CH_3$, $R_5 = -H$
sanguilutine	**51b**	$R_1 = R_2 = R_3 = R_4 = -CH_3$, $R_5 = -OCH_3$
sanguinarine	**51d**	$R_1 + R_2 = R_3 + R_4 = -CH_2-$, $R_5 = -H$
chelilutine	**51e**	$R_1 + R_2 = -CH_2-$, $R_3 = R_4 = -CH_3$, $R_5 = -OCH_3$

Chelirubine and Chelilutine Free Bases. Dostál and co-workers have also studied chelirubine and chelilutine as the free bases.[114] Chelirubine chloride (**49c**) and chelilutine chloride (**49e**), on treatment with sodium carbonate, form the corresponding free bases, which in turn yield the corresponding dihydro ether dimers, **50c**,**e**; treatment with aqueous ammonium hydroxide gave the corresponding dihydro dimeric amines, **51c**,**e**.

In the course of the NMR study of these benzo[*c*]phenanthridine alkaloids, the dimeric ethers **50c**,**e** underwent hydrolysis in chloroform-*d* to afford the corresponding 6-hydroxyl analogues, **52c**,**e**, which could not be isolated,

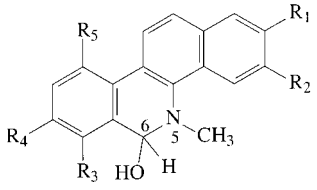

chelirubine	**52c**	$R_1 + R_2 = R_3 + R_4 = -CH_2-$, $R_5 = -OCH_3$
sanguinarine	**52d**	$R_1 + R_2 = R_3 + R_4 = -CH_2-$, $R_5 = -H$
chelilutine	**52e**	$R_1 + R_2 = -CH_2-$, $R_3 = R_4 = -CH_3$, $R_5 = -OCH_3$

and underwent spontaneous reverse condensation to a diastereomer of the ether. The ^{15}N chemical shifts were variously determined using either GHMBC or GSQMBC experiments and were referenced externally to liquid ammonia. As would be expected based on the discussion above (see Table 8), the ^{15}N resonance of the 6-hydroxy analogue, **52c**, observed at 49.7 ppm was roughly 10 ppm downfield of the dimeric dihydro ethers, **50c**,**e**, whose N-5 resonances were observed at 40.1 and 38.7 ppm, respectively.

Sanguinarine Pseudobase. More recently, Dostál and colleagues[115] reported a study of the benzo[*c*]phenanthridine alkaloid sanguinarine (**49d**). Sanguinarine is a quaternary benzo[*c*]phenanthrine widely distributed in plants of the *Papaveraceae* and other families. Treatment with hydroxide ion converts the quaternary alkaloid to its free base, often referred to using historical terminology as the pseudobase. The formation of the pseudobase has generally been assumed to be the first step in a transformation leading to the formation of the dimeric dihydro ether, the true "free base" of sanguinarine, and related benzo[*c*]-phenanthridine alkaloids. Treatment of sanguinarine free base with hydroxide or the appropriate alcohol readily leads to the formation of the corresponding 6-hydroxy or 6-alkoxyl analogues, **53a**−**c**.

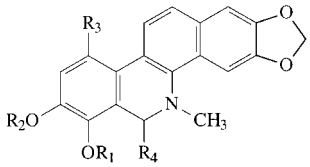

sanguinarine	**53a**	$R_1 + R_2 = -CH_2-$, $R_3 = -H$, $R_4 = -OH$
	53b	$R_1 + R_2 = -CH_2-$, $R_3 = -H$, $R_4 = -OCH_3$
	53c	$R_1 + R_2 = -CH_2-$, $R_3 = -H$, $R_4 = -OCH_2CH_3$
chelirubine	**53d**	$R_1 = R_2 = -CH_3$, $R_3 = -OCH_3$, $R_4 = -OH$
chelilutine	**53e**	$R_1 = R_2 = -CH3$, $R_3 = -OCH_3$, $R_4 = -OH$
chelerythrine	**53f**	$R_1 = R_2 = -CH_3$, $R_3 = H$, $R_4 = -OCH_2CH_3$
dihydrosanguinarine	**53g**	$R_1 + R_2 = -CH_2-$, $R_3 = R_4 = -H$
dihydrochelerythrine	**53h**	$R_1 = R_2 = -CH_3$, $R_3 = R_4 = -H$

The ^{15}N chemical shifts of **53a**−**c** in chloroform-*d* were determined using a GHMBC experiment. Chemical shifts are reported downfield of externally referenced liquid ammonia. The chemical shifts of **53a**−**c** were 50.3, 40.3, and 41.3, respectively. This study represents the first experimental evidence for the formation of 6-hydroxysanguinarine, **53a**.

Benzylisoquinoline and Quinoline Alkaloids. Marek and co-workers have also reported several studies of various members of the benzylisoquinoline family of alkaloids. The earliest study considered only armepavine (**54**).[94]

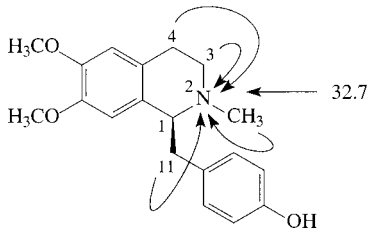

54

Armepavine was also the subject of a subsequent, more detailed NMR and X-ray crystallographic study.[116] A comprehensive study of a number of different isoquinoline

Table 9. ^{15}N Chemical Shifts of Various Benzo[*c*]phenanthridine Alkaloids Determined Using $^{1}H-^{15}N$ Long-Range Heteronuclear Chemical Shift Correlation Experiments at Natural Abundance[117]

alkaloid		δ ^{15}N	alkaloid		δ ^{15}N
chelerythrine chloride	**49a**	186.2[a]	bis(dihydrochelilutinyl)amine	**51e**	35.4[b]
sanguilutine chloride	**49b**	186.6[a]	6-hydroxydihydrosanguinarine	**53a**	50.3[b]
chelirubine chloride	**49c**	186.3[a]	6-methoxydihydrosanguinarine	**53b**	40.3[b]
sanguinarine chloride	**49d**	186.0[a]	6-hydroxydihydrochelerythrine	**53c**	50.3[b]
bis(dihydrochelerythrinyl) ether	**50a**	39.0[b]	6-hydroxydihydrochelirubine	**53d**	49.7[b]
bis(dihyrdosanguilutinyl) ether	**50b**	32.4[b]	6-ethoxydihydrosanguinarine	**53e**	41.3[b]
bis(dihydrochelirubinyl) ether	**50c**	40.1[b]	6-ethoxydihydrochelerythrine	**53f**	41.3[b]
bis(dihydrosanguinarinyl) ether	**50d**	41.2[b]	dihydrosanguinarine	**53g**	21.1[b]
bis(dihyrdochelilutinyl) ether	**50e**	38.7[b]	dihydrochelerythrine	**53h**	21.2[b]
bis(dihydrochelerythrinyl)amine	**51a**	35.8[b]	norcheleryhrine	**57**	298.6[b]
bis(dihydrosanguilutinyl)amine	**51b**	34.2[b]	chelidonine	**58a**	38.6[b]
bis(dihydrosanguinarinyl)amine	**51d**	38.4[b]	homochelidonine	**58b**	39.5[b]

[a] DMSO-d_6. [b] Chloroform-*d*.

alkaloids, including a summary of work done on the benzo[*c*]phenanthridines, protoberberines, benzylisoquinolines, aporphines, pavinanes, and the β-carboline-proaporphines, has recently been reported.[117]

Benzylisoquinoline Alkaloids: Armepavine, Papaverine, and Escholamine Iodide. Armepavine was the first of the benzylisoquinoline alkaloids to be studied.[94,116] Using a GHMBC experiment performed on a sample prepared by dissolving 30 mg of armepavine (**54**) in 500 μL of chloroform-*d*, correlations were observed from both of the 3- and one of the 4-methylene protons to the tetrahydroisoquinoline nitrogen resonating at 32.7 ppm. Correlations were also observed from the *N*-methyl and both of the 11-methylene protons, but the two-bond correlation from the 1-methine proton was not observed in the spectrum. Details of the optimization of the experiment were not provided in the initial study.[94] The subsequent study of armepavine reported the optimization of the GHMBC experiment at 5 Hz.[116]

Papaverine (**55**) an isoquinoline alkaloid, resonated at

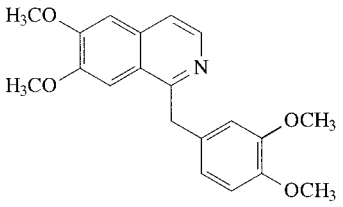

55

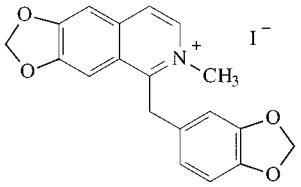

56

297.2 ppm, consistent with its fully aromatic nature. Finally, escholamine iodide (**56**), a quinolinium salt, resonated upfield of papaverine at 189.9, which is also consistent with the general range noted above in Tables 9 and 10 for the salts of the benzo[*c*]phenanthridine and protoberberine alkaloids, respectively.

Isoquinoline and Isoquinoline-Derived Alkaloids. In what is undoubtedly the most comprehensive long-range $^{1}H-^{15}N$ study to appear to date, Marek and co-workers[117] have reported the ^{15}N chemical shifts of members of a number of isoquinoline-derived alkaloids. Sufficient data are presented in this comprehensive work for generalities to begin to be drawn for the various families of alkaloids covered in the work. The various generalizations and

Table 10. ^{15}N Chemical Shifts of Various Protoberberine Alkaloids Determined Using $^{1}H-^{15}N$ Long-Range Heteronuclear Chemical Shift Correlation Experiments at Natural Abundance[117]

alkaloid		δ ^{15}N	alkaloid		δ ^{15}N
berberine chloride	**59a**	194.0[a]	tetrahydropalmatine	**60c**	48.5[b]
coptisine chloride	**59b**	194.1[a]	tetrahydropalmatine	**60c**	47.3[a]
canadine	**60a**	48.4[b]	tetrahydropalmatine	**60c**	47.1[c]
stylopine	**60b**	48.3[b]	oxoberberine	**61**	153.0[b]
			dihydroberberine	**62**	63.4[b]

[a] DMSO-d_6. [b] Chloroform-*d*. [c] Acetone-d_6.

categories of alkaloids described in this valuable work will be treated briefly in the following paragraphs. The benzylisoquinolines considered in this study, papaverine (**55**) and escholamine iodide (**56**), are treated in the preceding section.

Among the benzo[*c*]phenanthridine family, it was observed that the N-5 pyridinium-containing members of the group generally exhibited nitrogen resonances at approximately 186 ppm. Examples included chelerythine chloride (**49a**), sanguilutine chloride (**49b**), chelirubine chloride (**49c**), and sanguinarine chloride (**49d**). The ^{15}N chemical shifts for these alkaloids are collected in Table 9. The aliphatic (dihydro) members of the group, depending on the nature of the substitution at the 6-position, exhibited nitrogen resonances in the broad range of ~20 to 50 ppm. The 6-hydroxy analogues had nitrogens resonating the farthest downfield, near 50 ppm. Included in this group are 6-hydroxysanguinarine (**53a**), 6-hydroxychelerythine (**53c**), and 6-hydroxychelirubine (**53d**). The 6-alkoxyl derivatives and the bisether dimeric analogues exhibited nitrogen resonances in the range 38−41 ppm. The 6-alkoxy analogues included 6-methyoxysanguinarine (**53b**), 6-ethoxysanguinarine (**53c**), and 6-ethoxychelerythine (**53f**). The bisamine dimeric analogues (**51a**−**e**) had nitrogen resonances in the range 34−38 ppm. Chemical shift data are also included for the biethers **50a**−**e**. The nitrogen resonances of the 5,6-dihydro alkaloids were observed the farthest upfield, in the vicinity of 21 ppm for the two examples reported, dihydrosanguinarine (**53g**) and dihydrochelerythrine (**53h**). Chemical shifts were, again, not reported for the linking N−H resonances; all data for the bisamine dimers were taken in chloroform-*d*. The ring nitrogens of the bisamines resonated near 35 ppm. The only fully aromatic example described, norchelerythrine (**57**), resonated at 298.6 ppm, consistent with the pyridine-like nature of its nitrogen resonance. Finally, two 5,6,11,12-tetrahydroisoquinoline alkaloids were described which included chelidone (**58a**) and homochelionine (**58b**). The ring nitrogens for both resonated near 39 ppm.

Marek and co-workers[117] reported data for a more limited assortment of protoberberine alkaloids. The pyridinium

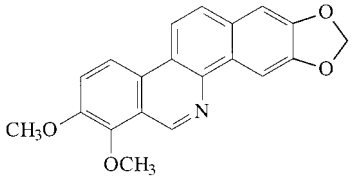

57

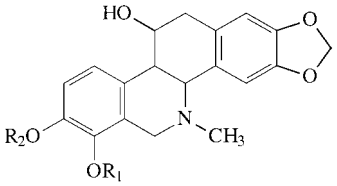

58a $R_1 + R_2 = -CH_2-$

58b $R_1 = R_2 = -CH_3$

chlorides resonated downfield of the corresponding members of the benzo[*c*]phenanthridine group by approximately 8 ppm at ~194 ppm. Examples included berberine chloride (**59a**) and coptisine chloride (**59b**). The tetrahydro ana-

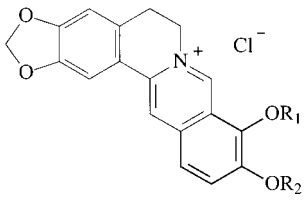

59a $R_1 = R_2 = -CH_3$

59b $R_1 + R_2 = -CH_2-$

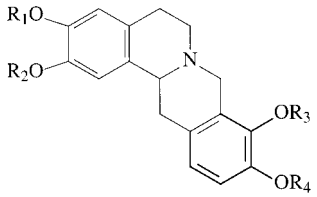

60a $R_1 + R_2 = -CH_2-$, $R_3 = R_4 = -CH_3$

60b $R_1 + R_2 = R_3 + R_4 = -CH_2-$

60c $R_1 = R_2 = R_3 = R_4 = -CH_3$

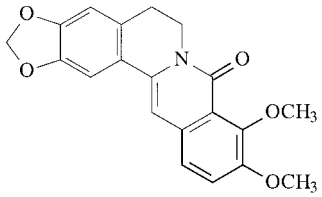

61

logues resonated at 47−48 ppm. Data for a reasonably extensive set of examples were reported, which included canadine (**60a**), stylopine (**60b**), and tetrahydropalmatine (**60c**) in multiple solvents (chloroform-*d*, DMSO-d_6, and acetone-d_6). In the three solvents in which data for tetrahydropalmatine were acquired, the observed chemical shift differences were <1.5 ppm. Oxoberberine (**61**), the sole amide of the group to be studied, resonated at 153.0 ppm, which is at about the downfield limit of amide ^{15}N chemical shifts. The sole dihydro analogue reported, dihydroberberine (**62**), resonated at ~63 ppm. The ^{15}N chemical shift data for the protoberberines are summarized in Table 10.

Peptides and Cyclic Peptides. To date, there have been relatively few long-range $^1H-^{15}N$ studies of peptides

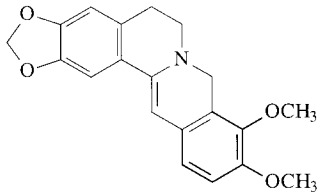

62

or cyclic peptides to appear. The earliest was a study of the cyclic peptide antibiotic quinomycin-A that was contained in the report by Koshino and Uzawa[63] demonstrating the feasibility of long-range $^1H-^{15}N$ studies at natural abundance. Next there appeared a study of the lipopeptides crambins-A and -B from the Caribbean cyanobacterium *Lyngbya majuscula* in which $^1H-^{15}N$ GHMBC was utilized.[118] Long-range $^1H-^{15}N$ experiments were extensively used by one of the authors in an effort to assign the nitrogen resonances of the thiopeptide antibiotic sulfomycin-I.[51] $^1H-^{15}N$ GHMBC data were employed in the elucidation of the structure of the antifungal antibiotic YM-75518, which contains a novel methoxy imino group in its structure.[119] Finally, a novel application of the $^1H-^{15}N$ PEP-GHSQC-TOCSY with the peptide bombesin (**67**) has been reported.[37]

Quinomycin-A. The cyclic peptide antibiotic quinomycin-A (**63**) was the first peptide natural product to be

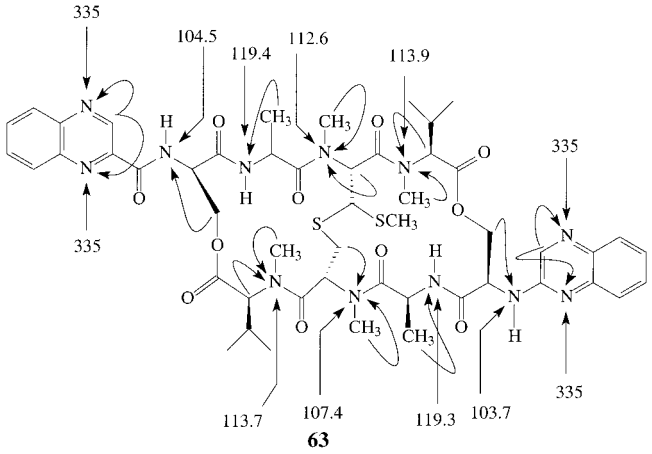

63

examined by long-range $^1H-^{15}N$ GHMBC at natural abundance.[63] Data were acquired using a sample prepared by dissolving 21 mg of the antibiotic in 400 μL of DMSO-d_6. The experiment was optimized for 8.3 Hz; data were acquired in 34 h and were referenced to $^{15}NH_4NO_3$. Chemical shifts have been adjusted for external liquid ammonia and are shown on the structure above. A mix of two- and three-bond long-range correlations were observed in the study. It is also interesting to note that relatively few of the possible two-bond correlations from the α-methine protons to their respective nitrogens were observed in the long-range data recorded.

Crambins-A and -B. The lipopeptides crambins-A (**64**) and -B were recently isolated from the butanol extract of

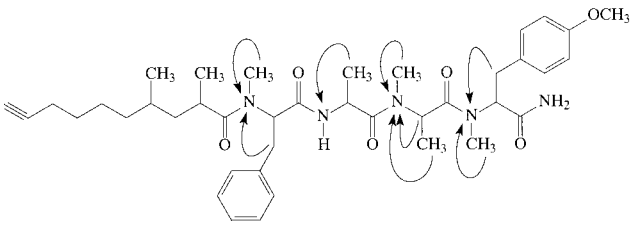

64

the marine cyanobacterium *Lyngbya majuscula* by Gerwick and colleagues.[118] Long-range $^1H-^{15}N$ GHMBC was employed in the elucidation of the structures of these linear pentapeptides. Although the data were acquired in DMSO-d_6, no details of the concentration of the sample, the optimization, or the observed ^{15}N chemical shifts were contained in the report. Only the long-range correlation pathways for crambin-A (**64**) were reported.

Sulfomycin-I. Sulfomycin-I (**65**) is a member of the

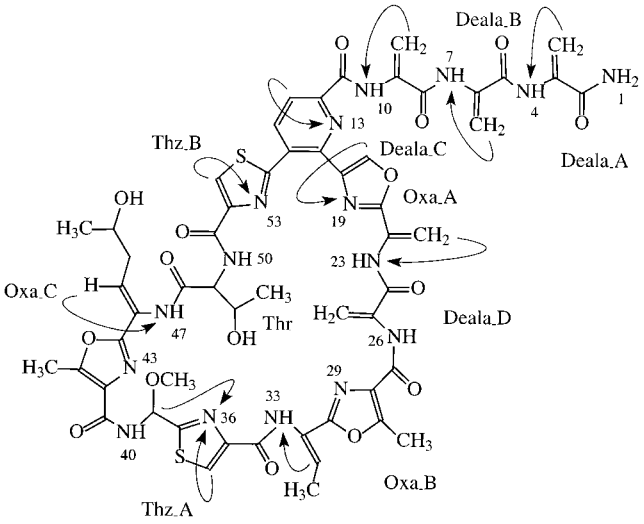

65

family of thiopeptide antibiotics elaborated by various *Streptomyces* spp. Several studies employing ^{15}N direct observation have been reported for various members of this family of antibiotics. The earliest such study was performed on nosiheptide.[120] During a study of the biosynthesis of nosiheptide, the ^{15}N resonances were totally assigned by direct observation methods using ^{15}N-labeled material.[121] More recently, nosiheptide was used as a model compound for the development of new inverse-detected 2D NMR pulse sequences.[122] Finally, the ^{15}N chemical shifts of thiostrepton and siomycin were also the subject of an early ^{15}N direct observation study.[123]

Long-range $^1H-^{15}N$ data were acquired at natural abundance for sulfomycin-I using a sample containing either 100 mg in 600 μL or 25 mg in 160 μL of DMSO-d_6 for studies employing 5- and 3-mm gradient inverse probes, respectively.[51] The data reported were acquired using a GHNMBC[49] pulse sequence, although the authors also commented negatively on the utility of the D-HMBC experiment to acquire these data. Experiments were optimized for long-range couplings ranging from 6 to 10 Hz. Chemical shifts are summarized in Table 11 and are reported downfield of external liquid ammonia.

YM-75518, a Novel Macrocyclic Peptide Lactone Antifungal Antibiotic. The antifungal antibiotic YM-75518 (**66**) was isolated from a fermentation broth of a *Pseudomonas* sp. grown from a soil sample collected in Indonesia.[119] The structure is comprised of a 15-membered macrolactone ring and a methoxy imino structure. Long-range $^1H-^{15}N$ data were acquired using the GHMBC experiment on a sample prepared by dissolving 4 mg of **66** in 550 μL of DMSO-d_6. The optimization of the experiment was not reported; chemical shifts were reported downfield of external liquid ammonia. While the ^{15}N chemical shift of the secondary amide nitrogen was typical, the methoxy imino nitrogen resonance observed at 408 ppm is noteworthy, and consistent with expectation, for this type of substituent.[8]

Table 11. ^{15}N Chemical Shifts of Sulfomycin-I (**65**) in DMOS-d_6[51] [a]

position	residue	δ ^{15}N
N-1	deala-A	99.8
N-4	deala-A	1215
N-7	deala-B	119.7
N-10	deala-C	118.6
N-13	pyridine	302.8
N-19	oxazole-A	255.8
N-23		117.0
N-26	deala-D	121.0
N-29	oxazole-B	no response
N-33		115.7
N-36	thiazole-A	310.6
N-40		123.0
N-43	oxazole-C	no response
N-47		117.3
N-50	threonine	110.3
N-53	thiazole-B	314.3

[a] Data were acquired using the GHNMBC pulse sequence.

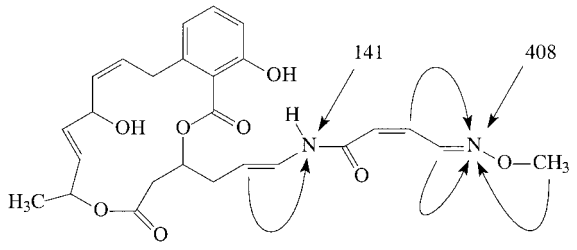

66

Application of PEP-GHSQC-TOCSY to the Identification of Proton Spin Systems of Bombesin. Williamson, Márquez, and Gerwick[37] recently reported a novel application of the PEP-GHSQC-TOCSY experiment using ^{15}N natural abundance to sort the amino acid spin systems of the peptide bombesin (**67**). The approach used by the

pGlu1 – Glu2 – Arg3 – Leu4 – Gly5 – Asn6 – Gln7 – Trp8

|

Met14 – Leu13 – His12 – Gly11 – Val10 – Ala9

67

authors takes advantage of the somewhat broader range of amide ^{15}N chemical shifts (20−50 ppm vs only 5−10 ppm for the α carbon chemical shift range), relative to the shift range of the α carbons, and exploits this broader shift range as a basis for sorting the homonuclear spin systems via the ^{15}N chemical shift.

The experiment used by the authors (see section entitled GHSQC-TOCSY) employs the idea of Cavanaugh et al.[38] of preserving equivalent pathways, or PEP, to enhance the sensitivity of the experiment by a factor of $2^{1/2}$. Following the labeling of the amide N−H protons of the various amino

Table 12. ^{15}N Chemical Shifts for the Peptide Bombesin (**67**) in DMSO-d_6 at 600 MHz[37]

amino acid	δ ^{15}N	amino acid	δ ^{15}N
p-Glu-1	115.8	Trp-8	112.3
Gln-2	112.6	Ala-9	115.4
Arg-3	113.2	Val-10	108.2
Leu-4	114.0	Gly-11	100.6
Gly-5	102.9	His-12	109.9
Asn-6	111.6	Leu-13	114.4
Gln-7	113.6	Met-14	112.5

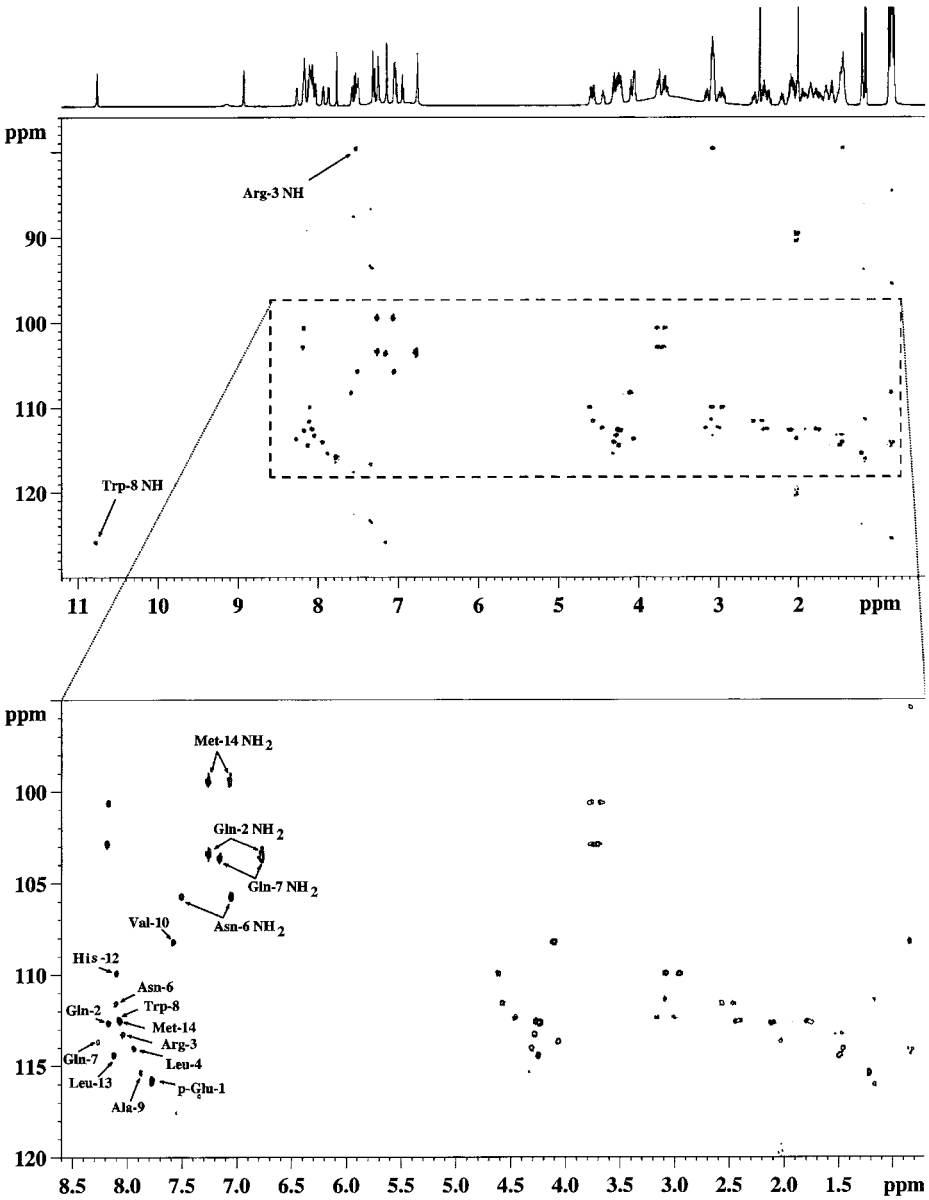

Figure 16. Natural abundance PEP-GHSQC-TOCSY spectrum of the linear peptide bombesin (**67**).[37] The experiment first establishes the direct $^{1}H-^{15}N$ chemical shift correlation, after which magnetization is propagated along the individual amino acid backbones. This technique provides a novel method for disentangling overlapping proton−proton spin-coupling networks of peptides. (Data generously provided by R. T. Williamson, B. Marquez, and W. H. Gerwick; reprinted with permission from Elsevier Science.)

acids with the chemical shift of the directly bound nitrogen, magnetization is propagated down the homonuclear spin system of the amino acid using a DIPSI-2 (TOCSY) sequence. In this fashion, the chemical shifts of the entire amino acid spin system can be uniquely sorted by the ^{15}N chemical shift of the nitrogen to which the α proton is directly bound, as shown schematically by **68**. ^{15}N chemical

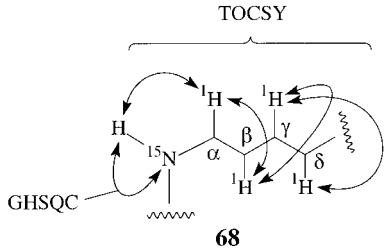

68

shifts for bombesin are collected in Table 12; the PEP-GHSQC-TOCSY spectrum is shown in Figure 16.

Miscellaneous Reports. Finally, several reports have appeared containing applications of long-range $^{1}H-^{15}N$ 2D NMR studies at natural abundance that cannot be readily grouped. Among this group are a study of dimethylpenta-3,4-dienal derivatives,[124] a study of P−S−N-containing ring systems,[125] a study of a series of Ritter reactions,[126] and an unsuccessful attempt to employ $^{1}H-^{15}N$ GHMBC to assign proton resonances of a degradation product of rubreserine.[127] Also included are studies of salicylaldoximes,[129] acylselenoureas,[130] arylglycines,[131] organometallic studies,[132−134] Schiff base podates,[135] and lithocholic acid analogues.[136]

2,2-Dimethylpenta-3,4-dienal Derivatives. Marek[124] has reported the utilization of $^{1}H-^{15}N$ inverse-detected 2D NMR methods to determine $^{1}H-^{15}N$ couplings of a series of 2,2-dimethylpenta-3,4-dienal derivatives (**69**, **70**, and **71**). ^{15}N chemical shifts and long-range $^{1}H-^{15}N$ couplings are summarized in Table 13. Long-range correlations were established using a GHMBC experiment optimized for between 4.2 and 8.3 Hz. Samples were prepared in 500 μL

Table 13. ^{15}N Chemical Shifts and $^{1}H-^{15}N$ Coupling Constants for a Series of 2,2-Dimethylpenta-3,4-dienal Derivatives in Chloroform-*d*[124]

compound	N-8	N-9	$^{1}J_{H-9,N-9}$	N-7′	N-8′	$^{2}J_{H-1,N-8}$	$^{2}J_{H-1,N-9}$	$^{2}J_{H-9,N-8}$
69a	306.3	149.2	97.0	365.4	367.8	3.4	8.5	3.4
70a	305.4	149.5	97.5	365.4	367.7	3.4	8.8	3.1
70b	311.2	143.9	92.0	370.4		3.4	8.3	2.5
70c	345.3					2.7		
70d	319.4	162.4	not obs	214.6		3.7	7.4	not obs
71b	313.2	144.7	91.5	370.8		3.5	7.9	3.2
71e	311.8	141.5	96.0	371.6		3.7	8.0	2.6

of chloroform-*d* using quantities that range from a few to >100 mg. Long-range $^{1}H-^{15}N$ coupling constants were measured using a phase-sensitive GSQMBC experiment (see section entitled GSQMBC). Chemical shifts were originally reported downfield of external liquid ammonia.

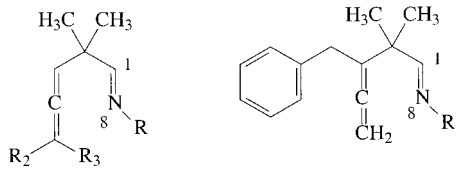

69 R_2 = -CH_3, R_3 = -H
70 $R_2 = R_3$ = -CH_3

71

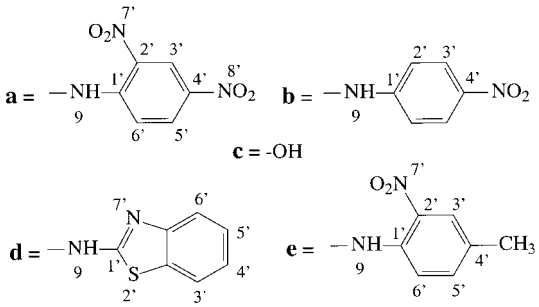

a = **b** = **c** = -OH

d = **e** =

Reaction of 2,4-(Naphthalene-1,8-diyl)-1,3,2,4-dithiaphosphetane 2,4-Disulfide with Hexamethyldisilazane. The reaction of 2,4-(naphthalene-1,8-diyl)-1,3,2,4-dithiaphosphetane 2,4-disulfide (**72**) with hexamethylsilazane was studied, in part, using $^{1}H-^{15}N$ GHMBC and GSQMBC[42] experiments optimized from 5 to 10 Hz.[125]

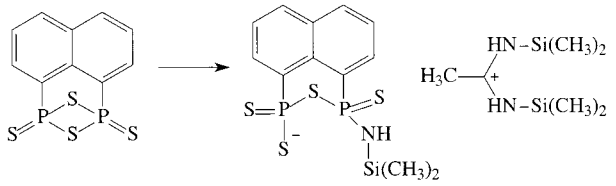

72 **73**

Chemical shifts were reported downfield of external liquid ammonia. Details of the sample preparation were not reported; data were acquired in acetonitrile-d_3. The reaction incorporated a molecule of the hexamethyldisilazane to give the structure shown by **73**. Two distinct nitrogen resonances were observed for samples run in methylene chloride-d_2 or acetonitrile-d_3. The nitrogen attached covalently to one of the phosphorus atoms after the opening of the P−S−P bond resonated at 68.5 ppm with a −76-Hz one-bond coupling. The equivalent nitrogens of the countercation resonated at 133.1 ppm with a −72-Hz one-bond coupling and long-range couplings to the methyl (−4.8 Hz) and trimethylsilyl methyl protons (−3.5 Hz).

A Study of the Product of a Ritter Reaction of a Schiff Base with Dimethyl Acetylenedicarboxylate. The reaction of the Schiff base whose structure is shown by **74** with dimethyl acetylenedicarboxylate (DMAD) afforded the adduct shown by **75**.[126] Long-range $^{1}H-^{15}N$

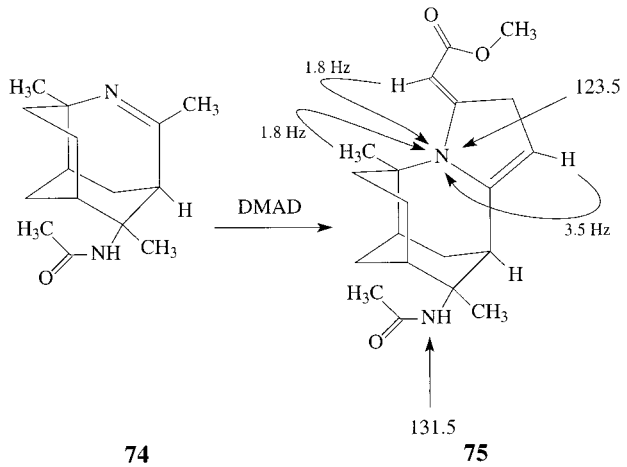

74 **75**

correlations were used in the elucidation of the structure. In particular, long-range $^{1}H-^{15}N$ coupling constants were used to aid in establishing the stereochemistry of the adduct shown. ^{15}N chemical shifts were determined using a GHMBC experiment; long-range couplings were extracted from a 1D GHSQC spectrum optimized for the long-range couplings. Nitrogen chemical shifts were originally referenced relative to nitromethane and have been adjusted and reported herein downfield of external liquid ammonia.

Blue Degradation Products of Rubreserine. The attempted application of long-range $^{1}H-^{15}N$ methods at natural abundance to colored degradants of rubreserine was a failed attempt to use a $^{1}H-^{15}N$ GHMBC experiment. The *o*-quinone analogue of the alkaloid physostygmine, **76**, reacts under ammonia gas to form isomeric, dimeric structures with a phenoxazine central core, one of which is shown by structure **77**.[127] The researchers used a $^{1}H-^{15}N$ GHMBC experiment optimized for 2 Hz in an effort "...to provide any useful information to confirm the assignment of the quaternary carbons in the central portion of these molecules". It is unclear from the brief mention of this attempt to utilize long-range $^{1}H-^{15}N$ NMR how the data would have been applied in the assignment of the quaternary carbons in this molecule. It is also unfortunate that the authors did not report whatever nitrogen chemical shift and long-range coupling pathway information may have been available from the experiment performed.

Spectral Assignment of Salicylaldoximes. Kohlemainen and co-workers[128] have studied a series of 4- and 5-substituted salicylaldoximes, **78a**−**h**, to examine the possibility of an intramolecular double bond improving correlations between NMR spectral parameters and substituent constants. The observed range of $^{15}N-OH$ chemical

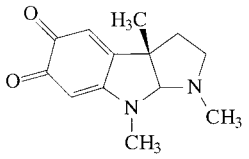

76

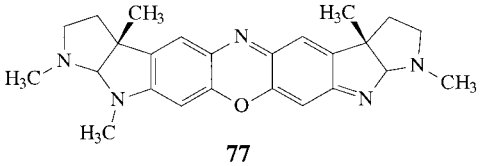

77

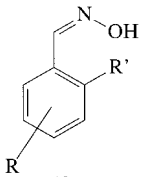

78

shifts (24.7 ppm) was found to be comparable to *p*-substituted benzaldoximes.[129] Electron-donor substituents shift the signal of the oxime upfield. Comparison of the 2-hydroxyl and 2-unsubstituted 4-*N*,*N*-dimethylamino-substituted analogues shows that the 2-hydroxyl group also shifts the nitrogen substantially (~21 ppm) upfield. This shift is believed to be due to superposition of the inductive/resonance effects of the 2-hydroxyl group and the intramolecular bonding between the oxime nitrogen (N·····H−O−C_2) The study concluded that the ^{13}C data do not support the contention that there is a mixture of "free" and "hydrogen-bound" forms of the salicylaldoximes in solution in DMSO-d_6. The ^{15}N chemical shifts of the salicylaldoximes reported in this study are presented in Table 14. The original data were referenced relative to nitromethane and are reported here downfield of liquid ammonia.

Acylselenoureido Thiophene-3-carboxylates and Their Benzo Analogues. Long-range ^{1}H−^{15}N GHMBC and GSQMBC experiments were employed in the characterization of a series of acylselenoureas represented by the general structure **79**.[130] Long-range couplings to the two

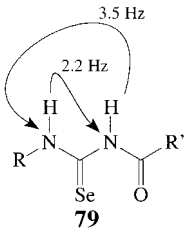

79

urea nitrogens were relatively small and were measured using the phase-sensitive GSQMBC experiment.

A series of acylselenoureas were prepared where the substituent group, R, was either a phenyl or a *tert*-butyl group. ^{15}N chemical shifts for the urea nitrogens of **80a** and **80b** were in the range 150−170 ppm downfield of liquid ammonia measured in $CDCl_3$ (Table 15). Photoisomerization gave the corresponding acylisoselenoureas, **81a** and **81b**. As expected, with the isomerization of the double bond, the N-3 resonance was shifted considerably

Table 14. ^{15}N Chemical Shifts of a Series of Salicylaldoximes, **78**, in DMSO-d_6[128]

compound	R′	R	C=N−OH δ^{15}N	other δ ^{15}N
78a	OH	5-NO_2	362.0	369.5
78b	OH	5-Cl	359.9	
78c	OH	5-Br	354.2	
78d	OH	5-OMe	356.9	
78e	OH	H	357.7	
78f	OH	4-OMe	344.6	
78g	OH	4-NMe_2	337.3	52.5
78h	H	4-NMe_2	358.0	50.4

Table 15. ^{15}N Chemical Shifts of a Series of Acylselenourea Analogues Measured in $CDCl_3$[130]

compound	substituent	^{15}N N-1	^{15}N N-3
80a	Ph	156.2	164.8
80b	t-Bu	156.1	163.9
81a	Ph	135.9	240.2
81b	t-Bu	133.8	241.4

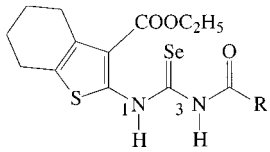

80

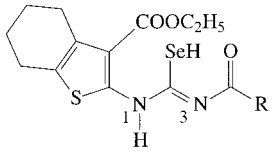

81

downfield from its position in the precursor selenourea. It is also interesting to note that the long-range coupling from the proton attached to N-1 to N-3 increased from 2.2 to 4.7 Hz following the photoisomerization to the selenoisourea. The authors also note that further details of the long-range heteronuclear couplings are to be published elsewhere. As of the date that this review was completed, this work had not been submitted for publication, insofar as we are aware.

A Study of the Resonance and Polar Effect of Substituents in *N*-Arylglycines. A study of the effect of various substituents on the ^{15}N chemical shift of a series of *N*-arylglycines, **82**, showed a strong dependence on a

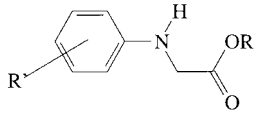

82

linear combination of inductive and resonance substituent constants.[131] The contribution of resonance to chemical shifts was much higher than that due to polar effects. Chemical shifts were originally reported using nitromethane as a chemical shift reference (see Table 16).

Organometallic Applications. Some examples of applications of long-range ^{1}H−^{15}N heteronuclear chemical shift correlation have begun to appear in the field of orgnometallic chemistry. Doubtless as more laboratories begin to gain experience using these techniques, such applications will become more numerous.

Interaction of Palladium with Pyridylpyrazole and Pyridylimidazoles. Three studies have recently appeared[132−134] that dealt with the study of the interaction of pyridylpyrazole and pyridylimidazole systems, respectively, with palladium. In the first study of the cyclopropanation of ketene silyl acetal with allylic acetates, novel η^3-allyl palladium pyridylpyrazoles were studied by long-range ^{1}H−^{15}N at natural abundance to establish the

Table 16. ^{15}N Chemical Shifts of Some Substituted *N*-Arylglycines (**82**) in DMSO-d_6

R′ substituent	R = H	R = Et
p-NO_2	77.8	76.4
p-CN	70.8	70.3
m-CN	62.5	
p-Ac	70.1	69.1
p-COPh	71.2	
p-CO_2Et	69.8	67.9
m-Cl	66.9	61.0
p-Cl	60.1	59.1
p-OPh	57.6	55.9
H	59.1	58.5
p-Me	56.8	57.9
p-OMe	55.3	53.0
p-OH	53.0	

Table 17. ^{15}N Chemical Shifts of Pyridylpyrazole−Palladium Complexes Determined Using $^1H-^{15}N$ Long-Range Heteronuclear Shift Correlation at Natural Abundance[132−134]

position	**83**	**84**
N-1	219.7	236.3
N-2	189.9	288.3
N-11	225.3	218.7

location of the double bonds in the pyrazole portion of the complex.[132] The starting complex, represented by **83**, carried bonds from the palladium to the pyridine nitrogen, N-11, and to the N-1 resonance of the pyrazole, which was sp^2 hybridized. Following treatment with sodium methoxide in a mixture of deuterated methylene chloride/methanol, double-bond isomerization occurred in the pyrazole ring, as reflected by the dramatic ^{15}N shifts observed in Table 17.

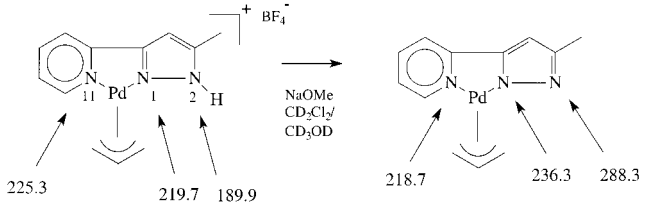

83 **84**

Behavior similar to that just described was noted in the subsequent study of the complex of palladium with a pyridylimidazole, **85**.[133] Treatment of **85** with base isomer-

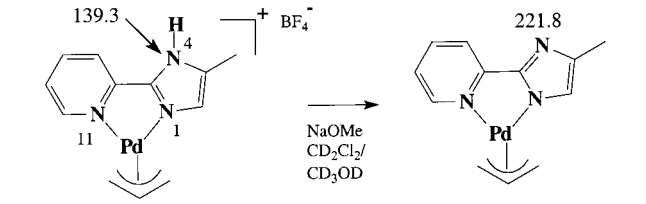

85 **86**

ized the double bonds of the imidazole ring, N-4 shifting downfield from 139.3 ppm in **85** to 221.8 ppm in **86**. No chemical shift data were given in this report for the other imidazole nitrogen or for the pyridine nitrogen.

Most recently, the asymmetric cyclopropanation of ketene silyl acetal (**87**) has been reported using these methods.[134] The structure of the palladium complex in DMSO-d_6 was studied using long-range $^1H-^{15}N$ methods at natural abundance.

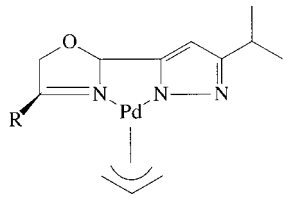

87

^{15}N chemical shifts were referenced in all three studies downfield of $^{15}NH_4NO_3$ and are reported here referenced to liquid ammonia. No details of the optimization of the experiments performed were given, nor were the specific long-range couplings observed reported.

Characterization of Schiff-Base Podates. Long-range $^1H-^{15}N$ studies at natural abundance have recently been directed toward the characterization of the cadmium binding of linear and three-armed podands by Jäntti and co-workers.[135] The podands were synthesized via the reaction of pyridine-2-carbaldehyde with a series of polyfunctional amines to afford **88** and **89**. Complexation with

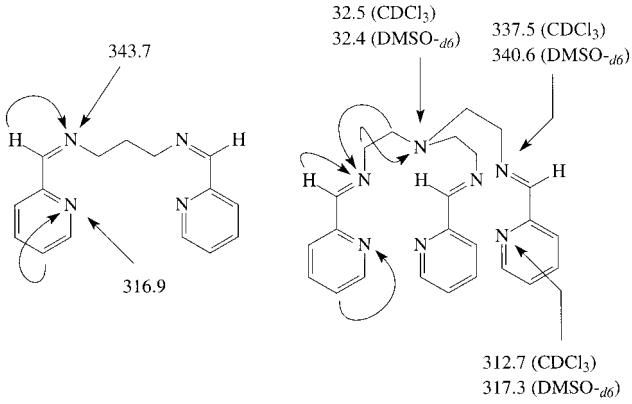

88 **89**

cadmium perchlorate was studied by ^{113}Cd and $^1H-^{15}N$ GHMBC NMR experiments. The ^{15}N chemical shifts for the imine nitrogen of **88** shifted from 343.7 ppm for the free ligand to 317.3 ppm for the cadmium complex. The pyridine nitrogen resonated at 316.9 ppm in the free ligand, but no correlation to this nitrogen was observed in the cadmium complex despite increasing the duration of the long-range delay to 200 ms (2.5 Hz). The authors attributed this behavior to either a very small scalar coupling or to the possibility of a dynamic process occurring in the complex at room temperature.

In the case of the three-armed podand, **89**, ^{15}N chemical shifts were recorded in both $CDCl_3$ and DMSO-d_6, as shown. Somewhat larger perturbations of the ^{15}N shifts of **89** were observed for the cadmium complex. The Schiff-base nitrogen shifted upfield from 340.6 ppm in DMSO-d_6 to 289.5 ppm; the pyridine nitrogen shifted upfield from 317.3 to 266.5 ppm. Despite the observation of correlations to the pyridine nitrogen for the cadmium complex of **89**, no correlations were observed in the $^1H-^{15}N$ GHMBC spectrum to the tertiary aliphatic nitrogen.

Silver Cation Complexation with 3α,3′α-bis(pyridine-*n*-carboxy)lithocholic Acid 1,2-Ethandiol Diesters. In an extension of efforts directed at the potential utilization of bile acids as carriers for drug molecules, a series of 3α,3′α-bis(pyridine-*n*-carboxy)lithocholic acid 1,2-ethandiol diesters were prepared.[136] Compounds such as **90** have been specifically used as "shuttles" to deliver drugs to liver targets. When analogues of **90** were treated with

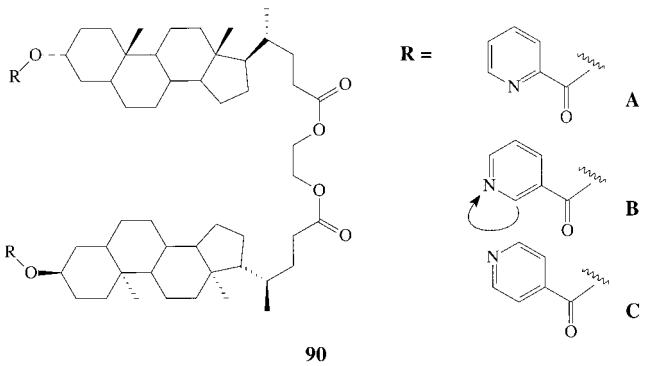

90

AgO_3SCF_3, significant shifts in the ^1H resonances of the pyridine residues were observed. When the pyridine was incorporated as a picolinato moiety (**90a**), theoretical calculations suggested that both the pyridine nitrogen and the ester carbonyl oxygen were involved. The pyridine nitrogen shifted upfield from 309.9 ppm as the free ligand to 267.7 ppm when silver cation was added. Similar behavior was observed for the nicotinate analogue (**90b**), the pyridine nitrogen shifting upfield from 310.4 to 260.3 ppm when silver cation was added. In the case of the isonicotinolate, **90c**, the pyridine nitrogen resonated at 314.1 ppm. No mention was made in the work of a shift induced at the pyridine nitrogen by the addition of silver cation. Chemical shifts were reported relative to nitromethane.

Conclusions

The applications of long-range $^1H-^{15}N$ heteronuclear shift correlation experiments at natural abundance that have appeared through mid 1999 have been reviewed. Every effort has been made to be comprehensive and exhaustive in the literature search that was conducted; we offer our apologies if we have missed any contributions to this growing field of research. Some papers published later in 1999 after the original draft of this review was submitted for publication are briefly surveyed in the section Notes Added in Proof. The issues of ^{15}N chemical shift referencing, the experiments that are available for the acquisition of direct and long-range $^1H-^{15}N$ heteronuclear shift correlation data, pulse calibrations, data processing, the extraction of pertinent information from the spectra, and other considerations have also been presented. We have provided tables of ^{15}N shift data for various types of compounds gleaned from the various literature sources cited herein. The range of structural types tabulated in this review is by no means comprehensive, and readers interested in other types of nitrogen-containing functional groups or heterocycles are directed to the excellent and far more comprehensive reviews of ^{15}N chemical shift data that have been published by Witanowski, Stefaniak, and Webb.[1−6]

The growing availability of 3-mm gradient inverse probes,[64,65] coupled with the recent development of a 1.7-mm submicro gradient inverse detection or SMIDG NMR probe[66,67] by Nalorac Corporation of Martinez, CA, will undoubtedly stimulate further studies in the area of long-range $^1H-^{15}N$ heteronuclear shift correlation NMR at natural abundance. The utilization of ^{15}N as a structural probe, in the opinion of the present authors, will open new avenues of investigation in the elucidation of natural products and other complex structures. We feel that this will be especially true as more groups have access to micro (3-mm) and submicro (1.7-mm) NMR probe technology, which reduces sample requirements for these experiments at 600 MHz below the 1-mg level for the first time.[61,62] The development of inverse-detection gradient 3-mm "cold metal" probes with rf coils and electronics cooled to the range 8−20 K can be expected to increase the sensitivity still higher, perhaps by as much as a factor of 3. If the anticipated gains in sensitivity are realized, long-range $^1H-^{15}N$ heteronuclear shift correlation studies performed on submicromole samples may become routine in laboratories with this advanced probe technology available to investigators.

At present, on the basis of the bibliography of work done in this area, which is available on request from the senior author by e-mail, all indications are that applications of long-range $^1H-^{15}N$ heteronuclear shift correlation at natural abundance are about to enter a period of burgeoning growth. In the first year that papers were published in this area, 1995, four papers appeared in the literature containing long-range $^1H-^{15}N$ data, and a fifth paper mentioned the utilization of these experiments albeit without specific mention of any data. In 1996 and 1997 nine and eleven papers appeared in the literature, respectively, which included long-range $^1H-^{15}N$ data. In 1998, to the best of our knowledge there were more than 20 papers that either had appeared or were in press. It is likely that there will be in excess of 20 papers this year, and we feel that it is highly probable that the rate of appearance of studies involving long-range $^1H-^{15}N$ studies at natural abundance will continue to increase for the foreseeable future.

Notes Added in Proof

Since the completion of the writing and submission of this review, papers have continued to appear in the literature that either directly report further work in the area of long-range $^1H-^{15}N$ heteronuclear shift correlation at natural abundance or are germane to this area of research. A new long-range heteronuclear shift correlation experiment, CIGAR-HMBC, which uses accordion optimization and which may be applicable to long-range $^1H-^{15}N$ experiments, has been reported.[137] Of particular interest to the question of experiment selection, a paper comparing the results obtained with the GHMBC, ACCORD-HMBC, and IMPEACH-MBC pulse sequences using strychnine (**5a**) as a model compound has appeared.[138] A new pulse sequence for the accurate measurement of long-range heteronuclear couplings has been reported by Williamson and co-workers.[139]

Williamson, Sitachitta, and Gerwick[140] have reported the utilization of the GHNMBC experiment[49] in a study of the biosynthesis of the cyanobacterial metabolite barbamide (**91**) that successfully determined the origins of the thiazole ring in the molecule's structure.

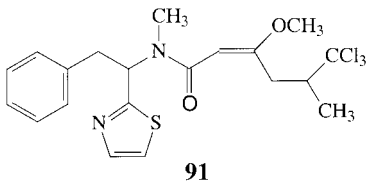

91

Tabata et al.[141] reported the application of gradient $^1H-^{15}N$ HMQC and HMBC in the elucidation of the structure of the cyclic peptide antibiotic zelkovamycin (**92**). The long-range couplings observed are shown on the structure. ^{15}N chemical shifts were referenced relative to formamide (115 ppm) and are shown as reported by the authors.

Long-range $^1H-^{15}N$ GHMBC spectra optimized for 3 Hz were used to determine the sites of metalation in 2,3-disubstitued quinoxalines. 2-Methoxyquinoxaline and 2-

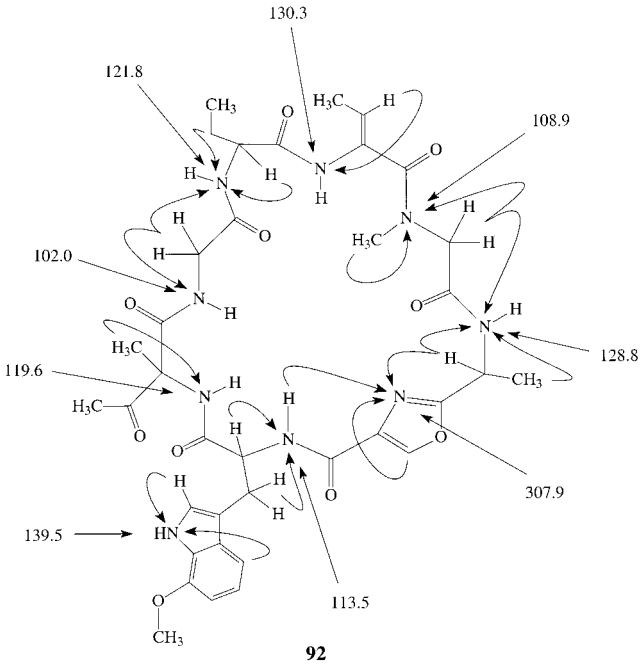

92

phenylquinoxaline were used as model compounds to assign the nitrogen chemical shifts of 2-methoxy-3-phenylquinoxaline (**93**). The assigned ^{15}N chemical shifts of **93** were then used as the basis for determining the site of metalation and subsequent substitution.[142]

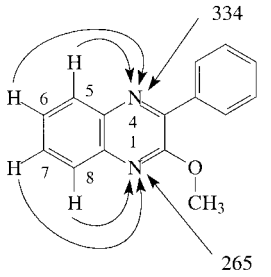

93

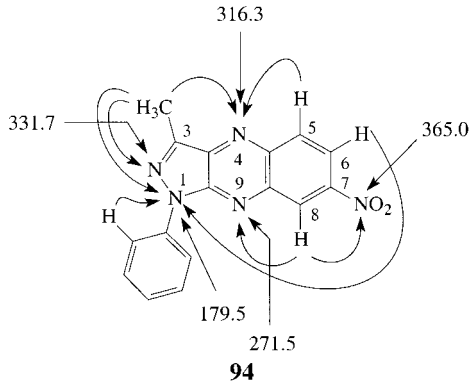

94

Kolehmainen and co-workers[143] in a similar study used ^{1}H−^{15}N GHMBC data to differentiate between isomeric pyrazolo[3,4*b*]quinoxalines, e.g., **94**. The data reported by these authors were from an experiment optimized for 5 Hz; chemical shifts were referenced relative to nitromethane and are shown here relative to liquid ammonia. Interestingly, in addition to several four-bond ($^{4}J_{NH}$) long-range couplings, these authors also reported the observation of a seven-bond ($^{7}J_{NH}$) correlation from H-6 of **94** to the N-1 ^{15}N resonance. To the best of our knowledge, this is the only time such a long-range correlation has been reported in long-range ^{1}H−^{15}N data taken at natural abundance.

Acknowledgment. The authors are very deeply indebted to colleagues worldwide who have graciously provided preprints of papers from their laboratories that have aided in making this review more comprehensive. We especially wish to thank Dr. Hiroyuki Koshino of The Institute of Physical Chemical Research (RIKEN), Saitama, Japan; Dr. Radek Marek of Masaryk University, Brno, Czech Republic; and Professor Erkki Kolehmainen, Department of Chemistry, University of Jyväskylä, Jyväskylä, Finland. We would also like to thank R. Thomas Williamson, Brian Marquez, and Professor William H. Gerwick of Oregon State University for providing preprints of their work and for permission to reproduce the PEP-GHSQC-TOCSY spectrum of bombesin shown in Figure 16. The permission of Pergamon Press/Elsevier Science and John Wiley & Sons, Ltd., to reproduce some of the figures contained in this review is also gratefully acknowledged.

Supporting Information Available: Supplementary tables of ^{15}N chemical shifts of various nitrogen-containing functional groups and heterocycles as well as figures showing the effect of ^{15}N pulse length on excitation range, and pulse sequence schematics for experiments applicable to ^{1}H−^{15}N correlation experiments are available free of charge via the Internet at http://pubs.acs.org.

References and Notes

(1) Mooney, E. F.; Winson, P. H. In *Annual Reports of NMR Spectroscopy*; Mooney, E. F., Ed.; Academic Press: New York, 1968; Vol. 2; pp 125−152.
(2) Witanowski, M.; Stefaniak, L.; Webb, G. A. In *Annual Reports of NMR Spectroscopy*; Mooney, E. F., Ed.; Academic Press: New York, 1972; Vol. 5a; pp 395−457.
(3) Witanowski, M.; Stefaniak, L.; Webb, G. A. In *Annual Reports of NMR Spectroscopy*; Webb, G. A., Ed.; Academic Press: New York, 1977; Vol. 7; pp 118−239.
(4) Witanowski, M.; Stefaniak, L.; Webb, G. A. In *Annual Reports of NMR Spectroscopy*; Webb, G. A., Ed.; Academic Press: New York, 1981; Vol. 11B.
(5) Witanowski, M.; Stefaniak, L.; Webb, G. A. In *Annual Reports of NMR Spectroscopy*; Webb, G. A., Ed.; Academic Press: New York, 1986; Vol. 18.
(6) Witanowski, M.; Stefaniak, L.; Webb, G. A. G. A. In *Annual Reports of NMR Spectroscopy*; Webb, G. A., Ed.; Academic Press: New York, 1993; Vol. 25.
(7) Witanowski, M.; Webb, G. A. *Nitrogen NMR*; Plenum Press: New York, 1973.
(8) Levy, G. C.; Lichter, R. L. *Nitrogen-15 NMR Spectroscopy*; Wiley: New York, 1978.
(9) Martin, G. J.; Martin, M. L.; Gouesnard, J.-P. *^{15}N NMR Spectroscopy, NMR Basic Principles and Progress*; Diehl, P., Fluck, E., Kosfeld, R., Eds.; Springer-Verlag: New York, 1981; Vol. 18.
(10) Berger, S.; Braun, S.; Kalinowski, H.-O. *NMR Spectroscopy of the Non-Metallic Elements*; Wiley: New York, 1997; pp 111−318.
(11) von Philipsborn, W.; Müller, R. *Angew. Chem., Intl. Ed. Engl.* **1986**, *25*, 383−486.
(12) Bax, A.; Griffey, R. H.; Hawkins, B. L. *J. Magn. Reson.* **1983**, *55*, 301−315.
(13) Bax, A.; Griffey, R. H.; Hawkins, B. L. *J. Am. Chem. Soc.* **1983**, *105*, 7188−7190.
(14) Müller, L. *J. Am. Chem. Soc.* **1979**, *101*, 4481−4484.
(15) Bax, A.; Subramanian, S. *J. Magn. Reson.* **1986**, *67*, 565−569.
(16) Bodenhausen, G.; Ruben, D. J. *Chem. Phys. Lett.* **1980**, *69*, 185−189.
(17) Bax, A.; Summers, M. F. *J. Am. Chem. Soc.* **1986**, *108*, 2083−2084.
(18) Carmeli, S.; Moore, R. E.; Patteson, G. M. L.; Corbett, T. H.; Valeriote, F. A. *J. Am. Chem. Soc.* **1990**, *112*, 8195−8197.
(19) Martin, G. E.; Crouch, R. C.; Sharaf, M. H. M.; Schiff, P. L., Jr. 34th Annual Meeting of the American Society of Pharmacognosy, San Diego, CA, July 18−22, 1993, Abstract P101.
(20) Uzawa, J.; Utumi, H.; Koshino, H.; Hinomoto, T.; Anzai, K. 32nd NMR Conference, Tokyo, Japan, November 4−6, 1993; pp 147−150.
(21) Hurd, R. E.; John, B. K. *J. Magn. Reson.* **1991**, *91*, 648−653.
(22) Ruiz-Cabello, J.; Vuister, G. W.; Moonen, C. T. W.; van Geldern, P.; Cohen, J. S.; van Zilj, P. C. M. *J. Magn. Reson.* **1992**, *100*, 282−302.
(23) Parella, T. *Magn. Reson. Chem.* **1998**, *36*, 467−495.
(24) Willker, W.; Leibfritz, D.; Kerssebaum, R.; Bermel, W. *Magn. Reson. Chem.* **1993**, *31*, 287−292.
(25) Martin, G. E.; Crouch, R. C. *J. Heterocycl. Chem.* **1995**, *32*, 1839−1842.
(26) Martin, G. E.; Crouch, R. C.; Andrews. C. W. *J. Heterocycl. Chem.* **1995**, *32*, 1759−1766.
(27) (a) Maudsley, A. A.; Wokaun, A.; Ernst, R. R. *Chem. Phys. Lett.* **1978**, *55*, 9−14. (b) Bax, A.; de Jong; P. G.; Mehlkopf, Smidt, J. *Chem. Phys. Lett.* **1980**, *69*, 567−570. (c) Barker, P.; Freeman, R. *J. Magn. Reson.* **1985**, *64*, 334−338.
(28) Crouch, R. C.; Davis, A. O.; Spitzer, T. D.; Martin, G. E.; Sharaf, M. H. M.; Schiff, P. L., Jr.; Phoebe, C. H., Jr.; Tackie, A. N. *J. Heterocyclic Chem.* **1995**, *32*, 1077−1080.

(29) Tackie, A. N.; Boye, G. L.; Sharaf, M. H. M.; Schiff, P. L., Jr.; Crouch, R. C.; Spitzer, T. D.; Johnson, R. L.; Dunn, J.; Minick, D.; Martin, G. E. *J. Nat. Prod.* **1993**, *56*, 653−670.
(30) Martin, G. E.; Hadden, C. E.; Sharaf, M. H. M.; Tackie, A N.; Schiff, P. L., Jr. *Magn. Reson. Chem.* **1999**, *37*, 529−537.
(31) Hadden, C. E.; Martin, G. E.; Schiff, P. L., Jr.; Tackie, A. N. *J. Heterocycl. Chem.* **1999**, *36*, 1114−1117.
(32) Reynolds, W. F.; McLean, S.; Tay, L.-L.; Yu, M.; Enriquez, R. G.; Estwick, D. M.; Pascoe, K. D. *Magn. Reson. Chem.* **1997**, *35*, 455−462.
(33) Griesinger, C.; Schwalbe, H.; Schleucher, J.; Sattler, M. In *Two-Dimensional NMR Spectroscopy—Applications for Chemists and Biochemists*, 2nd ed.; Croasmun, W. R., Carlson, R. M. K., Eds.; VCH: New York, 1994; pp 457−580.
(34) Bax, A.; Pochapsky, S. S. *J. Magn. Reson.* **1992**, *99*, 638−643.
(35) Wimperis, S.; Freeman, R. *J. Magn. Reson.* **1984**, *58*, 348−353.
(36) Martin, G. E.; Zektzer, A. S. *Two-Dimensionl NMR Methods for Establishing Molecular Connectivity, A Chemist's Guide to Experiment Selection, Performance, and Interpretation*; VCH: New York, 1988; pp 51−55.
(37) Williamson, R. T.; Márquez, B.; Gerwick, W. H. *Tetrahedron* **1999**, *55*, 2881−2888.
(38) Cavanaugh, J.; Palmer, A. G., III; Wright, P. E.; Rance, M. *J. Magn. Reson.* **1991**, *93*, 151−170.
(39) Shaka, A. J.; Lee, C. J.; Pines, A. *J. Magn. Reson.* **1988**, *77*, 274−293.
(40) Furihata, K.; Seto, H. *Tetrahedron Lett.* **1995**, *36*, 2817−2820.
(41) Furihata, K.; Seto, H. *Tetrahedron Lett.* **1996**, *37*, 8901−8902
(42) Marek, R.; Králík, L.; Sklenář, V. *Tetrahedron Lett.* **1997**, *38*, 665−668.
(43) Sheng, S.; van Halbeek, H. *J. Magn. Reson.* **1998**, *130*, 296−299.
(44) Wagner, R.; Berger, S. *Magn. Reson. Chem.* **1998**, *36*, S44−S46.
(45) Furihata, K.; Seto, H. *Tetrahedron Lett.* **1998**, *39*, 7337−7340.
(46) Hadden, C. E.; Martin, G. E.; Krishnamurthy, V. V. *J. Magn. Reson.* **1999**, *140*, 274−280.
(47) Kogler, H.; Sørensen, O. W.; Bodenhausen, G.; Ernst, R. R. *J. Magn. Reson.* **1983**, *55*, 157−163.
(48) Meissner, A.; Moskau, D.; Nielsen, N. C.; Sørensen, O. W. *J. Magn. Reson.* **1997**, *124*, 245−249.
(49) Farley, K. A.; Walker, G. S.; Martin, G. E. *Magn. Reson. Chem.* **1997**, *35*, 671−679.
(50) Farley, K. A.; Bowman, P. B.; Brumfield, J. C.; Crow, F. C.; Duholke, W. K.; Guido, J. E.; Robins, R. H.; Sims, S. M.; Smith, R. F.; Thamann, T. J.; Vonderwell, B. K.; Martin, G. E. *Magn. Reson. Chem.* **1998**, *36*, S11−S16.
(51) Martin, G. E.; Crow, F. W.; Kaluzny, B. D.; Marr, J. G.; Fate, G. D.; Gilbertson, T. *Magn. Reson. Chem.* **1998**, *36*, 635−644.
(52) Bax, A.; Marion, D. *J. Magn. Reson.* **1988**, *78*, 186−191.
(53) Titman, J. J.; Neuhaus, D.; Keeler, J. *J. Magn. Reson.* **1989**, *85*, 111−131.
(54) Bachmann, P.; Aue, W. P.; Müller, L.; Ernst, R. R. *J. Magn. Reson.* **1977**, *28*, 29−39.
(55) Hurd, R. E.; John, B. K.; Plant, H. D. *J. Magn. Reson.* **1991**, *93*, 666−670.
(56) Davis, A. L.; Keeler, J.; Laue, E. D.; Moskau, D. *J. Magn. Reson.* **1992**, *98*, 207−216.
(57) Vuister, G. W.; Boelens, R.; Burgering, M.; Kaptein, R.; van Zilj, P. C. M. *J. Biol. NMR* **1992**, *2*, 301−305.
(58) Vuister, G. W.; Ruiz- Cabello, J.; van Zilj, P. C. M. *J. Magn. Reson.* **1992**, *100*, 215−219.
(59) Bodenhausen, G.; Ernst, R. R. *J. Am. Chem. Soc.* **1982**, *104*, 1304−1309.
(60) Martin, G. E.; Hadden, C. E.; Crouch, R. C.; Krishnamurthy, V. V. *Magn. Reson. Chem.* **1999**, *37*, 517−528.
(61) Hadden, C. E.; Martin, G. E. *Magn. Reson. Chem.* **1999**, *37*, 385−388.
(62) Hadden, C. E.; Martin, G. E. *J. Nat. Prod.* **1998**, *61*, 969−972.
(63) Koshino, H.; Uzawa, J. *Kagaku to Seibutsu* **1995**, *33*, 252−258.
(64) Crouch, R. C.; Martin, G. E. *J. Nat. Prod.* **1992**, *55*, 1343−1347.
(65) Crouch, R. C.; Martin, G. E. *Magn. Reson. Chem.* **1992**, *30*, S66−S70.
(66) Martin, G. E.; Crouch, R. C.; Zens, A. P. *Magn. Reson. Chem.* **1998**, *36*, 551−557.
(67) Martin, G. E.; Guido, J. E.; Robins, R. H.; Sharaf, M. H. M.; Schiff, P. L., Jr.; Tackie, A. N. *J. Nat. Prod.* **1998**, *61*, 555−559.
(68) Martin, G. E.; Hadden, C. E. *Magn. Reson. Chem.* **1999**, *37*, 721−729.
(69) Krishnamurthy, V. V. Personal communication, 1998.
(70) Olson, D. L.; Peck, T. L.; Webb, G. A.; Magin, R. L.; Sweedler, J. V. *Science* **1995**, *270*, 1967−1970.
(71) Olson, D. L.; Lacey, M. E.; Sweedler, J. V. *Anal. Chem.* **1998**, *70*, 645−650.
(72) Olson, D. L.; Lacey, M. E.; Sweedler, J. V. *Anal. Chem.* **1998**, *70*, 257A−264A.
(73) Subramanian, R.; Webb, G. A. *Anal. Chem.* **1998**, *70*, 2454−2458.
(74) Webb, A. G. *Prog. NMR Spectrosc.* **1997**, *31*, 1−42.
(75) (a) Subramanian, R.; Sweedler, J. V.; Webb, G. A. 40th Experimental NMR Conference, Orlando, FL, February 28−March 5, 1999, P200. (b) Subramanian, R.; Sweedler, J. V.; Webb, G. A. *J. Am. Chem. Soc.* **1999**, *121*, 2333−2334.
(76) Crouch, R. C.; Martin, G. E.; Musser, S. M.; Grenade, H. R.; Dickey, R. W. *Tetrahedron Lett.* **1995**, *36*, 6827−6830.
(77) Reynolds, W. F.; Yu, M.; Enriquez, R. G. *Magn. Reson. Chem.* **1997**, *35*, 614−618.
(78) Carmeli, S.; Park, S.; Moore, R. E.; Patterson, G. M. L.; Yoshida, W. L. *Tetrahedron Lett.* **1993**, *34*, 6681−6684.
(79) Levy, G. C.; Lichter, R. L. *Nitrogen-15 Nuclear Magnetic Resonance Spectroscopy*; Wiley-Interscience: New York, 1979; pp 114−116.
(80) Crouch, R. C.; Martin, G. E. *J. Heterocycl. Chem.* **1995**, *32*, 1665−1669.
(81) Andrews, C. W.; Wisowaty, J.; Davis, A. O.; Crouch, R. C.; Martin, G. E. *J. Heterocycl. Chem.* **1995**, *32*, 1011−1017
(82) Martin, G. E. *J. Heterocycl. Chem.* **1997**, *34*, 695−699.
(83) Martin, G. E.; Crouch, R. C.; Sharaf, M. H. M.; Schiff, P. L., Jr. *J. Nat. Prod.* **1996**, *59*, 2−4.
(84) Kaczmarek, L.; Nantka-Mamirski, P.; Sefaniak, L.; Webb, G. A.; Davoust, D.; Basselier, J. J. *Magn. Reson. Chem.* **1985**, *23*, 853−855.
(85) Sharaf, M. H. M. Alkaloids of *Cryptolepis sanguinolenta* (Lindl.) Schlechter (*Asclepiadaceae*), Ph.D. Thesis, School of Pharmacy, University of Pittsburgh, Pittsburgh, PA, 1993; pp 177−192.
(86) Paulo, A.; Gomes, E. T.; Houghton, P. J. *J. Nat. Prod.* **1995**, *36*, 1485−1491.
(87) Cooper, M. M.; Lovell, J. M.; Joule, J. A. *Tetrahedron Lett.* **1996**, *37*, 4283−4286.
(88) Sharaf, M. H. M.; Schiff., P. L., Jr.; Tackie, A. N.; Martin, G. E. *J. Heterocyclic Chem.* **1998**, *35*, 1365−1369.
(89) Martin, G. E.; Hadden, C. E.; Blinn, J. R.; Sharaf, M. H. M.; Tackie, A. N.; Schiff, P. L., Jr. *Magn. Reson. Chem.* **1998**, *37*, 1−6.
(90) Hadden, C. E.; Sharaf, M. H. M.; Guido, J. E.; Robins, R. H.; Schiff, P. L., Jr.; Tackie, A. N.; Phoebe, C. H., Jr.; Martin, G. E. *J. Nat. Prod.* **1999**, *62*, 238−240.
(91) Bax, A.; Walker, G. S.; Farley, K. A. *J. Magn. Reson. A* **1996**, *119*, 134−138.
(92) Kusano, M.; Sotoma, G.; Koshino, H.; Uzawa, J.; Chijimatsu, M.; Fujioka, S.; Kawano, T.; Kimra, Y. *J. Chem. Soc., Perkin Trans. 1* **1998**, 2823−2826.
(93) Markgraf, J.; Richardson, P.; Livingston, R. C. *Magn. Reson. Chem.* **1993**, *31*, 694−695.
(94) Marek, R.; Dostál, J.; Slavík, J.; Sklenář, V. *Molecules* **1996**, *1*, 166−169.
(95) Kim, J.-S.; Shin-ya, K.; Furihata, K.; Hayakawa, Y.; Seto, H. *Tetrahedron Lett.* **1997**, *37*, 3431−3434.
(96) Koshino, H.; Lee, I.-K.; Kim, J.-P.; Kim, W.-G.; Uzawa, J.; Yoo, I.-D. *Tetrahedron Lett.* **1996**, *37*, 4549−4550.
(97) Verotta, L.; Pilati, T.; Tató, M.; Elisabetsky, E.; Amador, T. A.; Nunes, D. S. *J. Nat. Prod.* **1998**, *61*, 392−396.
(98) Kawamura, N.; Sawa, R.; Takahashi, Y.; Issiki, K.; Sawa, T.; Kinoshita, N.; Naganawa, H.; Hamada, M.; Takeuchi, T. *J. Antibiot.* **1995**, *48*, 435−437.
(99) Kawamura, N.; Sawa, R.; Takahashi, Y.; Isshiki, K.; Sawa, T.; Naganawa, H.; Takeuchi, T. *J. Antibiot.* **1996**, *49*, 651−656.
(100) Kawamura, N.; Sawa, R.; Takahashi, Y.; Sawa, T.; Naganawa, H.; Takeuchi, T. *J. Antibiot.* **1996**, *49*, 657−660.
(101) Shin-ya, K.; Kim, J.-S.; Furihata, K.; Hayakawa, Y.; Seto, H. *Tetrahehdron Lett.* **1997**, *38*, 7079−7082.
(102) Kato, Y.; Koshino, H.; Uzawa, J.; Anzai, K. *Biosci. Biotech. Biochem.* **1996**, *60*, 2081−2083.
(103) Arai, N.; Shiomi, K.; Takamatsu, S.; Komiyama, K.; Iwai, Y.; Liu, J.-R.; Ōmura, S. *J. Antibiot.* **1997**, *50*, 808−814.
(104) McDonnell, P. A.; Gauthier, A. D.; Ferro, M. P. *Magn. Reson. Chem.* **1998**, *36*, 35−38.
(105) Kolehmainen, E.; Puchala, A.; Suontamo, R.; Rasala, D.; Lysek, R. *J. Chem. Soc., Perkin Trans. 2* **1996**, 2383−2387.
(106) Ryoo, I.-J.; Song, K.-S.; Kim, J.-P.; Kim, W.-G.; Koshino, H.; Yoo, I.-D. *J. Antibiotics* **1997**, *50*, 256−258.
(107) Kondo, S.; Ikeda, Y.; Ikeda, D.; Nishizuka, T.; Gomi, S. *J. Antibiot.* **1998**, *51*, 232−234.
(108) Shariahama, H.; Koshino, H.; Uzawa, J.; Yamano, K.; Konno, K.; Nakatu, K. *Heterocycles* **1998**, *47*, 661−664.
(109) Kolehmainen, E.; Lappalainen, K.; Saman, D.; Holy, A.; Günter, J. *Magn. Reson. Chem.* **1998**, *36*, 442−444.
(110) Fukuzawa, S.; Matsunaga, S.; Fusetani, N. *Tetrahedron Lett.* **1996**, *37*, 1447−1448.
(111) Takishi, S.; Tuchiya, N.; Sato, A.; Negishi, T.; Takamatsu, Matsushita, Y.; Watanabe, T.; Iijim, Y.; Haruyma, H.; Kinoshita, T.; Tanaka, M.; Kodama, K. *J. Antibiot.* **1998**, *51*, 805−815.
(112) Marek, R.; Tousek, J.; Králík, L.; Dostál, J.; Sklenář, V. *Chem. Lett.* **1997**, 369−370.
(113) Dostál, J.; Slaík, J.; Potácek, M.; Marek, R.; Sklenář, V.; De Hoffman, E.; Rozenber, R.; Tinant, B.; Declercq, J.-P. *Phytochemistry* **1998**, *47*, 879−885.
(114) Dostál, J.; Slaqvík, J.; Potácek, M.; Marek, R.; Humpa, O.; Sklenář, V.; Tousek, J.; De Hoffman, E.; Rozenberg, R. *Collect. Czech. Chem. Commun.* **1998**, *63*, 1045−1055.
(115) Dostál, J.; Marek, R.; Slavík, J.; Táborská, E.; Potácek, M.; Sklenář, V. *Magn. Reson. Chem.* **1998**, *36*, 869−872.
(116) Marek, R.; Marek, J.; Dostál, J.; Slavik, J. *Collect. Czech. Chem. Commun.* **1998**, 1623−1630.
(117) Marek, R.; Humpa, O.; Dostál, J.; Slavík, J. *Magn. Reson. Chem.* **1999**, *37*, 195−202.
(118) Hooper, G. J.; Orjala, J.; Shatzman, R. C.; Gerwick, W. H. *J. Nat. Prod.* **1998**, *61*, 529−533.
(119) Suzumura, K.-I.; Takahashi, I.; Matsumoto, H.; Nagai, K.; Setiawan, B.; Rantiatmodjo, R. M.; Suzuki, K.-I.; Nagano, N. *Tetrahedron Lett.* **1997**, *38*, 7573−7576.
(120) Depaire, H.; Thomas, J. P.; Brun, A.; Olesker, A.; Lukacs, G. *Tetrahedron Lett.* **1977**, *16*, 1401−1402.

(121) Mocek, U.; Knaggs, A. R.; Tsuchiya, R.; Nguyen, T.; Beale, J. M.; Floss, H. G. *J. Am. Chem. Soc.* **1993**, *115*, 7557−7568.
(122) Gasmi, G.; Massiot, G.; Nuzillard, J. M. *Magn. Reson. Chem.* **1996**, *34*, 185−190.
(123) Olesker, A.; Valente, L.; Barata, L.; Lukacs, G.; Hull, W. E.; Tori, K.; Tokura, K.; Okave, K.; Ebata, M.; Otsuka, H. *J. Chem. Soc., Chem. Commun.* **1978**, 577−578.
(124) Marek, R. *Collect. Czech. Chem. Commun.* **1997**, *62*, 1747−1753.
(125) Kilián, P.; Marek, J.; Marek, R.; Tou-ín, J.; Humpa, O.; Novosad, J.; Woollins, J. D. *J. Chem. Soc., Dalton Trans.* **1998**, 1175−1180.
(126) Lin, Q.; Ball, G. E.; Bishop, R. *Tetrahedron* **1997**, *53*, 10899−10910.
(127) Poobrasert, O.; Cordell, G. A.; Bobzin, S. C. *J. Nat. Prod.* **1997**, *60*, 578−580.
(128) Kohlemainen, E.; Gawinecki, R.; Omialowski, B.; Trezbiatowska, K. *Magn. Reson. Chem.* **1997**, *35*, 778−784.
(129) Westerman, P. W.; Botto, R. E.; Roberts, J. D. *J. Org. Chem.* **1978**, *43*, 2590−2596.
(130) Pazdera, P.; Sibor, J.; Marek, R.; Kuty, M.; Marek, J. *Molecules* **1997**, *2*, 135−151.
(131) Gawinecki, R.; Kolehmainen, E.; Kucybła, Z.; Ośmiałowski, B.; Kauppinen, R. *Magn. Reson. Chem.* **1998**, *35*, 848−854.
(132) Satake, A.; Nakata, T. *J. Am. Chem. Soc.* **1998**, *120*, 10391−10396.
(133) Satake, A.; Koshino, H.; Nakata, T. *Chem. Lett.* **1999**, 49−50.
(134) Satake, A.; Kadohama, H.; Koshino, H.; Nakata, T. *Tetrahedron Lett.* **1999**, *40*, 3597−3600.
(135) Jäntti, A.; Wagner, M.; Suontamo, R.; Kolehmainen, E.; Rissanen, K. *Eur. J. Inorg. Chem.* **1998**, 1555−1562.
(136) Kolehmainen, E.; Tamminen, J.; Kauppinen, R.; Linnanto, J. *J. Inclusion Phenom. Mol. Recognit. Chem.* **1999**, *35*, 75−84.
(137) Hadden, C. E.; Martin, G. E.; Krishnamurthy, V. V. *Magn. Reson. Chem.* **2000**, *37*, 143−147.
(138) Martin, G. E.; Hadden, C. E. *Magn. Reson. Chem.* **2000**, *37*, 251−256.
(139) Williamson, R. T.; Marquez, B. L.; Kover, K. E.; Gerwick, W. H. *Magn. Reson. Chem.* **2000**, *38*, 265−273.
(140) Williamson, R. T.; Sitachitta, N.; Gerwick, W. H. *Tetrahedron Lett.* **1999**, *40*, 5175−5178.
(141) Tabata, N.; Tomoda, H.; Zhong, H.; Uchida, R.; Ōmura, S. *J. Antiobiot.* **1999**, *52*, 34−39.
(142) Chapoulaud, V. G.; Salliot, I.; Plé, N.; Turck, A.; Quéguiner, G. *Tetrahedron* **1999**, *55*, 5389−5404.
(143) Kolehmainen, E.; Kucybała, Z.; Gawinecki, R.; Pączkowski, J.; Kacała, A. *Tetrahedron* **1999**, *55*, 8475−8480.

NP9903191